Dilute Acid and Ionic Liquid Based Pretreatment of Lignocellulosic Biomass towards Fermentable Sugars

Thesis submitted in partial fulfillment of the requirements for the degree of

Doctor of Philosophy

by

Madhusmita Dash

Centre for Energy

Indian Institute of Technology Guwahati

Guwahati – 781039, Assam, India

December - 2017

I would like to dedicate this thesis to my loving Parents whose words of encouragement and push for tenacity ring in my ear. They supported me all the way since the beginning of my studies and made me strong enough to achieve my goal.

CENTRE FOR ENERGY
INDIAN INSTITUTE OF TECHNOLOGY GUWAHATI
GUWAHATI- 781039, ASSAM, INDIA

CERTIFICATE

This is to certify that the matter embodied in this thesis entitled ***"Dilute Acid and Ionic Liquid Based Pretreatment of Lignocellulosic Biomass towards Fermentable Sugars"*** is the result of investigations carried out by **Ms. Madhusmita Dash** (Roll No. 126151005) under our supervision, and to be submitted for the award of degree of Doctor of Philosophy to IIT Guwahati. We certify that she has fulfilled all the requirements according to the rules of the institute and this work has not been submitted elsewhere for a degree or diploma.

Dr. Kaustubha Mohanty
Professor
Department of Chemical Engineering
Indian Institute of Technology Guwahati

Dr. V. V. Dasu
Professor
Department of Biosciences and Bioengineering
Indian Institute of Technology Guwahati

ACKNOWLEDGEMENT

With immense gratitude I would like to acknowledge the valuable guidance, support, help and encouragement of my supervisor Prof. Kaustubha Mohanty, Department of Chemical Engineering, Indian Institute of Technology Guwahati. I sincerely thank him for being an excellent mentor and teacher throughout my research work. I would also like to acknowledge my sincere gratitude to my co supervisor Prof. V.V. Dasu, for his guidance and support. I owe my gratitude to the members of my doctoral committee Prof. V. S. Moholkar, Prof. G. Pugazhenthi and Prof. Sukhomay Pal for their insightful advices and suggestions throughout the research.

My sincere thanks to the Heads of Centre for Energy, Prof. P. Goswami and Prof. V.S. Moholkar for allowing me to use the Centre facilities in their respective tenures. Special thanks to the Head of Central Instrument Facility (CIF), IIT Guwahati, for providing me the analytical facilities of CIF.I am grateful to all the staff members of Centre for Energy for their help during my research work. I would also like to thank all my research group members, Dr. Soumya, Dr. Shanti, Dr. Himadri, Kulbhusan, Sanjeev, Sounak, Santosh, Madona, Bikashbindu, Pranab, Barasa, Sachankar, Munmi, Ranjeet and Proloy for their help throughout my research work. I am also thankful to my colleagues in Centre for Energy and my friends for their love and support throughout this period.

I would like to express my deep sense of gratitude to my parents, my brother and family for their unconditional love and support towards the completion of my PhD thesis. I extend my sincere thanks to my husband for his support. This journey would not have been possible without them.

Madhusmita Dash

ABSTRACT

Bio-energy from lignocellulosic biomass is cleaner, sustainable, and one of the renewable energy sources that could help meets some of our energy demand. Unlike fossil fuels, it can be grown and used repeatedly and its use can replace the fossil fuels. In addition to this, these materials are easily available either in the form of agricultural waste or forest residues and are economically viable. The current study focuses on physico-chemical characterization of three commonly available lignocellulosic biomasses of North-East India such as Castor (*Ricinus communis*), Jatropha (*Jatropha curcas*), and Miscanthus (*Miscanthus Sinensis*) for second generation biofuels production. Ultimate analysis (CHNSO), thermogravimetric analysis, X-ray diffraction, Fourier transformation infrared (FTIR), and oxygen bomb calorimeter techniques were used to characterize the above mentioned three lignocellulose biomasses. It was found that the cellulose content of three biomasses varied from 40% to 44%, hemicellulose content from 8% to 14% and lignin content varied from 21% to 30%. Chemical structure of lignocellulose is studied through FTIR. The crystallinity index of Castor and Jatropha was similar, i.e., 69%, whereas crystallinity index of Miscanthus was 72%. Due to the presence of higher carbon and cellulose content along with less moisture (10%–12%), ash (5%–10%), sulphur (0.1%–0.8%), and extractives (12%–20%) makes them very good feedstock for the production of alcoholic fuels through biochemical route.

Thermogravimetric analysis of these three lignocellulosic biomass under high purity nitrogen atmosphere were carried out over a temperature range of 25 ^{o}C–900 ^{o}C at three different heating rates of 10, 15, 20 ^{o}C min^{-1}. The profiles generated from thermal decomposition process signified that except dehydration there were three main stages of degradation occurred and were associated with three main components (hemicellulose,

cellulose and lignin). The temperature peaks at maximum weight loss rate obtained from differential thermogravimetric thermograms changed with increasing heating rate. The activation energy and pre-exponential factors were calculated by applying two model-free methods and compared. The kinetic parameters obtained from Kissinger and Ozawa methods were in good agreement with the experimental results. The value of kinetic parameters explained the thermal stability of the biomass. The thermal analysis could not infer the composition and chemical structure of lignocellulosic biomass; hence FTIR spectroscopic analysis has been carried out.

Bioethanol production from lignocellulosic feedstock is considered one of the most promising as it is abundant, cheap and renewable resource. Biomass can be an ideal feedstock for fermentative bioethanol production if properly hydrolyzed. The maximum yield of glucose from biomass requires efficient pretreatment and process optimization is needed to locate the best operational conditions. The efficiency of pretreatment is evaluated in terms of sugars yield, biomass structure alteration and ethanol yield. In the present study, optimization of dilute sulphuric acid pretreatment of Miscanthus followed by enzymatic hydrolysis and fermentation for production of bioethanol was carried out. Response surface methodology was employed for the simultaneous analysis of pretreatment conditions such as substrate loading, acid loading and pretreatment time on crystallinity (CrI %) of solid fraction and amount of xylose and arabinose (X+A) g L^{-1} present in the liquid fraction. The treatment of biomass with H_2SO_4% (v/v) = 0.5 at solid loading % (w/v) = 3.98 for 39.1 minutes exhibited optimum CrI % (82.09). The optimized conditions to obtain maximum (X+A) g L^{-1}(9.61) were; H_2SO_4% (v/v) = 1.47, solid loading % (w/w) = 4.75 and treatment time (min) = 60.17. There is a good correlation between the actual and predicted results. Saccharification results showed that the yield of glucose was higher (0.81 g/g cellulose) for the 5% pretreated biomass (X+A)

at 20 (FPU/g dry biomass) enzymes loading. The yield of glucose was 0.7 (g/g dry pretreated biomass) for the 5% pretreated biomass (X+A) at 20 (FPU/g dry biomass) enzymes

The combine effect of anions of ionic liquids (IL) and anti-solvents on pre-treatment and dissolution mechanism of biomass is not well studied. To reveal the above effect, three different ionic liquids containing fixed cation ($[EMIM]^+$) but varied anions were studied for Miscanthus dissolution. Results showed that, $[EMIM]^+[Ac]^-$ was very good in altering the cellulose structure and crystallinity followed by enzymatic digestibility with a sugar yield of 0.98 (g/g of cellulose). The IL $[EMIM]^+[HSO_4]^-$ was very efficient to remove lignin and partially solubilize hemicellulose, however, the sugar yield was low (0.47 g/g of cellulose) compared with $[EMIM]^+[MeSO_3]^-$ and even the untreated Miscanthus. The regenerated biomass with water-acetone mixture (1:1 v/v) as anti-solvent resulted in higher glucose yield. The hydrogen bond basicity (β value), correlated well with cellulose crystallinity, lignin removal and glucose yield. *N,N-diethyl-4-nitroaniline* (99% pure) was synthesized and its yield was higher with polar protic solvent (C_2H_5OH) and at higher reaction temperature.

CONTENTS

Chapter III

ABBREVIATIONS

OECD: Organization for Economic Co-operation and Development

IEO: International Energy Outlook

LCB: Lignocellulosic biomass

CE: Cellulosic Ethanol

CrI: Crystallinity Index

X+A: Concentration of xylose and arabinose present in filtrate after dilute acid hydrolysis

IL: Ionic liquid

RTIL: Room temperature ionic liquid

AC_WW: Biomass obtained after pre-treatment of Miscanthus using $[EMIM]^+[Ac]^-$ IL and regenerated with water anti-solvent

HS_WW: Biomass obtained after pre-treatment of Miscanthus using $[EMIM]^+[HSO_4]^-$IL and regenerated with water anti-solvent

MS_WW: Biomass obtained after pre-treatment of Miscanthus using $[EMIM]^+[MeSO_3]^-$ IL and regenerated with water anti-solvent

AC_HA: Biomass obtained after pre-treatment of Miscanthus using $[EMIM]^+[Ac]^-$ IL and regenerated with acetone water mixture anti-solvent

HS_HA: Biomass obtained after pre-treatment of Miscanthus using $[EMIM]^+[HSO_4]^-$IL and regenerated with water anti-solvent

MS_HA: Biomass obtained after pre-treatment of Miscanthus using $[EMIM]^+[MeSO_3]^-$ IL and regenerated with water anti-solvent

Lignin removal (%) WW: Lignin removal obtained after pretreatment of Miscanthus using IL and regenerated with water anti-solvent

Cellulose (%) WW: Cellulose content obtained in pretreated Miscanthus using IL and regenerated with water anti-solvent

Hemicellulose (%) WW: Hemicellulose obtained in pretreated Miscanthus using IL and regenerated with water anti-solvent

Lignin removal (%) HA: Lignin removal obtained after pretreatment of Miscanthus using IL and regenerated with acetone water mixture anti-solvent

Cellulose (%) HA: Cellulose content obtained in pretreated Miscanthus using IL and regenerated with acetone water mixture anti-solvent

Hemicellulose (%) HA: Hemicellulose obtained in pretreated Miscanthus using IL and regenerated with acetone water mixture anti-solvent

CrI WW: Crystallinity Index of pretreated Miscanthus using IL and regenerated with water anti-solvent

CrI HA: Crystallinity Index of pretreated Miscanthus using IL and regenerated with acetone water mixture anti-solvent

Glucose yield WW: Glucose yield obtained from pretreated Miscanthus using IL and regenerated with acetone water mixture anti-solvent

Glucose yield HA: Glucose yield obtained from pretreated Miscanthus using IL and regenerated with acetone water mixture anti-solvent

List of Tables

List of Figures

1 INTRODUCTION

Energy plays a vital role for promoting growth in economies and progress in our society. According to the International Energy Outlook (U.S. IEO2013), the world energy consumption is expected to rise by 56% from 2010 to 2040, i.e., 524 quadrillion Britishthermal units (Btu) to 820 quadrillion (Btu). The global energy demand from 2010 to 2040 for developing nations outside the Organization for Economic Cooperation and Development (non OECD) increases by 90% due to strong, long-term economic growth and increasing populations, whereas increase in energy demand is 17% for OECD countries. This triggers energy conservation and diversification. Several factors such as the rapid depletion of reserves and fluctuating prices of fossil fuels, national energy security, greenhouse gas emissions are key factors in facilitating development of alternative energy.

1.1 Global Energy Trends

Understanding the global energy trends is an essential component when trying to detect how and why energy resources have been and might be allocated. The key points that have given projections of future global energy trends through a period to, and beyond, 2030 are the energy mix, supply and demand, global population, non-OECD growth in affluence and global economic performance. An initial goal of the work was to look at the global energy mix, the overall contribution of renewable energy and biomass derived energy/fuels in particular. Both renewable and non-renewable energy sources are considered to provide context to the scale of biomass-based energy technologies.

1.1.1 Trends in the global energy mix

The composition of the energy mix varies from one country to another. To meet it's energy demands, each country uses the energy available to it, in different proportions. Since the industrial revolution, development has been largely driven by fossil fuels. Over the last few decades, 81% of the primary energy consumed worldwide came from fossil fuels: 31% oil, 29% coal, which predominated in global electricity generation, and 21% natural gas. The world energy demand is governed by the developing countries such as India, China and Brazil because of their demographic growth and the expansion of emerging economies that led to increased energy demand. Developed countries struggle with stagnant economies and high oil prices resulting in stable or decreasing energy consumption [1]. The total global energy consumption from all sources is expected to increase further in the next decade. The issues of energy security, greenhouse gas emissions, environment pollution, climate change, and sustained high world oil prices expanded the use of non-fossil renewable energy sources. Renewable energy sources could be trapped for hundreds of years and produces little or no waste products such as carbon dioxide or other chemical pollutants, so has minimal impact on the environment. Hence, in many countries the government policies and incentives want to see a mix of energy from renewable and non-renewable sources. A mix of sources increases the reliability of the energy supply, and brings economic benefits to many regional areas, as most renewable energy projects are located away from large urban centres and suburbs of the capital cities. According to IEO2016, in 2040, fossil fuels will account for nearly 78% of total world energy consumption.

Petroleum and other liquid fuels remain the largest source of energy, although their share of total world marketed energy consumption increased from 90 million

barrels per day (b/d) in 2012 to 100 million b/d in 2020 and 121 million b/d in 2040 [2]. Worldwide, demand for liquid fuels has increased as a result of huge expansion in transportation and industrial sectors which resulted in increased greenhouse gas emissions [3]. The decline in the use of liquid fuels in residential and power sectors results from rising world oil prices, which led to look for diversify liquid fuel source. In addition to economics, technological status, and potential supply, sustainable development of alternative liquid fuels should take environmental and social concerns into consideration. Alternative liquid fuels include biomass based biofuels which contribute less greenhouse gas emission than gasoline and needs to be part of the strategy to reduce greenhouse gas emissions while improving energy security. Hence, renewable resources such as biomass based alternative liquid fuels and chemicals have drawn much attention.

1.1.1.1 Renewable liquid fuels from lignocellulosic biomass

Liquid biofuels are one of the most exciting emerging areas of bioenergy, as they can be used as substitute for petroleum based fuels to resolve the demanding consumption of fossil fuels. The most common liquid biofuel is bioethanol, which is used as a gasoline substitute and biodiesel, which is used as a diesel substitute. Bio oils, which are the product of biomass pyrolysis, can be used to replace diesel or bunker oil in marine-type engines or industrial scale boilers.

Biomass and biomass derived materials are one of the most promising alternatives for renewable fuels and chemicals. Until the last millennium, when non-renewable liquid fuel and other energy security-based issues surfaced, bio-ethanol has found a new dimension, as an alternate biofuel or fuel additive as oxygenate. It was clearly understood that, to make bio-ethanol as a fuel additive or alternate fuel from food

grade materials has become a controversial topic because in the current world, there are several million people who do not get sufficient food. Therefore bio-ethanol from lignocellulosic biomass turned out to be a promising answer, against all scientific and socio-political debates. On the other hand, market wise, it encountered crucial competition with existing fossil fuels, as well as sugar or starch derived ethanol. However, complex structure of lignocellulosic biomass makes it resistant to enzymatic and chemical degradation and deconstruction of lignocellulosic matrix is an expensive procedure with respect to cost and energy [4]. Hence, to make cost-competitive lignocellulosic ethanol, it was essential to develop biorefinery and biofuel technologies to produce renewable liquid fuel and green chemicals.

1.2 Lignocellulosic biomass

Lignocellulosic biomass (LCB) refers to plant biomass, which is predominately composed of cellulose, hemicellulose, and lignin. In real, these polymers are organized into complex non-uniform three-dimensional structures to different degrees and it's complex structure and composition varies depending on the species and environmental conditions [5]. LCB is increasingly recognized as a valuable commodity, since lignocellulosic biomass refinery is analogous to petroleum refinery. The structure and compositions of LCB affect the hydrolysis of polysaccharides; therefore, understanding each component is important to efficiently utilize lignocellulosic biomass.

There are various forms of LCB resources in the world, which can be grouped into four categories, i.e., agricultural residues, forestry residues, energy crops and bio wastes [6]. The global production of plant biomass, of which over 90% is lignocellulose, amounts to about 200×10^9 tons/year, where about $8 - 20 \times 10^9$ tons of the primary biomass remains potentially accessible [6]. Lignocellulosic biomass, which is the most

abundant, bio-renewable and is available worldwide, represents a promising option for ethanol production considering their output /input energy ratio, low cost and higher ethanol yield. Furthermore, LCB holds enormous potential for sustainable production of chemicals and materials.

About one-third of biofuel production cost is associated with LCB cost. Its cost is directly proportional to the yield (ton per hectare) [7]. LCB in the form of agricultural and forestry residues are natural renewable resources. Use of agricultural residues for biorefinery is good for huge amounts of wastes that do not find any alternative use and are either left in the fields or are burned. However, from the economic point of view, LCB derived from energy crops, can be produced quickly, uses arid land and lower in cost that makes them promising renewable source for the production of liquid fuels, chemicals and bio-based materials.

One of the most important barriers in increased biomass utilization is the cost of the respective supply chain. A typical biomass supply chain includes several discrete processing steps which are (i) harvesting/collection of the biomass in the field/forest, (ii) in-field/forest handling and transport to move the biomass to a point where road transport vehicles can be used, (iii) storage, (iv) pre-processing (densification by increasing the bulk density), (v) transportation (biomass to biorefinery) and (vi) post-processing at the biorefinery [8].

Owing to the voluminous nature of the resource, low bulk density, moisture content are major challenges for transportation and storage of lignocellulosic biomass [9]. Again it's handling becomes a major issue since it requires bigger modes of logistics along with employment of a larger number of work-force. Therefore, lignocellulosic biorefinery need a strong backup and government support so that such an idea could go a

long way in strengthening the biomass supply chain, promotion of associated clean energy technologies and in making a significant dent in the present fuel scenario in the developing world.

1.2.1 Structural features of lignocellulosic biomass

LCB is mainly composed of three components; cellulose, hemicellulose and lignin together with smaller amount of pectins, proteins, extractives, and several inorganic materials. Also, the composition of these constituents varies in the same plant species depending on age, stage of growth, and other conditions. The polysaccharides (cellulose and hemicellulose) and lignin mainly present in cell walls of woody tissue and grasses. The cellulose fibrils are embedded in a network of hemicellulose and lignin. The recalcitrance of LCB comes from the crystallinity of cellulose, hydrophobicity of lignin, and encapsulation of cellulose by the lignin-hemicellulose matrix [10]. This results in the elimination of water from the cell wall and limits the accessibility of hydrolytic enzymes.

1.2.1.1 Cellulose

The primary building material of lignocellulosic biomass is cellulose. Cellulose is a very important polysaccharide because it is the most abundant organic compound on earth. Cellulose has a unique structure because it contains unbranched chains of β-(1→4)-D-glucopyranose units in $^{4}C_{1}$ conformation. Each glucose unit is rotated 180^{o} with respect to its neighbor, and the resulting disaccharide called cellobiose. The repeating unit of the cellulose chain is the disaccharide cellobiose and long-cellulose chains are arranged parallel to each other and are joined together using hydrogen bonds to form microfibrils. Extensive intra-molecular and inter-molecular hydrogen bonding networks are present in cellulose, which tightly binds the glucose units and makes cellulose a

relative stable polymer, and gives the cellulose fibrils high tensile strength. Cellulose is a water insoluble polymer. The chemical structure of cellulose was presented in Fig 1-1.

Cellulose is capable of forming number of crystal structures or allomorphs. These are cellulose I, II, III and IV [11, 12]. Cellulose I, or native cellulose, is the form found in nature. It occurs as metastable partially-crystalline microfibrils. Cellulose I, contain sheets of parallel hydrogen bonded chains that are stacked on top of each other through hydrophobic interactions. Native cellulose possesses mixtures of two different crystalline polymorphs designated cellulose I_β and I_α. These two crystal phases always coexist with each other in various proportions depending on the cellulose structure. Cellulose I_β is the dominant polymorph in higher plants (wood, cotton etc.) and tunicate (cellulose in tunicate animals). Cellulose from algae and microbes (bacterial cellulose) contains the predominant form of I_α. I_β form is more stable than I_α (metastable), because I_α can be irreversibly converted to I_β through annealing [13].

Depending on the application, raw cellulosic material is pretreated or processed to transform cellulose I to another crystal phase. Through the processes of dissolving the cellulose/regeneration and mercerization with alkali, cellulose I can be converted into a stable crystalline form, cellulose II. Cellulose II cannot be reconverted to cellulose I. Cellulose II contains two anti-parallel chains in the unit cell results in less intra-molecular and more inter-molecular hydrogen bonding as compared to cellulose I. Processing of cellulose I and cellulose II with ammonia or with certain amines such as ethylene diamine (EDA) yield cellulose III_I and cellulose III_{II} respectively. Cellulose III_I phase contains one chain in the unit cell [14,15]. The structure of cellulose III_{II} has not yet been reported. Treatment of cellulose III_I and cellulose III_{II} with glycerol at high temperature allows the preparation of cellulose IV_I and IV_{II} respectively. Credible proof that cellulose IV_I is not a genuine allomorph and it is generally accepted that cellulose

IV_I is a disordered form of cellulose I_β [16,17]. Inter-conversion of polymorph of cellulose was presented in Fig 1-2 [11].

Horikawa et al. studied the digestibility of cellulose I, II, $IIII_I$ and amorphous cellulose substrate as a substrate for enzymatic hydrolysis. They concluded that cellulose $IIII_I$ is more amenable to enzymatic hydrolysis than cellulose II hydrate because cellulose II changed to highly crystalline structure during saccharification. Further cellulose II hydrate is more digestible than cellulose I [18]. Wada et al. studied the enzymatic hydrolysis of cellulose I, cellulose II hydrate, and cellulose II. They reported that cellulose II hydrate showed faster hydrolysis rate than the hydrolysis of the other two substrates because cellulose II hydrate is an inflated structure with low density. The saccharification ratio of cellulose II was only slightly higher than that of cellulose I [19]. Thus, it can be concluded that order of saccharification efficiency of cellulose polymorph is: amorphous cellulose substrate > cellulose $IIII_I$ > cellulose II hydrate > cellulose II > cellulose I.

1.2.1.2 Hemicellulose

Hemicellulose is the second most natural abundant polysaccharide after cellulose. The “hemicellulose” term is used for heteropolymers (matrix polysaccharides) that normally occur in lignocellulosic biomass together with cellulose. In the plant cell walls hemicelluloses form a complex network of bonds that gives the best combination of mechanical support and transport properties by linking cellulose fibres into microfibrils and cross-linking with lignin [20, 21].The hemicellulose is located primarily in cell walls of plant cell and consists of different monomers (D-xylose, D-mannose, D-galactose, D-glucose, L-arabinose, D-glucuronic acid, D-galacturonic acid, α-D-4-O-methylglucuronic acid) and also some oxidation products, as for example, acetates. Most

hemicelluloses contain two to six of these sugars [22]. Unlike cellulose, hemicellulose has branched and amorphous structure. The structure and composition of hemicellulose depends on the plant type (especially hardwoods, softwoods and grasses) [23].

Usually hemicelluloses are classified according to the main sugar residues in the backbone. In seaweeds (red and green algae) only homopolymers of xylose, so-called homoxylans are present. Hemicellulose of hardwoods consist of *O*-acetyl-4-*O*-methylglucuronoxylans, is substituted at irregular interval with 4-*O*-methyl-α-D -glucuronic acid groups joined to xylose by α-1,2-glycosidic linkages, whereas *O*-acetyl galactoglucomannan mainly present in softwoods [24]. The annual plants such as grass, herbs and cereal straws contain generally more structurally diverse and complex hemicellulose. Hemicelluloses from annual plants contains β-D- xylopyranosyl main chain that can be heavily branched with Xylp - (xylopyranose), Araf- (furanose), Galp – (galactopyranose) mono-, di- and trisaccharide side chains. Acidic and neutral nature of the annual plant hemicellulose depends on whether they contain 4-*O*-methyl-D-glucuronopyranosyl or D-glucuronopyranosyl substituent. In these annual plant hemicelluloses are xylose and arabinose are two predominant monosaccharides and hence they are termed as arabinoxylans [25]. Different structures of hemicelluloses are shown in Fig 1-3 (a), Fig1-3(b) and Fig1-3 (c).

1.2.1.3 Lignin

Lignin is a hydrophobic “cementing” and insulating agent of plant cell walls. After carbohydrates, lignin is another nature’s dominant source of aromatic polymer [26, 27]. Lignin is an amorphous and an aromatic complex polymer of monolignols (aromatic alcohols) also referred as phenylpropane. Lignin structure predominantly constitutes of three different phenylpropane units such as p-coumaryl alcohol, coniferyl alcohol, and

sinapyl alcohol. These monolignols are incorporated into lignin polymer in the form of the *p*-hydroxyphenyl (H), guaiacyl (G), and syringyl (S), respectively [28]. The phenylpropanoid units, present in lignin are connected by both ether and carbon-carbon bonds. Depending on the source of lignocellulosic biomass the relative proportion of H, G and S-lignin's varies [29]. It has been observed that softwood lignins are mostly composed of G units and containing small amount of H units. Hardwood lignins usually contains G and S monolignols with trace amounts of H units, and herbaceous plants contain significant amounts of all three G, S, and H lignins but in different ratios [30]. Structure of the monolignols from which lignin is synthesised are shown in Fig 1-4 (a) and Fig 1-4 (b) represents schematic structural formula for lignin and the major inter unit linkages.

In LCB, lignin content, structure, subunits, and linkages with polysaccharides own their remarkable importance to cell wall recalcitrance. It also affects the transport of water, nutrients and metabolites and plays an important role in plant cell development. Lignin builds the complex structure of lignocellulose which protects the plants from the pathogen and insect attacks [31].

1.2.1.4 Other constituents of lignocellulosic biomass

LCB also contains smaller amounts of some other substances such as pectin, extractives, proteins, and ashes. Pectins are complex mixture of polysaccharides, and are rich in galacturonicacid. Structural types of pectins are Homogalacturonan, Rhamnogalacturonan I, Rhamnogalacturonan II [32]. Their composition and structure varies with the source and conditions of extraction, location, and other environmental factors. They are present in most primary cell walls and are particularly abundant in the non-woody parts of terrestrial plants. The highest concentrations of pectin are found in

the middle lamella of cell wall, where it helps in cell adhesion and wall hydration. Their crosslinking also influences wall porosity and plant morphogenesis [33].

LCB extractives are low-molecular-weight compounds; include resin (terpenes, lignans and other aromatics), fats, waxes, fatty acids, alcohols, steroids and higher hydrocarbons etc. These materials are chemically polar and non-polar in nature. They give color, odor and also protect plants from termites and microorganisms. Extractives content and composition varies among plant species, geographical site, season, and growing age. In plants they are mostly found in resin canals, the ray parenchyma cells, lower amounts present in the middle lamellae, intercellular and cell walls of tracheids and libriform fibers [34]. The functions of extractives are diverse, and functions of many extractives have not been completely understood, some are involved in plant protection, some are precursors of certain chemicals [35, 36].

Ash content of LCB is the mass fraction of incombustible material left after complete burning process in air, consisting mainly inorganic materials present in biomass. The most abundant elements present in biomass ash are Al, Ca, Fe, Mg, P, K, Si, Na and Ti [34].

1.2.1.5 Chemical interaction between carbohydrate and lignin

Lignocellulosic biomass recalcitrance is a major obstacle to achieve sustainable production of biofuels and chemicals. It arises mainly from the cellulose structure and amorphous cell-wall matrix containing lignin and hemicellulose assembled into a complex supramolecular network that coats the cellulose fibrils. Mainly four interpolymer (in between different components) and intrapolymer linkages such as ether, ester, carbon-carbon, and hydrogen bonds are identified among these three components [37].

Cellulose polymers are made up of two main linkages i.e., ether and hydrogen bonds. Glycosidic bonds of cellulose can be considered as ether bonds, as they connect two carbon atoms with an oxygen molecule. Hydrogen bonds form between two hydroxyl groups of different cellulose polymer chains. In hemicellulose, mostly ether and ester bonds are present whereas monomer of lignin contains ether and carbon – carbon bond [38].

Cellulosic glucan chains at the surface of the cellulose microfibrils can co-crystallize with hemicelluloses through the formation of hydrogen bonds from the – CH_2OH groups present in cellulose chains to the Glycosidic oxygens in the adjacent hemicellulose chains. This association would form a tightly bound monolayer of the hemicellulose on the surface of the cellulose microfibril, and would function as part of the 'glue' which holds the microfibrils together in the cell wall. Lignin is connected to hemicellulose via ester and ether bonds. Still bonding of lignin with polysaccharides is not yet conclusively defined [39, 40]. In addition, chemical structure of plant cell walls may vary depending on which tissue of the plant they belong to (e.g., leaves, stems, young or old tissue), environmental stress condition experienced by the plant during growth (e.g., drought, disease, mechanical stress by wind etc.) [41]. Fig 1- 4 (c) presents grass lignin-carbohydrate complexes involving ferulic acid [42,43].

1.3 Bioethanol

Bioethanol is currently produced from sugars, starchs and lignocellulosic biomass (wood, straw, and even household wastes) through alcoholic fermentation. Simple sugars produced from LCB by pretreatment followed by enzymatic hydrolysis process results in bioethanol. Lignocellulosic ethanol is expected to be commercialized during the next decade and partly replace the first generation ethanol. The importance of lignocellulosic ethanol is evident as it only requires inexpensive cellulosic biomass as feedstock, which

is abundantly and easily available throughout the world. Consequently, this also avoids food versus fuel competition and decrease the environmental risks i.e., soil degradation and water and air pollution which are associated with first generation biofuels [44, 45].

1.3.1 Applications of bioethanol

Bioethanol is a liquid biofuel, which is a petrol additive/substitute. Ethanol blended with petrol as E10 ("E" numbers represents the percentage of ethanol fuel in the ethanol – gasoline mixture by volume) or less are used in more than 20 countries around the world, led by the United States, where ethanol represented 10% of the U.S. gasoline fuel supply in 2011 [46]. Since late 1970s, blends from E20 to E25 have been used in Brazil. U.S. and Europe commonly used E85 for flexible-fuel vehicles. Hydrous ethanol or E100 is used in Brazilian neat ethanol vehicles and flex-fuel light vehicles and hydrous E15 for modern petrol cars in the Netherlands [47].

Bioethanol is a high octane fuel, it has broader flammability limits, higher flame speeds and higher heats of vaporization than gasoline. Combustion of bioethanol results in cleaner emissions (carbon dioxide, steam and heat) and could be a carbon neutral fuel source. The disadvantages of bioethanol include its lower energy density than gasoline, its corrosiveness, low flame luminosity, low vapor pressure, miscibility with water, and toxicity to ecosystems [48].

Bioethanol finds wide variety of applications, apart from its use as fuel. Its other uses are solvent in liquor industry, personal care industry (i.e., pharmaceutical, toiletry, perfumery and fragrance industries), manufacture of chemicals such as ethyl acrylate and ethyl acetate, and manufacture of solvent based paints, printing inks, lacquer thinners etc.

1.3.2 Research challenges in ethanol production from lignocellulosic biomass

Advantages of cellulosic ethanol (CE) have been widely reported. The stages to produce CE using the biochemical approaches are: pretreatments, enzymatic hydrolysis, microbial fermentation of the sugars, distillation, and dehydration. Costs of ethanol and process energy used for large scale production of cellulosic ethanol are dependent on technologies used for conversion of feedstock [49]. However, pretreatment of LCB has pervasive impacts on all other major steps in the overall biochemical conversion from choice of feedstock to size reduction, enzymatic hydrolysis, fermentation, product recovery, residue processing, and co-product potential [50]. Pretreatment of LCB include deconstructing the lignocellulosic structure to decrease crystallinity of cellulose, increase biomass surface area, remove hemicellulose, break the lignin barrier, minimizing the formation of inhibitors for subsequent fermentation steps and lignin recovery for conversion into valuable co-products. Pretreatments include physical, chemical, thermal and biological methods, and their combinations. Pretreatment is one of the most expensive processing steps for the production of ethanol from lignocellulosic biomass [51]. Hence, pretreatment process is a major bottleneck in cellulosic ethanol production and commercialization. Also, lignocellulosic ethanol technologies include other bottlenecks such as enzymatic saccharification of the pretreated biomass, and fermentation of the hexose and pentose sugars released by hydrolysis and saccharification.

Therefore, extensive research is needed on optimization and study of parameters of pretreatment technologies to develop new pretreatment technologies in a cost effective

manner for enhanced production of cellulosic ethanol. Also other problems require substantial R&D efforts for improved efficiency and process economics.

1.3.3 Importance and options of bio-ethanol in India

India's growing population and economy generated an increasing demand for energy. Crude oil has been the major source to meet the energy demand, and its demand increases dramatically every year. India imports nearly 70% of its annual crude petroleum requirement, which is approximately 110 million tons. The prices are in the range of US$ 50-70 per barrel, and the expenditure on crude purchase is in the range of 1600 billion per year. Hence, any fluctuation in price or any problems in the global oil market would affect continuous supply, which would hit India's economy very hard [52]. In addition to this, the fast depleting global petroleum resources and the risk of climate change, forcing the Indian government and energy industry to consider long-term expansion of alternative fuels, especially liquid transportation fuels in order to increase energy security. Bioethanol from lignocellulosic biomass is one of the important alternatives being considered due to the easy adaptability of this fuel to existing engines and has the potential to contribute in creating a clean environment [53].

Now in India, the current share of bioethanol in the consumption of gasoline is extremely low. In the first phase of the project, blending of ethanol in gasoline was 5% and the government had made it mandatory in nine states and four Union Territories. These states are Andhra Pradesh, Goa, Gujarat, Haryana, Karnataka, Maharashtra, Punjab, Tamil Nadu and Uttar Pradesh. The four Union Territories include Chandigarh, Dadra and Nagar Haveli, Daman and Diu and Pondicherry [52]. The blending targets for ethanol in gasoline was proposed as 10% by 2011-2012, however not fully implemented yet [54].

Indian distilleries use molasses as the feedstock for ethanol production. Presently, Indian sugar industries are producing approximately 2.7 billion liters of ethanol per year and out of this, only a minor share is available for fuel use and its production cost is higher than oil-derived gasoline [55]. The government's decision for mandatory blending of ethanol in automotive fuels would mean that to look for alternative feedstocks such as lignocellulosic biomass for making ethanol to meet the requirements economically and would not create food verses feed disputes [56].

1.3.4 The future perspectives of lignocellulosic ethanol in India

The main issues to be addressed for lignocellulosic ethanol production process involve feedstock availability, its variability, sustainability and the transformation of the feedstock into the ethanol. Though, the generation of lignocellulosic biomass residues in India from agriculture is considerably large [57], but the actual availability of a major share of these residues for bioethanol production is questionable. Again there is a direct competition for land between food crops and natural vegetation with feedstocks used for the production of bioethanol such as maize, sugarcane stand, Miscanthus etc. Thus, the feedstock selection and comprehensive relation between policies (such as bioethanol usage) and land-use activities such as human settlement, bioethanol production, food production as well as the resulting effects on the spatial extent of natural land needs careful planning for future lignocellulosic ethanol production [54]. Also, the technologies for lignocellulosic ethanol production are under various stages of development which needs extensive R&D in this field to overcome technical and economical hurdles, along with the environmental benefits. This would make the lignocellulosic ethanol program successful at commercial scale [58].

1.4 The source, availability and production of lignocellulosic biomass in India

Among renewable energy sources only lignocellulosic biomass can be used to produce heat, electricity and fuel in a form and scale that is compatible with existing transportation and power generation infrastructure. It also can be used to produce chemicals and materials. In rural areas lignocellulosic biomass plays a very important role as it comprises the major energy source to majority of households in India. In India, 32% of the total primary energy use still comes from biomass and more than 70 % of the population depends on it for energy needs. LCB has the potential to give significant employment in the rural areas [59].

The availability of major amount of LCB in India is from agriculture as many states in India have an agricultural-based economy. The overview of report shows that although India has a considerable amount of area under forest cover but majority of it comes under Govt. protection policy and thus, forest biomass was shown as nil. Again other fraction of LCB in India comes from solid waste residue, timber industry, self-owned sources like farm trees, grasses in unused lands etc. [60]. Therefore, lignocellulosic biomass including agricultural residues, wood and grasses etc. is available in vast quantities in India.

However, in India still LCB is not the preferred renewable energy source for biofuel production because of the following challenges involved in ensuring reliable LCB supply chain: (I) fluctuation in availability of LCB round the year depends on cropping patterns, (II) absence of organized formal biomass markets, (III) lack of robust business model for management of biomass collection, transportation, processing and

storage. Another major challenge is the cost of biomass storage and transportation to biorefinery, which is consistently rising with time [61].

In order to get constant supply of LCB throughout the year, industrial biomass can be grown from numerous types of plants including miscanthus, bamboo, napier grass, and a variety of tree species, ranging from eucalyptus to oil palm (palm oil) that can be grown on marginal and degraded lands. The particular plant used is usually not important to the end products, but it does affect the processing of the raw material.

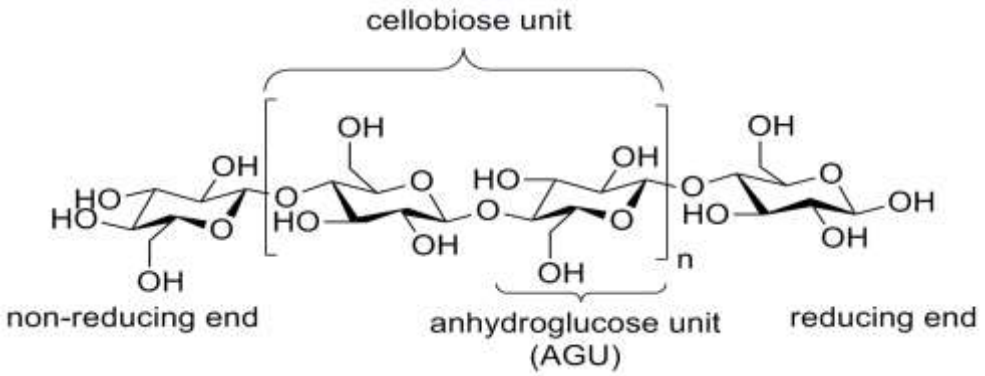

Fig 1-1: Schematic representation of the cellulose chain

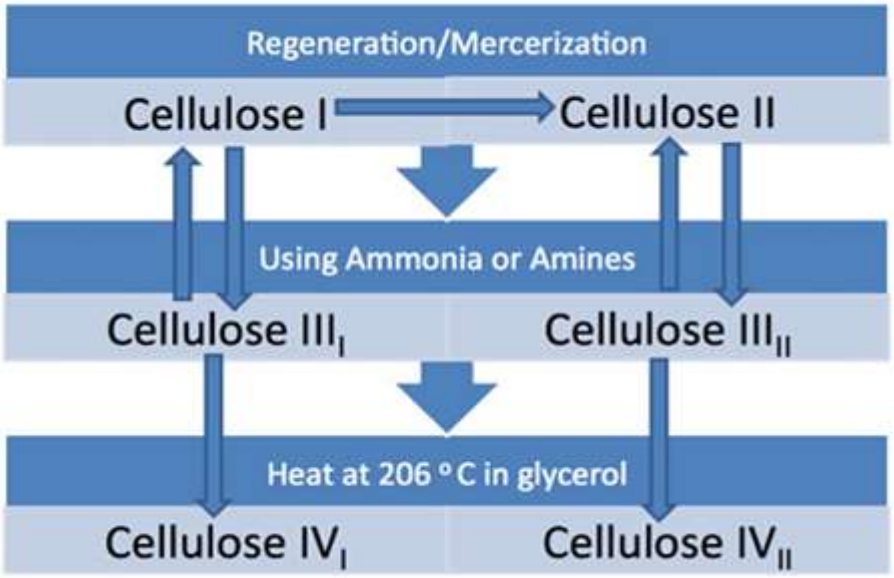

Fig 1-2: Interconversion of polymorphs of cellulose. Cellulose I, is native or natural source of cellulose. Cellulose II obtained from cellulose I by solubilisation in a solvent followd by regeneration with antisolvent. Or by mercerisation, which involves the swelling of native cellulose fibres in concentrated sodium hydroxide upon removal swelling agent. Cellulose III $_I$ and III $_{II}$ are formed by treatment with amonia or amines from celluloses I and II, respectvily. Polymorphs IV $_I$ and IV $_{II}$ are derived from III $_I$ and III $_{II}$ respectvily by heating to 206 ^oC in glycerol (Adapted from O'Sullivan et al. [11])

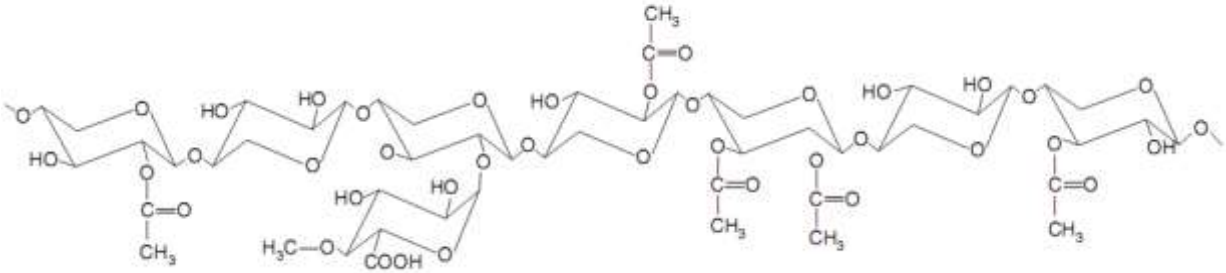

Fig 1-3 (a): Structure of *O*-acetyl-(4-*O*-Me-glucurono) xylan from hardwood

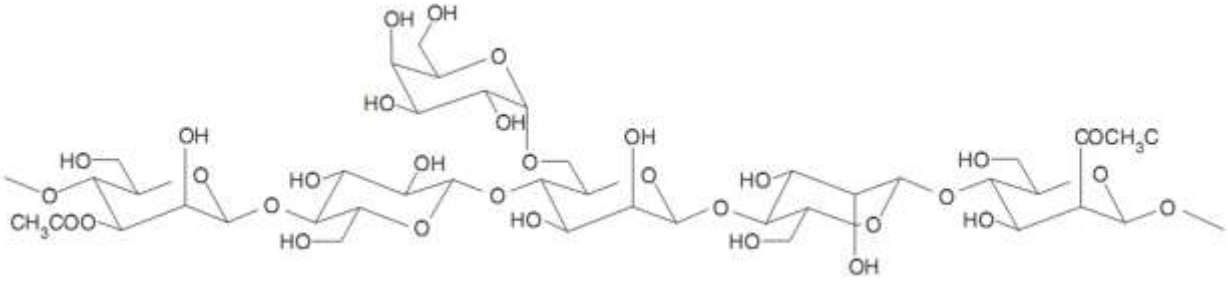

Fig1-3 (b): Structure of *O*-acetyl-galactoglucomannan

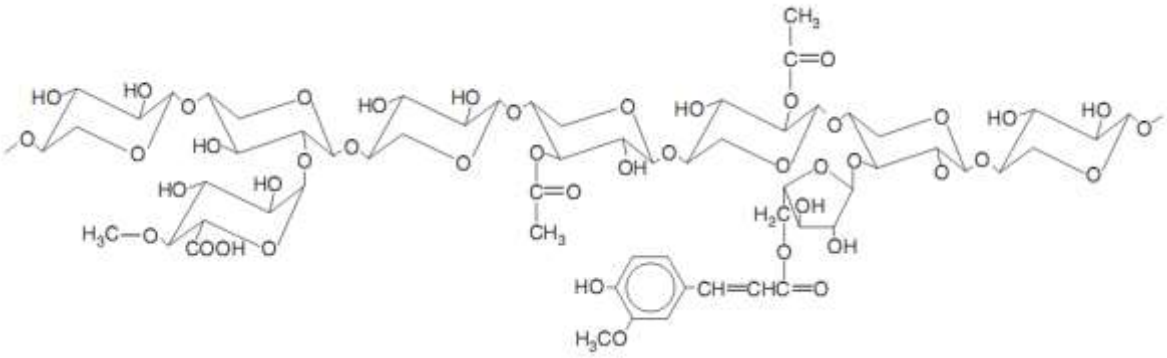

Fig1-3 (c): Structure of xylan from annual plants

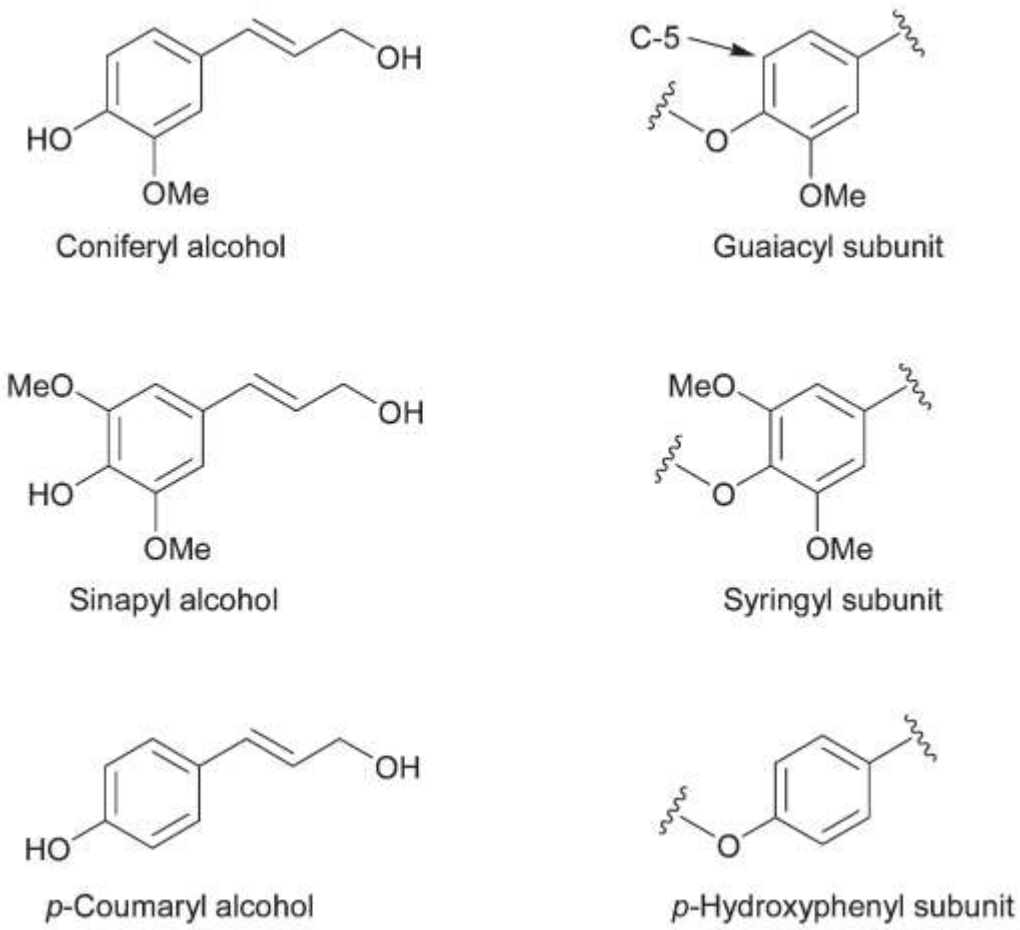

Fig 1-4 (a): Structure of the monolignols from which lignin is synthesised. The monomers vary in the substitution at the C-3 and C-5 positions

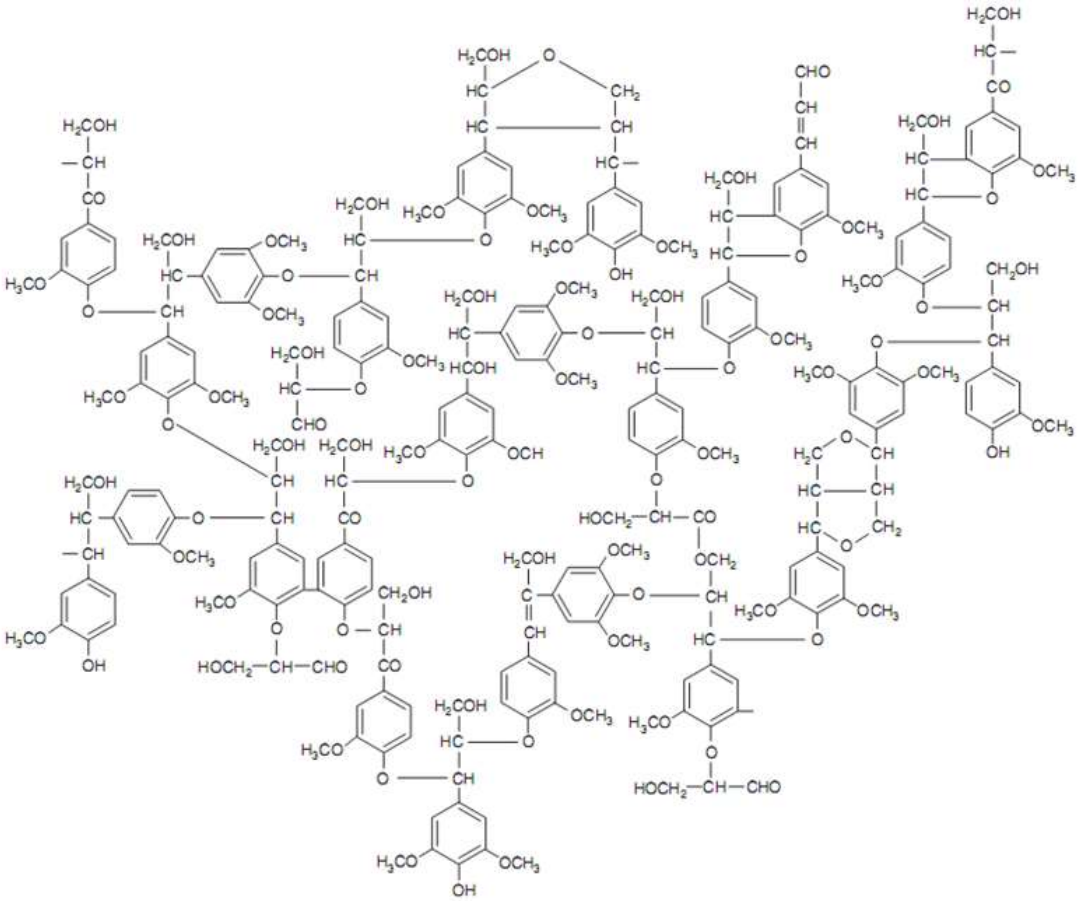

Fig 1-4 (b): Schematic structural formula for lignin. The structure illustrates the major inter unit linkages

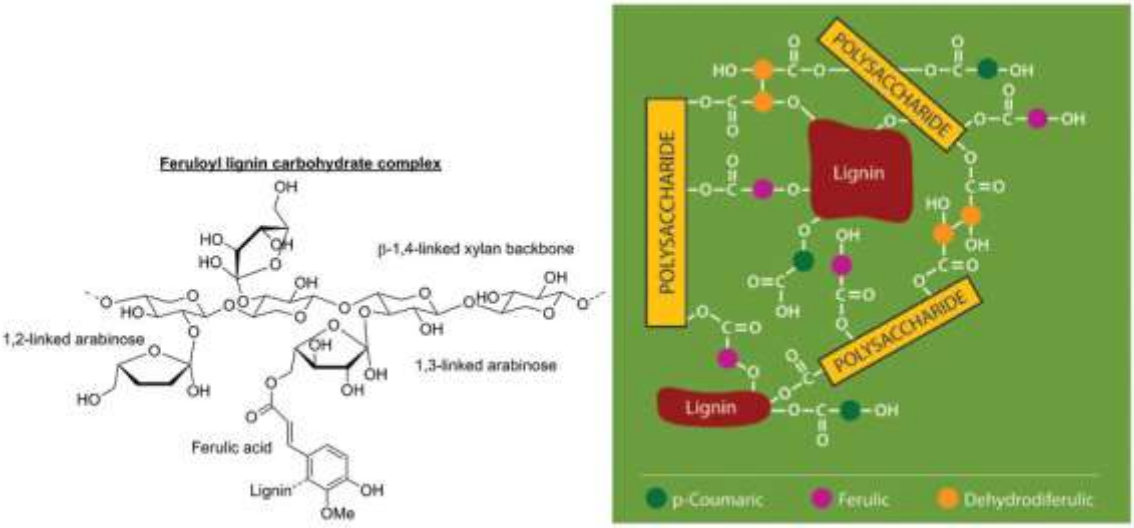

Fig 1-4 (c): Grass lignin-carbohydrate complexes involving ferulic acid (left). The network that is formed, mediated by ferulic acid, is explained on the right (Adapted from Houghton et al. [42])

2 LITERATURE REVIEW AND OBJECTIVES

2.1 Analysis of lignocellulosic biomass in India and selection of suitable feedstock for bioethanol production

For commercial cellulosic ethanol production in India, sufficient lignocellulosic biomass supply is a key factor. In India lignocellulosic biomass are available in different form and potential feedstock includes agricultural residues (crop straws and bagasse), herbaceous crops (grasses, bamboos), short rotation woody plants, forestry residues, waste paper and other wastes (municipal and industrial) [62]. Agriculture has a significant role in the India's economy. About 500 million tons of crop residues are generated out of total agriculture produce per year, and are generally used for animal feed, livestock bedding, packaging material, used as direct fuel for cooking in households, sold to the paper industry, etc. or burned in the farms after harvesting [63]. As a result, currently limited amount of agricultural residues may be available and its potential towards national bioethanol demand need to be calculated [64]. Zone wise distribution of available agro-feedstocks is shown in Table 2-1 [62]. About 23% of India's land is also covered by forest [63]. Large amount of forestry waste and other agro industrial wastes are readily available in India and are potential source for cellulosic ethanol. However, their availability for cellulosic ethanol needs to be looked carefully. The graduated spread of bioethnol all over India demands exploration of other biomass sources in the near future. As a result, besides forestry waste and other agro industrial wastes, herbaceous crops are being identified as a potential source. Herbaceous crops

including bamboo, Miscanthus, and softwood including reed, pine, which are mostly present in North-East India and Himalayan forest can serve as potential feedstock for ethanol [65].

Miscanthus is a C4 grass genus of 20 species originates in subtropical and tropical regions of Africa and southern Asia, with one species *(M. sinensis*) extending north into temperate eastern Asia. Miscanthus is a perennial, tall grass with C4 photo-synthesis and native to the East Asian region including Korea, China, and Japan, North-East region of India. It is an ideal bioenergy crop as it can grow in marginal land and has high biomass yield potential, with long sustainable productivity up to more than 15 years after the first establishment, and high carbon sequestration capacity [66]. Miscanthus is cultivated in southern India, whereas it grows wild in North-East India. Miscanthus can adapt to several different habitats, but easily grow at moist, well-drained soil in full sun to part shade and it has tall reed- or cane-like plants, usually 1-2 meters. Miscanthus is commonly used as an ornamental plant in United States and is used for dyeing. In India, people use it as cattle feed which dramatically boosts milk production. In England and United States, Miscanthus is cultivated and used as a biomass fuel or fibre source. Dry Miscanthus of twenty tons is equal to 12 tons of coal; and 30 tons are equal to 12,000 liters of oil [67, 68]. Miscanthus has several advantages for energy production, such as high yield, excellent carbon sequestration and soil building along with low mineral content. All these make it a good choice for potential energy crop. Hence, cultivation of this crop in land which are not suitable for food crops or any other valuable crops will boost the rural economy of North-East India and helps to stabilize India's energy security.

Castor plant (Ricinus communis) is a plant species of the spurge family, Euphorbiaceae and belongs to genus *Ricinu*s. It is native to the south-eastern

Mediterranean Basin, Eastern Africa, and India, but now it extend to all tropical and sub-tropical countries. It is a fast growing annual biennial or perennial plant, which can reach size of small tree. It can be grown on a wide range of soils especially in semi-arid and arid regions. In India Castor plant leaf, root and seed oil are used for medicinal purpose. In the silk producing regions of North-East India, castor leaves are fed to Muga and Eri/Endi silkworm larvae till they get into the chrysalis stage. Castor seed oil is also a very good source for biodiesel production. Hence, in India, it is cultivated throughout the country in gardens, fields and in waste places, which has mainly two varieties such as red stem castor plant and green stem castor plant [69, 70, 71]. It was observed that the Castor plant stem remain unused, which makes it as a choice for energy crop for biomass fuel through thermochemical or biochemical conversion process.

Jatropha (Jatropha curcas) belongs to the genus Jatropha in spurge family, Euphorbiaceae, that is indigenous to the American tropics, most likely Mexico and Central America, but now this is cultivated worldwide. It is a drought resistant, perennial plant that has excellent adoption capacity to a large variety of soil condition, whereas it prefers arid and semi-arid environments. This plant grows even in the soils with very low fertility and low nutrient content. *Jatropha curcas* is shrub or small to medium tree and can reach a height of 3 to 5 meters; however, in favourable condition it can reach even 8-10 feet height. It grows relatively quickly. This plant is widely found in most of the regions of India and it is cultivated in many states including North-East India. The chemicals produced from Jatropha seed oil, latex, leaves have various medicinal and pharmaceutical applications. Apart from this, it's seed oil is the major source for biodiesel. It is a substitute of fossil fuel and it's suitability for waste land cultivation makes it a good source for CO_2 capture. It's wood remain unused, which can be used as biomass fuel production through thermal or biochemical conversion process. In this way,

this source can be used in a more productive way, which will enhance the energy security for the country [72].

2.2 Overview on biochemical conversion of lignocellulosic biomass to fermentable sugar for bioethanol production

Second-generation ethanol productions from various lignocellulosic materials are considered as potential source to obtain ethanol as a fuel. Biochemical conversion route for ethanol production from lignocellulosic biomass comprises of four major unit operations: (1) pretreatment, (2) formation and detoxification of inhibitors (3) hydrolysis, (4) fermentation, and (5) product separation/distillation [73]. Pretreatment is mainly used to deconstruct the recalcitrant structure of lignocellulosic biomass and increase surface area to optimize cellulose accessibility to cellulase enzyme [74]. There are several pretreatment technologies available, depending on the pretreatment method selected, will solubilize, hydrolyze and separate cellulose, hemicellulose, and lignin components [75]. Effective pretreatment is essential for optimal successful hydrolysis and downstream operations [76]. Therefore, pretreatment of biomass is the focus of this thesis and will be reviewed in more detail under a separate section.

The pretreatment process highly affects the hydrolysis step [77]. During this hydrolysis reaction, cellulosic materials and hemicelluloses are hydrolysed into monomeric free sugars available for fermentation to produce ethanol [78]. The pretreated feedstock can be hydrolyzed by two different methods that involve either acidic hydrolysis or enzymatic hydrolysis. The acidic hydrolysis technology divided into two categories i.e. dilute acid hydrolysis and concentrated acid hydrolysis. Dilute acid hydrolysis requires high temperature, high pressure and produces inhibitors such as furfural and 5-hydroxymethyl-furfural (HMF) for fermentation [79]. On the other side,

concentrated acid hydrolysis requires low temperature and pressure, produces higher amount of free sugars and lower concentrations of inhibitors [80]. The enzymatic hydrolysis is catalyzed by cellulolytic enzymes and is carried out under mild conditions. Except comminution, unlike acid hydrolysis pretreatment is needed to increase the rate of enzymatic hydrolysis. Moreover, enzymatic hydrolysis is much slower than acidic hydrolysis but several inhibitory compounds are formed during acid hydrolysis and acids are associated with greater environmental liabilities [81]. The saccharification of LCB will be described in detail under a separate section.

The inhibitors for enzymatic hydrolysis and microorganisms for ethanol production are generated during acid hydrolysis or pretreatment of lignocellulosic biomass. The type and content of inhibitors in hydrolysate or pretreated slurries, depends on the feedstock and the pretreatment processes such as acidic, alkaline etc. [82]. The inhibitors of enzymatic hydrolysis and microorganisms for ethanol production includes furans (furfurals and 5-Hydroxy methyl furfural (5-HMF)), phenolic compounds, weak acids (acetic acid, levulinic acid, formic acid etc.), raw material extractives (acidic resins, tannic and terpene acids), heavy metal ions (iron, chromium, nickel and copper), and bio-alcohols or other fermentation products [83]. However, among soluble sugars, furan derivatives, and organic acids, phenolics are much more inhibitory for enzymatic hydrolysis as phenolics can lead to precipitation and irreversible inhibition of enzymes [84,85]. Acidic inhibitors (aromatics, aliphatic acids) and raw material extractives mostly inhibit the growth and metabolism by allowing the higher permeation of cell membrane in microorganisms [86,87,88] whereas furans and phenolic compounds have more inhibition degree of severity on fermenting microorganisms [76].

There are several different approaches which can be considered to reduce the concentration of inhibitors for saccharification and fermentation with the aim of

improving bioethanol production. To avoid formation of inhibitors during pretreatment, use of less severe pretreatment technique is required along with the optimization of operational conditions. However, to overcome the LCB recalcitrance, a harsh pretreatment is required. Therefore, it is difficult to stop the formation of inhibitors. This leads to another approach, i.e. separation of solid and liquid fractions of the pretreated material, proper washing of solid residues and enzymatic hydrolysis of washed solid residues in an optimal environment to obtain high sugar yield [83]. However, it would be economically expensive since more process units are required. Again to use sugar rich pretreatment liquid hydrolysate, detoxification of the pretreated hydrolysate would be needed before fermentation. Hence, detoxification of lignocellulosic hydrolysates is an important area of research. A number of detoxification methods including physical (evaporation, membrane based filtrations), physico-chemical (Rota evaporation with organic solvents), chemical (Calcium hydroxide over-liming, application of other alkalis such as sodium hydroxide, sodium dithionite, sodium disulphite, adsorption on activated charcoal, ion-exchange) and biological (changes in fermentation strategies, laccase, peroxidases, using of microorganisms such as *T. reesei*, *C. ligniaria*, *I. occidentalis* in the hydrolysates) have been proposed to transform inhibitors into inactive compounds or to reduce their concentration [89]. Again, recently developed genetic engineered competitive strains are more tolerant towards the inhibitors. Larsson et al. have successfully attempted the heterologous expression of laccase in *S. cerevisiae* [90]. Among all detoxification methods, chemical detoxifications have been the most popular approaches [83].

Fermentation of lignocellulosic hydrolysate is carried out to ferment monomeric sugars (glucose and xylose) into ethanol using microbial catalysts. Microorganisms such as yeasts and bacteria are being used to ferment cellulosic material. However, the most

frequently used microorganism in industrial processes is the robust yeast *Saccharomyces cerevisiae* (Baker's yeast) [91]. Under anaerobic condition *S. cerevisiae* can only ferment hexoses to produce ethanol [92], as the overall equation shows:

$$C_6H_{12}O_6 \longrightarrow 2C_2H_5OH + 2\,CO_2 \qquad \textbf{2-1}$$

Glucose ***Ethanol*** ***Carbon dioxide***

Theoretically, maximum conversion of ethanol from glucose is 0.51 g EtOH/g glucose. The fermenting efficiency of the yeast in ethanol yield is (> 90% theoretical yield), tolerance for ethanol (>40.0 g/L), ethanol productivity (>1.0 g/L/h), and able to grow in simple, inexpensive media and undiluted hydrolysates with resistance to inhibitors [93]. The problems of ethanol production from hexose and pentose sugars can be solved by using hybrid, genetically engineered or co-culture of two yeast strains [94]. Yeast strains such as *Pichia stipitis* (NRRL-Y-7124), *S. cerevisiae* (RL-11) and *Kluyveromyces fagilis* (Kf1) were reported as good ethanol producers from different types of sugars [95]. *K. Marxianus* is thermo tolerant yeast which is capable of co-fermenting both hexose and pentose sugars and can survive the temperature of 42–45 °C [96]. *S. cerevisiae* co-cultured with pentose utilizing yeasts like *Pichia fermentans* and *Pichia stipitis*, and efficiently utilized hexose and pentose sugars [97,98]. Many bacteria are able to metabolize and ferment both hexose and pentose sugars such as *Escherichia coli*, *Klebsiella oxytoca* and are used for industrial exploitation to produce ethanol. *Zymomonas mobilis only* ferments glucose and fructose to produce ethanol at high yields [93]. Hence, some attempts have also been made to genetically modify the yeast or bacteria as biocatalysts to produce high ethanol yield from lignocellulosic hydrolysate.

The processes used in fermentation to produce bioethanol are separate hydrolysis and fermentation (SHF), simultaneous saccharification and fermentation (SSF) and simultaneous saccharification and co-fermentation (SSCF) and consolidated

bioprocessing (CBP). In SHF, enzymatic hydrolysis and fermentation are performed sequentially. Therefore, enzymatic hydrolysis can be operated at its optimum temperature for higher yield of monomeric sugars. Fermentation allows microorganisms to be used at their optimum temperature for optimizing sugar utilization. In SSF, both enzyme and fermentation microorganisms are added to the same fermenter to perform both cellulose hydrolysis and fermentation of hexose sugars at the same time whereas SSCF is co-fermentation of hexose and pentose sugars in the same reactor [99]. Both SSF and SSCF are preferred over SHF as it offers following potential benefits which include use of only a single fermenter along with the elimination of associated equipments, low cost, end product inhibition on the enzyme is substantially reduced and possibility of microbial contamination during fermentation is reduced along with higher ethanol yield [100]. Another process is consolidated bio processing (CBP) in which enzyme production, hydrolysis and fermentation of all kinds of soluble sugars are allowed to be operated in a single step [101].

Certain fermentation parameters such as substrate and enzyme type and concentration, type of microorganism along with other usual process parameters affect the efficiency of hydrolysis and fermentation [102]. These process parameters include temperature, pH, incubation time, initial solid load and microbial load, agitation, and accumulation of soluble by-product in the fermentation broth [103].

Conventional recovery process of ethanol from fermentation broth is an energy-intensive distillation processes [104]. In recent years different alternative ethanol separation technologies have been investigated. A number of technologies have been examined for continuous ethanol removal from fermentation broth to maintain the ethanol concentration in the broth at low such that inhibitory effects on the growth of cells and on the specific ethanol conversion rate are reduced [105]. Hence, a lot of

research was carried out in finding more economically attractive separation techniques, such as ethanol extraction with CO_2 [106], solvent extraction [107], vacuum fermentation, adsorption [108], and pervaporation [109] etc.

Generally, the unfermented residual consisting of water and organic materials, are collected after ethanol recovery and dried. These materials can further be used for thermal energy or biogas or animal feed depending on their composition [110].

2.3 Effective pretreatment is a key-factor for digestibility of lignocellulosic biomass to produce fermentable sugars

Pretreatment is an important tool to change the microstructure, macrostructure and chemical composition of lignocellulosic biomass [111]. An effective pretreatment must break the lignin seal, reduce crystallinity of cellulose, increase surface area, swelling pores in the biomass structure, minimize carbohydrate losses, inhibit the formation of inhibitors for saccharification and fermentation, and enhances the enzyme efficiency to achieve the high yield of fermentable sugars[112]. After pretreatment, most of the lignocellulosic components should recover in a useable form in separate fractions. This upstream operation affect the cost of most other operations including size reduction prior to pretreatment, enzymatic hydrolysis and other downstream operations [21]. In addition, the pretreatment process itself must have low capital and operational cost, should avoid high consumption of expensive chemicals and chemical reagents polluting the environment and should require low energy input [113]. Above key features for the effective pretreatment of lignocellulosic biomass helps in developing promising pretreatment technologies. Finding optimal operating pretreatment conditions can contribute to overcome the major issues and challenges of lignocellulosic bioethanol

production in a biorefinery approach. Fig 2-1 represents effect of pretreatment on ultrastructure of lignocellulosic biomass [111].

2.3.1 Various methods of pretreatment

To date, several pretreatment methods have been investigated, which can be broadly classified into following categories: physical (comminution, microwave and extrusion), chemical (alkali, dilute acid, organosolv, ozonolysis and ionic liquids), physico-chemical (wet oxidation, steam explosion, liquid hot water, ammonia fiber explosion, wet oxidation and CO_2 explosion), biological pretreatment and combined/hybrid pretreatment [114,115]. The selection of suitable pretreatment technology depends on lignocellulosic biomass composition and structure, and end products [116]. In particular, each pretreatment method has some advantages and disadvantages as shown in Table 2-2 [99].

Physical pretreatment methods include comminution, extrusion, pyrolysis and irradiation (gammarays, electron beam or microwaves). Size reduction of LCB through comminution includes chipping (size of the materials is usually 10-30 mm after chipping), milling (ball milling, two roll milling, hammer milling, colloid milling, and vibro energy milling), grinding (size of the materials is usually 0.2-2 mm after milling or grinding) [117]. In general, physical pretreatment works on the LCB by increasing the accessible surface area and pore size, decreasing the degree of polymerization of cellulose and its crystallinity, and partial depolymerization of lignin [113]. The energy consumption is higher in physical pretreatments, environmentally un-friendly and non-suitable for commercial process [118].

Chemical pretreatment uses chemicals such as acids (H_2SO_4, HCl, H_3PO_4, HNO_3, organic acids), alkalis (NaOH, $Ca(OH)_2$, KOH, hydrazine, NH_3, NH_4OH), oxidizing

agents, organic solvents, and salts [119]. These are the most widely studied chemical pretreatment techniques for LCB and have been reported to have significant effect on the native structure of lignocellulosic biomass [120]. Acid pretreatment can be done with dilute or strong acids. Organic acids such as oxalic acid, acetyl salicylic acid and salicylic acid, maleic and fumaric acids are also used for LCB pretreatment. The organosolv pretreatment method involves organic solvents, such as methanol, ethanol, acetone, glycols or phenols, with or without the addition of a catalyst agent. ILs are organic salts composed of cations and anions, typically, large organic cations and small inorganic anions used for lignocellulosic biomass pretreatment. Pretreatment with oxidizing agent includes using ozone gas as an oxidant [116]. Chemical pretreatment of the lignocelluloses has become one of the most promising methods to modify the crystalline structure of cellulose, decrease the degree of polymerization (DP) and remove/or modify hemicelluloses and lignin [121]. Further, in the pulp and paper industry chemical pretreatment has been used for delignification of cellulosic material [122]. It has been employed to enhance LCB digestibility in an industrial pretreatment process [113].

Physico-chemical pretreatment uses both chemical and physical processes in order to break the recalcitrance structure of the lignocellulosic material. Technologies such as steam explosion, ammonia fibre explosion (AFEX), ammonia recycling percolation (ARP), soaking aqueous ammonia (SAA), wet oxidation, CO_2 explosion, liquid hot water etc. comes under physico-chemical pretreatment category [51]. Physico-chemical methods exert the actions on LCB through increasing the accessible surface area, decreasing the cellulose crystallinity, dissolving hemicellulose and altering the lignin structure [118].

Biological pretreatment uses microorganisms especially fungi that are able of producing enzymes to degrade lignin, hemicelluloses and polyphenols present in the biomass and makes LCB more accessible for hydrolysis and subsequent bioethanol production [123]. The microorganisms, such as brown-, white- and soft-rot fungi, actinomycetes and bacteria, are used to degrade LCB. White and soft-rot fungi primarily used for delignification of LCB, while brown-rot primarily attacks cellulose and hemicelluloses with only small lignin modifications [124]. The selected white-rot fungi such as *Phanerochaete chrysosporium*, *Ceriporia lacerate*, *Cyathus stercolerus*, *Ceriporiopsis subvermispora*, *Pycnoporus cinnarrbarinus*, *Coriolus versicolor* and *Pleurotus ostreaus* have been identified as the best delignifying organisms on different LCB [118,125]. From both economic and environmental perspectives, the advantages of biological pretreatment over physical/chemical pre-treatments include simple techniques, low energy consumption, no or reduced generation of toxic compounds and reduced downstream processing costs [126]. However, this pretreatment still faces some drawbacks which includes substantial loss of holocellulose (cellulose and hemicellulose), needs large space to perform and long pretreatment time negatively affecting its wide spread application and is found less attractive commercially [127].

A single pretreatment method can have risks, such as technological problem, environmental pollution, high-energy consumption, long reaction time, high requirement for reactor corrosion resistance, and the absence of the requirement for industrial production. Also, it can be concluded that till date a single pretreatment method has not been established which can eradicate above risks at a time. Hence, combined/hybrid pretreatment came into picture. Combined pretreatment include mechanical crushing - chemical, physical or biological treatment, mechanical crushing - microwave - chemical processing, and mechanical crushing - solid base catalyst - ionic liquid treatment,

mechanical crushing - alkaline peroxides- steam explosion etc. [128,129,130]. This method integrates the advantages of single pretreatment methods and has shown potential for significant improvements to overall process productivity. However, still lot of research needs to be done in order to develop combined pretreatment methods to obtain their full potential.

2.3.1.1 Pyrolysis

Pyrolysis of LCB is a form of treatment that thermally decomposes LCB materials through heating in the absence of oxygen to produce bio oil (condensable gas), synthetic gas (non-condensable gas), and bio char [131]. Bio oil is a complex mixture of many compounds such as aldehydes, ketones, acids, furans, phenolic compounds, anhydro sugars mainly levoglucosan (1,6-anhydro-β-d-glucopyranose) [132]. The composition of the bio oil mainly depends on the operating conditions during pyrolysis, as well as the type of feedstock used [133]. Bio oil can be further upgraded and converted into various value-added organic compounds and speciality chemicals. Understanding the cellulose pyrolysis behavior has increased importance as cellulose is the major component of LCB and the main pyrolysis product of cellulose is levoglucosan. Levoglucosan can be subjected to acid hydrolysis for production of fermentable glucose [134]. Pyrolysis of cellulose can be divided into the following types: slow pyrolysis, fast pyrolysis, flash pyrolysis and catalytic pyrolysis [135]. Pyrolysis of lignocellulosic biomass can be used as a pretreatment technology combined with acid hydrolysis to produce fermentable sugars. It has shown that presence of alkali and alkaline earth metals in LCB affect the choice of cellulose pyrolysis reaction pathway and suppressed the formation of levoglucosan [134,136].

Thermogravimetric analysis (TGA) has been widely used to study lignocellulose pyrolysis. Some researchers reported that the decomposition regions of hemicellulose and cellulose are in ranges of around 220–315 ºC and 315–400 ºC, respectively, with maximum weight losses at 268 ºC and 355 ºC. Lignin decomposition usually took place in the range from 180 ºC upto 900 ºC with an unclear maximum weight loss [137].

Non-isothermal solid-state kinetic data from TGA (Thermogravimetric analysis) are analyzed by several methods [138,139]. These methods are classified into two types: model-fitting and model free methods. In model fitting methods, different models are fitted to the data and a suitable model is chosen when it gives the best statistical fit with an ability to directly determine the kinetic parameters from a single TGA measurement. Especially for non-isothermal data, several models were found to be statistically equivalent, but the fitted kinetic parameters obtained may differ by an order of magnitude and hence it is difficult to select an appropriate model. Higher values of kinetic parameters were usually obtained for non-isothermal data by application of model-fitting methods [140]. Model-free methods require several TGA measurements at different heating rates to perform the kinetic analysis. Simplicity and the avoidance of errors connected with the choice of a kinetic model are the main advantages of the model free analysis [141].

Kinetic analysis through model-free methods can provide information about the possible reaction types involved and kinetic parameters. Model-free (iso-conversional) methods determine the activation energy as a function of extend of decomposition and temperature. Again it predicts kinetic parameters over a wide temperature range. Hence model-free kinetics are extensively used to study the kinetics of a variety of physical processes [142,143].

Jeguirim and Gwenaelle (2009) proposed that the activation energy and pre-exponential factor of hemicellulose were 110 KJmol^{-1} and 20 s^{-1} respectively [144]. Rogers R.N. (2008) proposed that activation energy of cellulose is 198.03 kJ mol^{-1}, whereas less stable arabinose has 82.48 kJ mol^{-1}[145].

2.3.1.2 Acid Pretreatment

Acid pretreatment involves the use of inorganic acids (sulfuric, nitric, hydrochloric, and phosphoric acids) and organic acids (formic, acetic, oxalic, maleic and propionic acids) to break the recalcitrance structure of the lignocellulosic material [75,146,147]. Dilute or concentrated acids can be used for the pretreatment.

Concentrated acid treatment carried out with acid concentration in the range of 10–30%, in mild temperature (T< 100 ^{o}C) at one atmosphere pressure for longer retention time [148]. Concentrated strong acids such as sulfuric acid and hydrochloric acid are powerful agent used for treating lignocellulosic materials [149]. Concentrated acid hydrolyzed both cellulose and hemicellulose with 90% of theoretical yield for both glucose and xylose and subsequent enzymatic hydrolysis step is not required [150, 151]. In addition, sugar conversion rate is higher than enzymatic hydrolysis. Lower operating temperature and pressure of this process minimize the production of inhibitors [152]. The major drawbacks of concentrated acid hydrolysis are higher toxicity and corrosivity. Therefore, the acid must be recovered and corrosive resistant equipment required, that causes high operational and maintenance costs [153].

Dilute acid is the most extensively studied pretreatment technology, as it is cheap and effective [154]. The dilute acid-pretreatment process usually uses temperatures between 100 - 240 °C and pressures ~10 atm. In this chemical pretreatment process, acid concentration is in the range of 0.2 to 2.5 % (w/w) and the residence time ranges from a

few minutes to hours depending upon the pretreatment conditions [51]. During dilute acid treatment, mainly hemicellulose is hydrolyzed, with poor removal of lignin. Removal of hemicellulose and partial degradation of lignin increases the porosity and enhance the enzymatic digestibility of cellulose [155]. The main advantage of the low concentration acid in the dilute acid treatment process is that recovery of acid does not required. At high temperature and pressure monomer sugars are degraded and the resulting degradation products inhibit the microbial fermentation process [149].

Pretreatment of biomass with dilute sulfuric acid is a very favorable method because sulfuric acid is a low-cost and easily available chemical for industrial applications, with low safety and environmental concerns. The dilute sulfuric acid pretreatment used for the hemicellulose and lignin solubilization of biomass and produce reactive cellulose to improve the enzymatic digestibility and to solubilize sugars for its further fermentation. The dilute sulfuric acid pretreatment is found to be very economical and efficient to make the cellulose more accessible for enzymatic hydrolysis [156,157,158]. Further, this pretreatment method not only solubilises the hemicelluloses, but also converts it into fermentable sugars. However, detoxification step is required to remove inhibitors before fermentation. Corrosive nature of dilute sulphuric acid requires corrosive resistant material for reactor [111,154].

In dilute acid pre-treatment many factors e.g., solid loading, acid loading, reaction time, temperature significantly affect the production of efficient fermentable sugars and reactive cellulose [154,159]. Hence optimization of this process is needed to improve the performance of a system to get the maximum benefit from it and used to obtain conditions for factors, which produces the best possible response. In general, optimization of a process could be achieved by either one-variable-at-a-time or statistical methods. The former having major limitation is that it does not include the interactive

effects among the variables studied as a result the process response is a direct function of the single varied parameter. In addition to this, this process is also labor intensive and time consuming whereas the statistical optimization procedures allow to consider interaction of variables. Among the most suitable multivariate optimization methods used in pretreatment optimization is response surface methodology (RSM) [160,161].

Sasmal et.al (2011, 2013) studied the pretreatment of areca nut husk fibre and Bonbogori (*Ziziphus rugosus*) using dilute sulfuric acid and optimized the process using the Taguchi method of optimization to enhance the enzymatic digestibility of treated biomass. They showed that for areca nut husk the maximum sugar yield through saccharification obtained at optimized reduction in the crystallinity was found to be around 49.8%. They found optimum acid concentration (2.5%), solid loading (1%), and time of operation (30min), respectively for *Z. rugosus* to reduce crystallinity [162,163].

2.3.1.3 Ionic liquid Pretreatment

Recently, it has been shown that some ionic liquids (ILs) can be used as non-derivatizing solvents for disruption of lignocelluloses. These salts have extremely low vapor pressure, high thermal and chemical stability and can effectively dissolve complex macromolecules and various polymeric compounds under mild conditions [164,165]. The tunable solvent properties of ILs makes it suitable for lignocellulosic biomass pretreatment and fractionation so as to facilitate the enzymatic hydrolysis to produce reducing sugars which can be subsequently converted to bio-ethanol through fermentation process [166].

The efficacy of a given IL in the dissolution of lignocellulosic biomass depends on the selection of cations and anions to be involved in the structure of ILs [167]. Swatloski et al. studied dissolution of cellulose with ionic liquids, containing 1-butyl-3-

methylimidazolium cations ($[C_4mim]^+$) were screened with a range of anions that are (Cl^-), ($[PF6]^-$), Br^-, SCN^-, and $[BF_4]^-$. Plus, they investigated the solubility of cellulose in ionic liquids for the chloride salts with variations in cation alkyl-substituent from butyl through octyl. They found $[C_4mim]Cl$ solubilize considerable amounts of cellulose (upto 25 wt%) with assistance of microwave irradiation and forming highly viscous solutions [168]. Zakrzewska et al. reviewed the use of different ILs in the fractionation of lignocellulosic materials and reported that one of the major advantages is that ILs can be designed according to the requirement of a specific dissolution or functionalization [169]. da Costa Lopes et al. presented fractionation of wheat straw using different ionic Liquids such as 1-butyl-3-methylimidazolium hydrogen sulfate ($[bmim][HSO_4]$), 1-butyl-3-methylimidazolium thiocyanate ([bmim]-[SCN]), and 1-butyl-3-methylimidazolium dicyanamide ($[bmim][N(CN)_2]$). They observed that a high-purity lignin-rich fractions was achieved with [bmim][SCN], in contrast high purity carbohydrate rich materials which was obtained with $[bmim][N(CN)_2]$ and no hemicellulose rich material was recovered with $[bmim][HSO_4]$ [170]. Fractionation of wheat straw using 1-ethyl-3-methylimidazolium acetate ($[emim][CH_3COO]$) and recovery of IL was studied by da Costa Lopes et al. Using this IL, optimized pre-treatment methodology allowed to obtain carbohydrate rich fractions and a separate lignin fraction recovered with 87 wt% purity. This carbohydrate rich fractions has a very high enzymatic digestibility followed by high glucose yield [171]. Effect of parameters such as different pretreatment time and temperatures on the wheat straw pretreatment, using the ionic liquid 1-ethyl-3-methylimidazolium acetate ([emim][OAc]) was demonstrated by da Silva et al. They found that cellulose-rich fraction contains glucan (81.1% w/w biomass), up gradation of carbohydrate content in the hemicellulose fraction (96% wt) and lignin purity (97% wt) were produced with the initial biomass loading

37.1% (w/w) at 140 ^{o}C for 6 h pre-treatment [172]. Carvalho et al. reported pre-treatment of Wheat straw with [bmim][HSO_4], resulted a solid fraction comprised of mainly cellulose and lignin and a liquor rich in hemicellulosic sugars, furans and organic acids [173]. Verdia et al. studied the pre-treatment of *Miscanthus giganteus* with 1-butyl imidazolium hydrogen sulphate and investigated the influence of the solution acidity on the fractionation of biomass by varying the 1-butylimidazole to sulphuric acid ratio. Higher acidity led to shorter pre-treatment times and reduced hemicellulose content in the treated pulp [174].

The most frequently used ionic liquids for dissolution of lignocellulosic biomass is 1-butyl-3-methylimidazolium chloride (BMIMCl) [175]. Imidazolium and pyridine, two of the best cations, containing aromatic moieties have shown to improve the dissolution of wood [176,177]. ILs contain anions such as chloride, acetate, formate, phosphonate have high hydrogen-bond acceptor (HBA) strength and are represented by the β values in terms of Kamlet-Taft solvatochromic parameters which is an indicator of their effectiveness in cellulose dissolution [178]. IL is thought to dissolve cellulose by intercalating into and breaking up the hydrogen bonding network of the cellulose whereas the cation interact with oxygen atoms on the hydroxyl groups of cellulose. Aromatic cation, allows it to interact through ring, or π--π, stacking with the lignin to dissolve lignocelluloses. Cellulose rich pulp separated from IL by using different protic and aprotic solvents. To make the IL pretreatment process cost effective and industrially feasible in bulk scale, detail study is needed [179]. Anti-solvents, such as water, is generally added to the solution to precipitate cellulose rich material from ILs. Some researchers reported that the cellulose content in the regenerated lignocelluloses can be enriched, using organic solvent-water mixtures [43]. Acetone–water mixture (1: 1 (vol %)) used by the Rogers group, [180,181] while Viell et al. used an ethanol–acetone

mixture (1: 1 (vol %)) [182]. Dibble et al. studied the optimization of anti-solvent composition comprising ethanol and acetone to avoid cellulose gelling [183].

2.4 Enzymatic Saccharification

Hydrolysis of cellulose using cellulolytic enzymes is another limiting step in the lignocellulosic bioethanol production. The rate of saccharification is influenced by factors such as enzyme activity, nature of the substrate, enzyme and substrate concentration, product inhibition, pH and temperature. Unlike chemical hydrolysis, it can be performed at low temperatures (30 °C–50 °C) and atmospheric pressure, mild conditions of pH (4.8), there is no sub-products formation, increasing the yield of glucose production. However, it is highly substrate specific and is greatly affected by their structure (degree of crystallinity, specific surface area and lignin content in lignocelluloses). Pretreatment of raw lignocellulosic material increase enzymatic efficiency and productivity by changing their structure. Increased amounts of substrate may cause a decrease in hydrolysis yields because of lower contact between substrate and enzymes, nonspecific binding to lignin [184].

2.5 Objectives

Thus, based on the above brief discussions, it seems that there is a good scope to carry out research on lignocellulosic biomass to produce fermentable sugars. Three unexploited lignocellulosic biomasses available in plenty in India viz. Miscanthus (*Miscanthus sinensis*), Castor (*Ricinus communis*) and Jatropha (*Jatropha curcas*), were taken and characterized followed by thermal kinetic parameters analysis to choose the best feedstock among these three for fermentable sugar production.

Throughout the research, the following objectives were established and accomplished.

1. Screening of best lignocellulosic feedstock from three selected biomass based on physico-chemical characterization and thermal-kinetic study with an aim to achieve better yield of fermentable sugars.
2. Optimization of the dilute acid pretreatment process using RSM for the best biomass followed by optimization of enzymatic hydrolysis process to achieve high yield of fermentable sugars.
3. Understanding the role of different anions in ionic liquids and anti-solvents for dissolution and regeneration of the best biomass and its relation to glucose yield through enzymatic hydrolysis.
4. Optimization of chemical synthesis of *N, N-diethyl-4-nitroaniline* to measure the Kamlet–Taft solvent parameters of different ionic liquids and co-relation between the hydrogen bond basicity (β value) of different ionic liquids with cellulose crystallinity, lignin removal and glucose yield from the best biomass.
5. Comparison of dilute acid pretreatment and ionic liquid pretreatment for the best biomass.

Table2-1 Zone wise distribution of available agro-feedstocks (Source: EIA "A Market intelligence Report" September2012, (Adapted from Kumar et al. [62]))

Indian region	States	Available agro feedstocks	Approximate range of cost of feedstocks (INR/t)
North-West	Rajasthan ,Gujarat	Stalks of mustard, julieflora, maize, dhaniya, soybean, cotton, tuver and sesame	1300 – 2500
Central and South-West	Madhya Pradesh, Maharashtra	Cotton stalk, soy husks and mustards, maize stalks and chilly, rice husk, juliflora and bamboo	1500 – 2800
South	Andhra Pradesh, Karnataka, Tamilnadu, Kerala	Rice husk, juliflora, ground nut and coconut shell, bengal gram, chilly stalk, cane trash, maize and channa steam	1200 – 2500
North-East	Jharkhand, West Bengal	Wood chips, rice husk and sugar cane	1100 – 2600
North	Punjab, Haryana, Himachal Pradesh, Uttaranchal, UttarPradesh	Rice husk and straw, mustard stalk, straw and wheat husk, juliflora and cane trashes	1550 – 3000
Central and South-East	Odisha, Chattisgarh	Rice husk, cotton stalk, saw dust and juliflora	1100–2600

Table 2-2 Advantages and disadvantages of different pretreatment methods (Adapted from Zabedet al. [99])

Category	Pretreatment method	Advantages	Disadvantages
Physical	Mechanical grinding	▪ Break the structure of lignocellulose ▪ Reduce cellulose crystallinity ▪ Increase surface area	▪ High energy input ▪ Cannot remove hemicellulose and lignin
	Irradiation	▪ Can be combined with other treatment ▪ Increase surface area ▪ Improve glucose yield	▪ High cost ▪ Slow rate of reaction ▪ Energy intensive ▪ Not eco-friendly
	High energy electron radiation	▪ Reduce cellulose polymerization degree	▪ High cost
	High temperature pyrolysis	▪ Decompose cellulose rapidly	▪ Energy consumption ▪ Low productivity
Chemical	Dilute acid	▪ Significant improvement of cellulose hydrolysis ▪ High reaction rate and high yields ▪ Less corrosion problem and inhibitor formation compared to concentrated acid pretreatment ▪ Most widely used method in industrial application	▪ Little lignin removal ▪ Requirement of washing the pretreated biomass and neutralization before enzymatic hydrolysis ▪ Requirements of disposal of neutralization salts
	Concentrated acid	▪ Complete removal of cellulose crystalline structure ▪ Achievement of amorphous cellulose ▪ High reaction rate	▪ Formation of inhibitors ▪ Corrosion of equipment ▪ Need for acid recovery
	Alkali	▪ Operation at low temperature ▪ Alteration in lignin structure ▪ Lower degradation of sugars	▪ Conversion of alkali to irrecoverable salts or incorporation as salts into the biomass

		compared to acid pretreatment	▪ Necessity of pH adjustment
	Ozonolysis	▪ Selective lignin degradation with minimal effects on cellulose and hemicellulose ▪ Low inhibitor formation ▪ Operation at ambient temperature and pressure	▪ Highly reactive, flammable, corrosive and toxic properties of ozone ▪ High generation costs due to large energy demand ▪ Exothermic characteristics of process may require cooling systems
	Ionic liquids	▪ No toxic or explosive gases are formed ▪ Minimum degradation of desired products ▪ Operation at low temperature	▪ Expensive ▪ Requirement of washing before use ▪ Lack of mature commercial IL recovery methods
	Organosolvo	▪ Obtain pure cellulose, hemicellulose, lignin ▪ Minimum cellulose loss (less than 2%) ▪ Low sugar degradation	▪ Requirement for removal of solvent from the system ▪ High costs of chemicals ▪ Formation of inhibitors
Physico-chemical	Steam explosion	▪ Partial hydrolysis of hemicelluloses ▪ Lignin transformation ▪ Increases accessible surface area ▪ Decrease in the degree of polymerization ▪ Cost effective ▪ No significant environmental constraints	▪ Less effective for softwood ▪ Partial degradation of pentoses and lignin ▪ Loss of yield and formation of inhibitors
	Acid catalyzed steam explosion	▪ Industrially developed ▪ Removal of hemicellulose ▪ Increased surface area ▪ Increased enzyme	▪ Formation of inhibitors ▪ Produce reactive loss and toxicity

		accessibility ▪ Low environmental impact	
	Liquid hot water	▪ Does not require any catalysts or chemicals ▪ Increased accessible surface area ▪ No or little inhibitor formation	▪ High water demand ▪ High energy requirement ▪ Hemicellulose degradation
	Ammonia fiber explosion (AFEX)	▪ Increased surface area ▪ Reduction in cellulose crystallinity ▪ Removal of lignin ▪ No inhibitors formation	▪ Environmental concerns ▪ Large amount of ammonia increase cost ▪ No utilization beyond lab scale
	Ammonia recycling percolation (ARP)	▪ Removal of lignin ▪ Reduction in cellulose crystallinity ▪ Alteration of lignin structure ▪ Low inhibitor formation	▪ High energy requirement ▪ Environmental concern
	Soaking aqueous ammonia (SAA)	▪ Formation of low inhibitors ▪ Low energy requirements	▪ Environmental concerns
	Wet oxidation	▪ Increased digestibility of cellulose ▪ Formation of low inhibitors ▪ Removal of lignin	▪ High costs for oxygen and catalysts ▪ Requirement of high pressure and temperature
	CO_2 explosion	▪ Effective removal of lignin ▪ Low sugar degradation ▪ Low temperature	▪ Requirement of costly equipment
Biological	Brown rot, white rot and soft rot fungi	▪ Reduction in the degree of polymerization of cellulose and hemicellulose ▪ No chemical required ▪ Mild environmental conditions ▪ Low capital costs ▪ Low energy demand ▪ Low inhibitor formation	▪ Very slow rate of degradation and delignification ▪ Loss of carbohydrates as consumed by microbes ▪ Long residence times (10–14days)

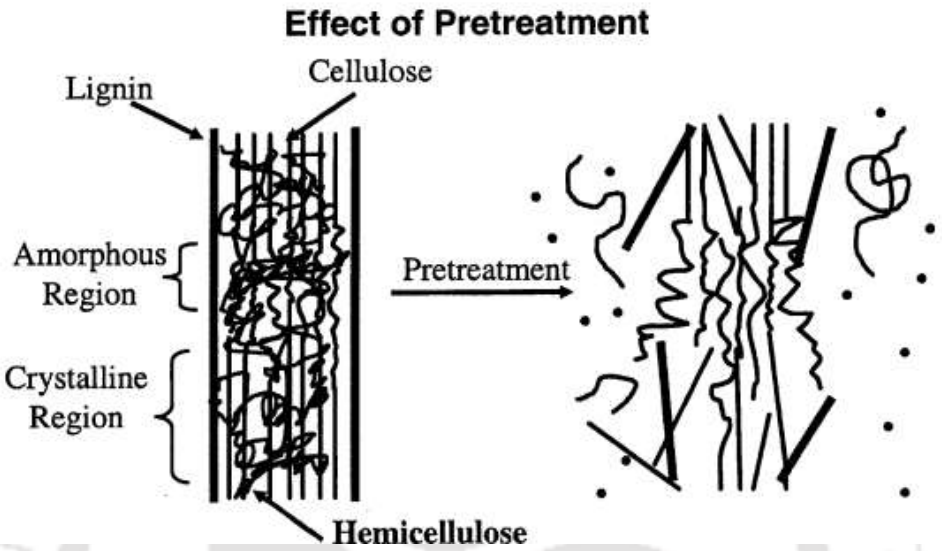

Fig 2-1: Effect of pretreatment on ultrastructure of lignocellulosic biomass (Adapted from Mosier et al. [111])

3 MATERIALS AND EXPERIMENTAL METHODS

3.1 Biomass collection and sample preparation

Castor, Jatropha and herbaceous Miscanthus were collected from local forest near IIT Guwahati and various parts of IIT Guwahati campus. Leaves and roots were removed, the stems of Castor, Jatropha and the stalks of Miscanthus were crushed into small pieces of size 1-2 cm and cleaned thoroughly using tap water until the washings became clean and colourless. Then they were sun dried for two days and stored in airtight plastic container. These dried samples were ground into powder using house hold grinder and passed through a mesh (BSS 60) to get uniform powder of particle size of less than 0.25 mm. Before characterisation, sample was dried for 24 h at 60 ± 3 ºC. The remaining crushed fibres were stored in desiccators at room temperature. The scientific classification of lignocellulosic feedstock is presented in Table 3-1.

3.2 Characterization of raw materials

The systematic characterization of powder biomass samples were carried out in this study to estimate the efficiency of these biomasses towards biofuel production and shown in Fig 3-1.

3.2.1 Compositional analysis

In this study, determination of cellulose, hemicellulose, lignin and extractives content of lignocellulosic biomass were included in compositional analysis. Estimation

of these components is useful for thermal and biochemical conversion of biomass for bio-fuel production.

3.2.1.1 Determination of Extractives

Lignocellulosic biomass extractives are low-molecular-weight compounds; include resin (terpenes, lignans and other aromatics), fats, waxes, fatty acids, alcohols, steroids and higher hydrocarbons etc. These materials are chemically polar and non-polar in nature. They give color, odor and also protect plants from termites and microorganisms. Extractives content and composition varies among plant species, geographical site, season, and growing age. In plants they are mostly found in resin canals, the ray parenchyma cells, lower amounts present in the middle lamellae, intercellular and cell walls of tracheids and libriform fibers. These materials have influence on the determination of structural carbohydrates and lignin and also they can be used as substitution of petrochemicals [185,186]. Therefore, extractions of these compounds are required before processing of lignocellulosic biomass for biofuel production.

For determination of extractives, each lignocellulosic biomass sample (5 g) was successively extracted with n-hexane followed by ethanol and distilled water using a soxhlet extraction apparatus for 6 h. For solvent extraction, biomass samples were transferred inside a cotton cellulose thimble and placed in the Soxhlet tube. The extraction solvent was taken into a distillation flask and the Soxhlet tube was placed onto this flask equipped with a condenser. The heating of solvent was done by a heating mantle for reflux. The extraction solvent n-hexane was used in first step to separate the compounds from biomass such as non-polar lipids, hydrocarbon compounds and terpenoids, etc. In the second step, hexane extracted biomass was extracted with ethanol

to separate polar compounds such as chlorophyll, polar waxes, sterol etc. Finally, distilled water was used as extraction solvent to extract inorganic materials and non-structural sugars etc. After each extraction, the solvent and extractive were separated using a rotary evaporator with a reduced pressure [187,188,189].

3.2.1.2 Determination of cellulose, hemicellulose and lignin content

The cellulose, hemicellulose and lignin content of raw Miscanthus, Castor and Jatropha was performed using NREL protocols [190]. 300 mg of biomass and 3 mL 72 % H_2SO_4 were incubated at 30 °C for 1 h while the sample was stirred every 5 to 10 minutes without removing the sample from the bath. The solution was diluted to 4% H_2SO_4 with 84 mL of DI water and autoclaved for 1 h at 121 °C. The reaction was quenched by slowly cooling to near room temperature before removing the biomass by filtration. The filtrate was used to determine acid soluble lignin as well as carbohydrates. A portion of the filtrate was neutralized with $CaCO_3$ and monomeric sugars (glucose, xylose, arabinose) were determined from the filtrate by High pressure liquid chromatography (HPLC) equipped with a refractive index detector (Perkin Elmer Series 200), using Repromer H^+, 9 µm (300 × 7.8 mm) column with the following chromatographic conditions: eluent - H_2SO_4 9 mM, flow rate - 0.5 mL min^{-1} at room temperature. Before injection each samples were filtered through 0.2 µm nylon filter. The injection volume was 20 µL with a run time of 35 min. Concentration of glucose, xylose, and arabinose was determined using average peak areas compared with the calibration standard and expressed as g L^{-1} sugar. Acid-insoluble lignin was quantified gravimetrically from the solid after overnight heating at 105 °C (the weight of acid-insoluble lignin + ash) and then 575 °C for at least 6 h (the weight of ash). The

absorbance of the filtrate at 245 nm wavelength was measured on a UV-Visible spectrophotometer (TMSPC-8, Shimadzu Corporation) to quantify acid soluble lignin.

3.2.2 Proximate and Ultimate analysis

Proximate analysis is defined as the determination of moisture, ash, volatile matter and fixed carbon content in biomass samples.

Moisture content present in biomass is classified in to two types i.e., extrinsic moisture and intrinsic moisture. Extrinsic moisture content is influenced by weather and mainly achieved during harvesting whereas intrinsic moisture content does not influenced by the weather [191]. Intrinsic moisture was calculated after every sample was sun dried for 2 days to remove extrinsic moisture.

Moisture quantification in biomass is required as it significantly affects the gross calorific value i.e., it lowers the energy content, which leads to lower fuel efficiency of biomass. More moisture content, required large boiler dimensions, incomplete combustion which increases fumes, reduces combustion temperature in furnace and heat loss increases from stack, lower grind capacity and transportation difficulties [192,193]. From this, it is clear that biomass with low moisture content is suitable for thermal conversion process where as high moisture content is suitable for biochemical process such as fermentation. The moisture content of the biomass was determined using the method described in ASTM3173-87 [194].

Ash content is the mass fraction of incombustible material left after complete burning process in air, consisting mainly inorganic materials present in biomass. The most abundant elements present in biomass ash are Al, Ca, Fe, Mg, P, K, Si, Na and Ti. These elements have a significant impact on the ash melting behavior, slagging, fouling,

sintering and corrosion and high ash content of the biomass reduces its heating value [192, 195]. In addition to this, the cations (K^+, Mg^{2+}, Ca^{2+}, Al^{3+}, Mn^{2+}, Fe^{3+}, Cu^{2+} and Zn^{2+}) present in the ash inhibits the enzymatic hydrolysis of cellulosic substrates into readily fermentable sugars. High concentrations of some elements may be a sign of biomass contamination with soil or sand. Dirt (soil or sand) in the biomass also adds to the mineral content, are called extractable ash. These are easily removed by simple extraction or washing techniques [185].

The ash content of biomass was determined according to procedure ASTM E1755 – 01 [196]. 1.0(±0.1) g of dried biomass sample was taken in crucible and placed in muffle furnace at 575± 10 ^oC for 3 h. Then the crucible was taken from the furnace and putted in desiccator to room temperature. The weight difference gives the ash content of biomass.

The concept of volatile matter refers to the part of the biomass that is liberated when biomass is heated at high temperature in the absence of air, excluding moisture. The components liberated usually as a mixture of combustible gases (short and long chain hydrocarbons, aromatic hydrocarbons) and incombustible gases (carbon dioxide, sulphur dioxide, nitrogen oxides). Usually, biomass has very high volatile content (up to 80 percent), which helps in easier ignition of biomass [197]. High volatile content requires secondary air and distribution aspects for effective combustion, which leads to dark smoke, heat loss, pollution hazard and soot deposition on boiler surfaces [193].

The volatile matter in the biomass was estimated using the procedure given in ASTM D 3175-07 [198]. 1.0 (±0.1) g of demoisturized biomass sample was taken and putted in muffle furnace at 950±10 ^oC for 7 min and removed immediately from the furnace and placed in the desiccator. The difference in weight represents the volatile of the biomass.

Fixed carbon content of biomass is the mass remaining after volatile materials are driven off, excluding ash and moisture content. This value can give information about heating value. It was determined by subtracting the percentages of moisture, volatile matter, and ash of biomass sample from 100.

The aim of ultimate analysis of biomass is to determine the amount of elemental constituents such as carbon (C), hydrogen (H), nitrogen (N), sulfur (S), oxygen (O) and other elements present in biomass. Knowledge of such elements helps to estimate quantity (theoretical) of air required for complete biomass combustion and the volume and composition of combustion gases [193]. From this analysis calorific value of biomass can be calculated using different methods such as Demirbas etc. [199].

The major elements present in biomass which mostly affect the above factors are C, H, N, S and O. This analysis of biomass was carried out on a dry basis using CHNSO elemental analyzer (Variael CUBE, Germany).

3.2.3 Thermogravimetric Analysis

Thermogravimetric analysis is a fast technique for determining the weight and rate of weight change of material with temperature or time under controlled atmosphere. The devolatilization characteristics and kinetics of thermal decomposition of biomass is extensively studied using TGA [185,188]. From TGA the major component of biomass (Cellulose, hemicellulose and lignin) determined quantitatively because several literature reveals that thermal degradation of lignocellulosic biomass follow first order reaction kinetics or pseudo-first order reaction kinetics and henceforth the rate of degradation of lignocellulosic biomass is directly proportional to the concentration of its individual components [200,201]. The rate of decomposition of lignocellulosic biomass in active pyrolysis zone depends upon the amount of carbohydrate present in biomass i.e. higher

the amount of carbohydrate than lignin results fast decomposition and formation of gases such as CO_2 and CO [185]. The value of T50 (temperature at level of 50% weight loss) and R50 (rate of weight loss at T50) gives the approximate idea about above rate of decomposition which is useful for gasification process. Overly, the kinetic analysis of TGA thermogram is essential for pyrolysis and gasification process.

Thermogravimetric analysis of all three lignocellulosic biomass samples (Castor, Jatropha and Miscanthus) was performed using METTLERTOLEDO, Switzerland (Model no TGA851e/LF/1100) thermogravimetric analyzer. In order to prevent heat and mass transfer limitations, a sample of 10±0.5 mg was taken and studied for the thermal degradation characteristics from 25 to 900 ^{o}C at the heating rate of 10 ^{o}C/min in 40 mL min^{-1} flow of nitrogen as the purge gas. The reproducibility of generated data was determined by repeating the experiments for three times and was found to be very good. The apparatus provides continuous measurement of weight loss vs. temperature using software (STAR). The TG and DTG curves were used for quantitative determination of main composition (Cellulose, hemicellulose and lignin) and thermal characteristics of biomass sample.

3.2.4 Crystallinity Index

The crystallinity index (CrI) is an empirical measure of relative crystallinity of biomass. The biomass composition significantly affects CrI of cellulose, and increased proportionally with the crystalline cellulose content [202]. The hydrogen bonds formed between β-1,4-glucan chains and Van-derwaals forces between the glucose molecules in cellulose and hemicellulose determine cellulose crystallinity [203,204]. Crystallinity of lignocelluloses retards the enzymatic hydrolysis of polymeric sugar molecules and with

increase in crystallinity there is increased retardation of enzymatic hydrolysis, which leads to lower yield of fermentable sugar as well as ethanol, hydrogen [205].

In the present study, X-ray diffraction (XRD) method was used to detect cellulose crystallinity index (CrI) of lignocellulosic biomass using X-ray diffractometer (Brucker D8 Advanced, Germany). The XRD analyses were performed on the X-ray diffractometer operating at 40 kW, 40 mA using copper Kα (λ = 1.5406 Å).The XRD patterns were collected in the 2θ range from 5° to 40° with a step size of 0.02° and the exposure time of 1 s. Crystallinity index (CrI) was determined by Segal's method [206].

$$CrI\ (\%) = 100 \times [(I_{002} - I_{am}) / I_{002}] \quad \textbf{3-1}$$

in which, I_{002} is the diffraction intensity at peak position $2\theta \sim 22^0$ for cellulose I, and $2\theta \sim 21^0$ for cellulose II and I_{am} is the intensity due for the amorphous portion (i.e., cellulose, hemicellulose, and lignin) at about $2\theta \sim 18^0$.

3.2.5 FTIR Analysis

Fourier transform infrared spectroscopy (FTIR) analysis gives better understanding of chemical structure of three raw lignocellulosic biomass samples and their extracts (hexane, ethanol and water) [187]. With this technique, it is possible to reveal the intrinsic mechanism of solvent (hexane, ethanol and water) extraction and the interaction of lignocellulosic biomass with above solvents.

FTIR absorption spectra of the subjected biomass samples and their extracts were obtained in the 4000–400 cm^{-1} region using a spectrophotometer (Shimadzu, Model-IR Affinity1) by diffuse reflectance method by dispersing samples on IR grade potassium bromide. Spectra were collected at a resolution of 4 cm^{-1} with 30 scans.

3.2.6 Determination of gross calorific value

Determination of gross calorific value is important because it is a characteristic for each biomass, which is used to design gasifier and also useful to know the efficiency of boiler or furnace [207]. Gross calorific value estimate the energy content (higher heating value) of biomass sample using oxygen bomb calorimeter (Model No: RBC, Reico Equipments and instruments Pvt. Ltd.) and detail procedure described in ASTM manual [208]. Approximately 1.0 g of ground sample of each biomass were measured and placed into pre-weighted crucibles. A cotton thread was attached to the nichrome ignition wire and placed in contact with the sample. Approximately 5 mL of distilled water added to the bomb and the bomb was pressurized with pure oxygen in between 20 and 30 atm. The outer jacket of bomb calorimeter was filled with 2000 mL of distilled water and constant temperature was maintained by circulating water at 25 ^{o}C. The electrical energy for ignition discharged from nichrome wire about 40V.

3.3 Experimental procedure for non-isothermal kinetic study

The experiments were performed using thermogravimetric analyzer METLER TOLEDO, Switzerland (Model noTGA 851e/LF/1100), at three different heating rates i.e.10, 15, 20 ^{o}C min^{-1} under high purity nitrogen atmosphere at a flow rate of 40 mL min^{-1}. The experiments were conducted on the above three biomass within a temperature range of 25 ^{o}C to 900 ^{o}C. The thermogravimetric analysis was performed and the kinetic parameters i.e. activation energy, pre-exponential factor were calculated from various model free methods used in this study.

3.3.1 Kinetic Theory

Thermal degradation of lignocellulosic materials under control environment involves number of reactions in parallel and series listed elsewhere [209], which makes the kinetics very complicated. Therefore a TG analysis is used to obtain kinetic data of various reaction parameters i.e, temperature and heating rate. According to the International Congress on Thermal Analysis and Calorimetry (ICTAC), to estimate kinetic parameters, multiple heating rate method is the best as compared to single heating rate method. In this study, two model-free multiple heating rate methods such as Kissinger and Ozawa were applied to determine the kinetic parameters. These two model-free non-isothermal methods allow determining the kinetic parameters of a solid state reaction without knowing the reaction mechanism and also there is no need to calculate *E* (activation energy) for each conversion in order to calculate kinetic parameters. The Kissinger and Ozawa methods are differential and integral thermal analysis methods respectively, because of their simple and fast calculation and broad adaptation of temperature range these two were frequently used to calculate the kinetic parameters at multiple heating rates [210].

In non-isothermal decomposition of lignocellulosic biomass, the reaction rate is generally expressed by the following expression:

$$\frac{d\alpha}{dt} = K(T)f(\alpha) \qquad \textbf{3-2}$$

where *α, t, K(T), f(α)* represent the degree of conversion of the process, time, temperature-dependent rate constant and differential function of the kinetics mechanism, respectively. α is calculated as follows:

$$\alpha = \frac{m_0 - m}{m_0 - m_f}$$

where, m_0 is the initial mass of the sample, m is the actual sample mass and m_f is the residual mass after thermal degradation.

According to Arrhenius's equation, the temperature-dependent rate constant, *K (T)* is defined as

$$K(T) = Aexp\left(-\frac{E}{RT}\right) \quad \textbf{3-3}$$

where, *A* is the pre-exponential factor, *E* is the activation energy and *R* is the gas constant.

Combining eq (**3-2**) and (**3-3**), it results

$$\frac{d\alpha}{dt} = Aexp\left(-\frac{E}{RT}\right) f(\alpha) \quad \textbf{3-4}$$

Moreover, under non-isothermal conditions the heating rate $\beta = \mathrm{dT/dt}$

Substituting the value of β in eq (**3-4**), it results

$$\frac{d\alpha}{dT} = \frac{d\alpha}{dt}\frac{dt}{dT} = \frac{A}{\beta} exp\left(-\frac{E}{RT}\right) f(\alpha) \quad \textbf{3-5}$$

3.3.1.1 Kissinger Method

Kissinger method of TG analysis is widely used to describe thermal decomposition behavior of biomass [210,211]. A model-free non-isothermal method is developed by Kissinger [212] where there is no necessity to calculate *E* for each conversion value in order to estimate kinetic parameters. In this method the above general rate equation (**3-4**) is differentiated, which results

$$\frac{d[d\alpha/dt]}{dt} = Aexp\left[\frac{E}{RT}\right]\frac{d[f(\alpha)]}{dt} + Af(a)\frac{d[exp[E/RT]]}{dt} \quad \textbf{3-6}$$

where β is the constant heating rate dT/dt and $\frac{d[exp[E/RT]]}{dt} = E\beta/RT^2\, exp\left(-\frac{E}{RT}\right)$

When $T = T_m$, then $\frac{d[d\alpha/dt]}{dt} = 0$ where T_m is the peak temperature of the DTG curve and eq. **3-5** becomes

$$0 = \frac{d[f(\alpha)]}{dt} + f(a)\, E\beta/RT_m{}^2 \qquad \textbf{3-7}$$

$\frac{df(a)}{da} = f'(\alpha)$ then $\frac{d[f(\alpha)]}{dt} = f'\frac{d\alpha}{dT}$ substituting this in equation (**3-6**) yields

$$0 = Aexp\left(-\frac{E}{RT_m}\right) f'(\alpha) + E\beta/RT_m{}^2 \qquad \textbf{3-8}$$

Rearranging the equation (**3-8**) and taking natural logarithm, results

$$\ln\left[\frac{\beta}{T_m{}^2}\right] = \ln\left[\frac{AR}{E}\right] + \ln\left[-f'(\alpha)\right] - \frac{E}{RT_m} \qquad \textbf{3-9}$$

In case of first order reaction, $\ln\left[-f'(\alpha)\right] = 0$ and eq. (**3-9**) becomes

$$\ln\left[\frac{\beta}{T_m{}^2}\right] = \ln\left[\frac{AR}{E}\right] - \frac{E}{RT_m} \qquad \textbf{3-10}$$

eq. (**3-10**) is widely known as Kissinger equation.

By using this method the apparent value of activation energy (E) is calculated from the slope of the plot of $\ln\left[\frac{\beta}{T_m{}^2}\right]$ against 1000/T_m at different heating rates (β) where slope is equal to $-\frac{E}{R}$.

3.3.1.2 Ozawa Method

Ozawa method [213] of TG analysis is also used to describe thermal decomposition behavior of biomass. For non-isothermal conditions, for a given degree of reaction, the analytical integration of above eq. (**3-5**) can result in eq. (**3-11**).

$$g(\alpha) = \frac{A}{\beta}\int_0^T exp\left(-\frac{E}{RT}\right) dT \qquad \textbf{3-11}$$

where $g(\alpha)$ is an integral function of the kinetics mechanism

One of the simplest approximations results to the eq. (**3-12**), which is Ozawa method.

$$\ln(\beta) = \ln\frac{AE}{Rg(\alpha)} - 5.331 - 1.052\frac{E}{RT} \quad \textbf{3-12}$$

By using this method the apparent value of activation energy (E) is calculated from the slope of the plot of $\ln(\beta)$ against $1000/T_m$, which explains the linear relation with a given value of (α) at different heating rates where slope is equal to $-1.052\frac{E}{RT}$.

3.4 Experimental procedure for dilute acid pretreatment of Miscanthus

3.4.1 Chemicals and reagents

Glucose, xylose, arabinose, acetic acid, formic acid, furfural, hydroxymethyl furfural, furfural, were of HPLC grade used as standards in high performance liquid chromatography were purchased from Sigma Aldrich, USA. Sulphuric acid and acetonitrile were of HPLC grade used as mobile phase in high performance liquid chromatography were procured from Spectrochem Pvt. Ltd. Sulphuric acid used for pretreatment, and other chemicals used in these studies were of analytical grade and procured from Merck and Rankem India Ltd.

3.4.2 Substrate

Lignocellulosic biomass (Miscanthus) was used for dilute acid pretreatment. The collection of Miscanthus and preparation of sample for dilute acid pretreatment is described in previous section.

3.4.3 Dilute acid pretreatment

Methodology for dilute acid pretreatment of Miscanthus is presented in Fig 3-2. Dilute acid pretreatment of Miscanthus was carried in 250 mL Erlenmeyer flasks with 100 mL working volume. Miscanthus was pretreated with sulphuric acid in the range 0.5

to 2.5 % (v/v) having solid loading rate in the range 1 to 6 % (w/v) and autoclaved at 121 ^{o}C and 15 psi for range of time (15 to 60 min). After hydrolysis, wet material was filtrated by a vacuum pump to separate solid material from aqueous solution. The solid material was washed with water up to neutral pH, and then dried in an oven at 60 ^{o}C for 12 h. Then some amount of total dried material was weighed and analyzed for carbohydrate and lignin content and remaining part was subjected to enzymatic hydrolysis followed by fermentation. The liquid phase was stored at 4 ^{o}C for analysis of glucose, xylose, arabinose, acetic acid, formic acid, furfural and hydroxyl methyl furfural content.

3.4.3.1 Response surface methodology (RSM)

Response surface methodology (RSM) consists of a group of mathematical and statistical techniques useful for analysis of the effects of several independent variables on response of interest through modeling [214]. Optimization of the variables of the process to get optimum values for response is the main objective of RSM and again it also quantifies interaction among one or more measured responses and the vital input variables [215]. In this study the 16 version of Minitab was used to develop the experimental plan, data analysis and optimization of process variables and response through RSM.

RSM is a sequential procedure. Screening of important parameters obtained either through RSM or other source of knowledge like preliminary experiments or literature. Then suitable model for data analysis and optimization of process parameters and response is selected through considering lack of fit tests and other adequacy measures. Finally graphical optimization method and numerical optimization techniques are used for optimization study [216].

First and second order models are mainly used approximating polynomial models in RSM. Designs used for first-order models are called first-order designs and those used for second-degree models are referred to as second-order designs. 2^k factorial (k is the number of control variables), Plackett–Burman, and simplex designs are mainly used in first-order designs. 3^k factorial, central composite, and the Box–Behnken designs are commonly used in second order designs [214]. The adequacy and significance of the model was justified by the analysis of variance (ANOVA).

In order to determine the optimum settings of the control variables leads to a maximum (or a minimum) response over a certain region of interest requires a 'good' fitting model. In RSM optimization techniques used according to the nature of fitted model. The steepest ascent (or descent) is a main technique used for first order model optimization and the method of ridge analysis is commonly used for second order model optimization. The visualization of the optimization can be obtained by the response surface plot and contour plot. The surface plot is three dimensional plots represent the relationship between the response and independent variables whereas two dimensional contour plot represents three dimensional surface by plotting constant z coordinate slices, called contours [217].

3.4.3.2 Experimental Design for dilute acid pretreatment

Design of experiments and optimization of dilute acid pretreatment process was carried out using RSM. In this study dilute acid pretreatment of Miscanthus was mainly influenced by three independent variables such as autoclaved time (min), acid loading % (v/v) and solid loading % (w/v). For this purpose central composite design (CCD) was adopted as central composite design is well suited for fitting a quadratic surface and usually works well for the process optimization by carrying minimum number of

experiments [218]. Central composite design was employed for above three independent variables, consisting of 20 experimental runs having total blocks one with eight cube points, six axial points (α = 1.68179) and six central points with one replicate. Each variable was studied at two different levels (-1 and 1), two axial points (α = ± 1.68179) and a center point (0) which is the midpoint of each factor range. Crystallinity (%) of dilute acid pretreated biomass and pentose sugar (xylose and arabinose) in g L^{-1} present in hydrolysate was two response variables as these two factors controls the glucose yield and ethanol production. Actual values for experimental range and corresponding levels of independent variables are shown in Table 3-2. After acquiring data related to each experimental point of Central composite design; it is required to fit a mathematical equation to describe the behavior of the response according to the levels of values studied. The interaction of the independent variables and the response variables were described by following second order polynomial.

$$Y = \beta_0 + \sum_{i=1}^{K=3} \beta_i X_i + \sum_{i=1}^{K=3} \beta_{ii} X_i^2 + \sum_{1 \le i \le j}^{K=3} \beta_{ij} X_i X_j + \varepsilon \qquad \textbf{3-13}$$

where Y is the predicted response, K is the number of variables i.e., three. $\beta_0, \beta_i, \beta_{ii}, \beta_{ij}$ are the regression coefficients for intercept, linear, quadratic and interaction terms, respectively, and X_i, and X_j are the independent variables and ε is the residual error associated to the experiments. The regression equation was optimized for maximum value of response variables to obtain the optimum conditions using Minitab version 16. Analysis of variance (ANOVA) was used for data analysis and estimation of statistical parameters. The regression model derived from the coefficients of the model used to calculate the predicted value and variations between predicted value and experimental value were explained by the determination of R^2 value. Response surfaces and two

dimensional contour plots were obtained using the fitted quadratic polynomial equation obtained from regression analysis.

3.4.3.4 Validation of Experiments

Optimal conditions for the crystallinity percentage of pretreated Miscanthus and pentose sugar concentration mg mL^{-1} present in hydrolysate depended on acid concentration; autoclave time and solid concentration were obtained using the predictive equations of RSM. The experimental and predicted values were compared for validation of Experiments.

3.4.4 Analytical Methods

3.4.4.1 High pressure liquid chromatography (HPLC) analysis

The structural carbohydrates and lignin present in raw material and residue obtained after dilute acid treatment of raw material was determined according to the National Renewable Energy Laboratory (NREL, Golden, CO) analytical procedures for biomass [190] and was described in the previous section (Determination of cellulose, hemicellulose and lignin content). The liquids obtained after dilute acid pretreatment of Miscanthus was analyzed for glucose, xylose, arabinose, acetic acid, formic acid, furfural and hydroxyl methyl furfural content. After enzymatic hydrolysis of pretreated Miscanthus, the liquid part was analyzed for glucose.

The quantification of sugars and organic acids was carried out by HPLC system equipped with a refractive index detector (Perkin Elmer Series 200), using Repromer H+, 9 µm (300 × 7.8 mm) column with the following chromatographic conditions: eluent - H_2SO_4 9 mM, flow rate - 0.5 mL min^{-1} at room temperature. Before

injection each samples were filtered through 0.2 µm nylon filter. A complete analysis was carried out by 60 min. Total chrom- Navigator Chromatography data system was used control all the modules of HPLC as well as collect, store and reprocess the data obtained from the detector. The concentration was quantified using average peak areas compared with the standard and expressed as g L^{-1} sugar.

The degraded product like furfural and hydroxy methyl furfural present in liquid part obtained from dilute acid hydrolysis of Miscanthus was quantified by HPLC system equipped with UV detector (Agilent Technologies 1220 Infinity LC) using Eclipse XDB–C18, 5 µm (3 × 150 mm) coulm. UV detection was made at 277 nm at room temperature. The flow rate was set to 1 mL min^{-1} and injections of 20 µL were made. The ratio of acetonitrile and the deionized water was 5% to 95% used as mobile phase. All analytical samples were filtered through 0.2 µm Nylon filters prior to HPLC analysis. A complete analysis was carried out by 20 minute. OpenLab chromatography data system was used control all the modules of HPLC as well as collect, store and reprocesses the data obtained from the detector. Quantification obtained by comparing average peak area with the standards.

The structural carbohydrates (Cellulose and hemicellulose) of the raw material and the pretreated solid were calculated by multiplying the sugar concentration of six and five carbons in the hydrolysates, by the stoichiometric factors 0.90 and 0.88, respectively. The acetyl groups were calculated as the product of the acetic acid concentration by the stoichiometric factor 0.983 [190] .

3.4.4.2 Crystalline structure analysis using X-ray diffraction

The crystallinity and crystalline structure of the Miscanthus samples before and after pretreatment was analyzed by x-ray diffraction (XRD) (Brucker D8 Advanced,

Germany) operating at 40 kW, 40 mA. Dried biomass samples (approximately 0.5 g) were mounted onto a quartz substrate for each analysis. The radiation was copper Kα (λ = 1.5406 Å), and scans were obtained between 5° and 40° with a step size of 0.02° at 1 s per step. The crystallinity of untreated and dilute acid treated biomass was determined and has described in previous section (*Crystallinity Index*).

In this study the average crystallite size was calculated from peak obtained from the 002 lattice plane of biomass samples using the following Scherrer equation. Gaussian function was used for deconvolution of the peak.

$$L = K\lambda/(\beta cos\theta) \quad \textbf{3-14}$$

where θ is the usual Bragg angle corresponding to the (002) plane, λ is the radiation wavelength (0.15406 nm), K is a constant and often taken as 0.9 and β is full width half maximum. Thus, we see that β and L are reciprocally related: the greater the broadening the smaller the crystallite size and vice-versa.

3.4.4.3 Thermogravimetric analysis of the raw material and pretreated raw material

Thermal decomposition of raw sample and pretreated sample was studied and the procedure has described in previous section (Thermogravimetric Analysis).

3.4.4.4 FTIR analysis of the raw material and pretreated raw material

Fourier transform infrared spectroscopy (FTIR) analysis was used for analyzing the chemical structure of Miscanthus sample before and after dilute acid pretreatment and the procedure has described in previous section (FTIR Analysis).

3.4.4.5 Morphological characterization through FESEM

Field Emission Scanning Electron Microscope (FESEM) analysis was conducted to view and compare the morphological structure change before and after dilute acid pretreatment. Firstly, dried samples were mounted on carbon tape coated aluminium stubs and then sputter-coated with gold particles prior to imaging under FESEM (ZEISS, Sigma).

3.4.5 Enzymatic hydrolysis of pre-treated biomass

The residue of Miscanthus obtained at optimized pretreated condition, were hydrolyzed by the enzyme Cellulase (Accelerase 1500, Material Number A30173) was gifted by Genencore International, B.V. (Netherlands). Enzymatic activities (FPU) were measured according to the methods described by NREL standard procedure (NREL, 2007) [219].

In the first study, experiments were performed with 10% (w/v) pretreated biomass loading in sodium citrate buffer (0.05 M, pH 4.8). This solution was supplemented with 0.01% (w/v) sodium azide to prevent hydrolysate from microbial contamination. The enzyme cellulase was added at different loading i.e. 10, 20, 25 FPU g^{-1} (Filter Paper Unit per dry biomass sample). The saccharification was carried out in 250 mL Erlenmeyer flask with 50 mL working volume at 30 ^{o}C and 150 rpm for 84 h, Sample aliquots (1mL) were taken periodically and kept in boiling water bath for 10 minutes and centrifuged. Supernatants were stored at 4 ^{o}C for reducing sugars analysis.

In the second study, hydrolysis was performed at different pretreated biomass loading i.e., 5%, 10 % (w/v) in sodium citrate buffer with optimized cellulase concentration. We applied the same hydrolysis conditions given in the first study.

3.5 Experimental procedure for ionic liquids pretreatment

3.5.1 Chemicals and reagents

The ionic liquids 1-ethyl-3-methylimidazolium acetate ($[EMIM]^+[Ac]^-$), 97%; 1-ethyl-3-methylimidazolium methanesulfonate ($[EMIM]^+[MeSO_3]^-$), ≥95% and 1-ethyl-3-methylimidazolium hydrogen sulphate ($[EMIM]^+[HSO_4]^-$), 95%; *4-nitroaniline*, ≥99%, Reichardt's dye, 90%; Iodoethane, 99% were obtained from Sigma-Aldrich, India. N, N-diethyl-4-nitroaniline was prepared from our laboratory. Analytical grade of sodium citrate, citric acid, sodium hydroxide, sulfuric acid, ethanol, acetonitrile, glucose, and xylose were purchased from Merck, India. Potassium carbonate, 98%, was purchased from HiMedia Labs., India. Commercially available cellulase enzyme (Accelerase 1500, material number A30173) used in this study was supplied by Genencore International, B.V., Netherland.

3.5.2 Substrate

Miscanthus was used for ionic liquids pretreatment. The collection of Miscanthus and preparation of sample for IL pretreatment has described in previous section (Sample collection and preparation).

3.5.3 Kamlet-Taft solvent parameters measurement

The Kamlet-Taft solvatochromic parameters are used for the quantitative measurement of hydrogen bond donating ability (α), hydrogen bond accepting ability (β), and dipolarity/polarizability (π^*) properties of solvents as contributing to overall solvent polarity. In this study Kamlet–Taft parameters of ionic liquids ($[EMIM]^+[Ac]^-$, $[EMIM]^+[MeSO_3]^-$, $[EMIM]^+[HSO_4]^-$) were measured spectrophotometrically at 100 ^oC

using three dyes such as *4-Nitroaniline* (4NA), *N,N-Diethyl-4-nitroaniline* (DENA), and Reichardt's dye (RD). Solutions of these dyes were prepared in ethanol to a concentration of 1 mg mL^{-1}. 2 µL of 4NA, 2 µL of DENA and 20 µL of RD were pipetted into three separate vials (2 mL) and the ethanol was evaporated under vacuum pressure. Dye concentrations of 12 mM, 8 mM, and 28 mM respectively were obtained by adding 1.25 mL of ionic liquid to each vial. The dye was dissolved in an ionic liquid by keeping the solution in a water bath sonicator for 10 minutes and then the solution was vortexed for 10 minutes. Solution was then loaded into a dry quartz cuvette to measure the absorbance spectra at 100 °C between 350 nm and 700 nm using Ultraviolet-Visible spectrophotometer (TMSPC-8, Shimadzu Corporation). Temperature was controlled by a Cary1 1 Peltier temperature controller.

3.5.3.1 Calculation of the Kamlet-Taft Values

The π^* parameter of the ionic liquid was determined from the measured wavelength maximum of *N,N-diethyl-4-nitroaniline* (DENA) in Kilokeyser (kK, 10^{-3} cm^{-1}), using eq. **3-15**:

$$\pi^* = \frac{\nu(\text{DENA})\text{max} - 27.52}{-3.183} \qquad \textbf{3-15}$$

The β value was calculated using the solvatochromic shift of 4-nitroaniline relative to *N,N-diethyl-4-nitroaniline*, eq. **3-16** :

$$\beta = \frac{1.035 \times \upsilon\,(\text{DENA})_{\text{max}} - \upsilon(4\text{NA})_{\text{max}} + 2.64}{2.8} \qquad \textbf{3-16}$$

The α value was calculated by using $E_T(30)$ and π^* values from eq. **3-17**:

$E_T(30)$ = 28591/λ_{max} where λ_{max} is the maximum wavelength of Reichardt's dye in nm.

$$\alpha = \frac{ET(30) - 14.6(\pi* - 0.23) - 30.31}{16.5} \quad \textbf{3-17}$$

3.5.4 Pre-treatment and regeneration of the biomass samples

The methodology for dissolution of Miscanthus using ILs and regeneration of biomass using different anti-solvents towards fermentable sugar production are shown in Fig 3-3. In the present study, three different ionic liquids were used in order to evaluate the effect of different anions on Miscanthus pre-treatment at 100 ^{o}C for 24 h. The chosen ionic liquids were dried in a 105 ^{o}C oven for 24 h. 0.9 g of dried and powdered (particle size of less than 0.25 mm) Miscanthus sample was placed in a test tube and 3 g of ionic liquid was added and mixed well by mechanical stirring using a glass rod for 5 min. The mixture was then covered with aluminium foil and was incubated for 24 h at 100 ^{o}C in a hot air oven. All experiments were carried out in duplicates. A dark viscous Miscanthus suspension was obtained after 24 h pre-treatment. This solution was then cooled to room temperature and the solubilized biomass in ILs was regenerated by precipitation from solutions with anti-solvents. The pre-treated biomass was precipitated by adding approximately 5-fold IL-biomass volume of anti-solvent into the solution with vigorous stirring for 5 min. Deionized water, and water-acetone (1:1, v/v) were used as anti-solvents for precipitating biomass from IL respectively. The residue was then collected by centrifugation of the solution at 6000 rpm for 5 min, further washed with respective anti-solvents, and dried at 90 ^{o}C overnight in the oven. Flow chart for dissolution of Miscanthus using ILs and regeneration of biomass using different anti-solvents followed by enzymatic hydrolysis to produce glucose is show in Fig 3-4.

3.5.5 Compositional analysis of raw and regenerated biomass

Compositional analysis of untreated and IL treated Miscanthus was performed using NREL protocols [190] and was described in the section (Determination of cellulose, hemicellulose and lignin content).

3.5.6 Analytical Methods

3.5.6.1 XRD analysis of raw and regenerated biomass

The untreated and pre-treated Miscanthus were dried and characterized with powder X-ray diffraction (PXRD). The procedure for XRD analyses and Crystallinity index (CrI) has described in the previous section (Crystallinity Index).

3.5.6.2 FTIR analysis of raw and regenerated biomass

The FTIR spectra of the raw and IL pre-treated Miscanthus samples between 500 and 4000 cm^{-1} at 4 cm^{-1} resolution at room temperature were recorded using a FTIR spectrophotometer (Shimadzu, Model-IRAffinity1). All samples were dried and mixed well with potassium Bromide (KBr) for FTIR measurement using diffuse reflectance method. The spectra were presented as relative absorbance percentage (%) of wave number (cm^{-1}). Sets of 30 scans were collected for each sample. An empirical crystallinity index, also known as lateral order index (LOI), was obtained from FTIR spectra by using following equation [220].

$$LOI = A_{1420-1430} / A_{898} \quad \textbf{3-18}$$

where $A_{1420-1430}$ is the intensity of the absorption bands at 1420–1430 cm^{-1} and 897 cm^{-1}.

3.5.7 Enzymatic hydrolysis of raw and regenerated biomass

Enzymatic saccharification of untreated and IL pre-treated Miscanthus was performed using Cellulase enzyme at 50 ^{o}C and 150 rpm in an orbital shaker incubator. The enzyme Cellulase (Accelerase 1500, Material Number A30173) was gifted by Genencore International, B.V. (Netherlands) and Cellulase activity (FPU) was determined based on NREL standard procedure (NREL, 2007) [219]. Cellulase was loaded at 20 FPU g^{-1} substrate. Enzymatic hydrolysis of Miscanthus samples were carried out in 50 mM sodium citrate buffer solution (pH4.8) for 120 h with 5% (w/v) biomass loading. 2% (w/v) sodium azide was added to the reaction medium to prevent the growth of organisms during the digestion. The reaction was monitored by withdrawing aliquots (300 µL) at 12, 24, 36, 48, 60, 72, 84, 96, 108 and 120 h for glucose analysis. The samples were centrifuged at 10,000 rpm for 6 minutes and glucose content was measured using high-performance liquid chromatography (Perkin Elmer Series 200). Analysis was performed on HPLC equipped with an RI detector. Separation was achieved using Repromer H^{+}, 9 µm (300 × 7.8 mm) column. The detail procedure was described in previous section (High pressure liquid chromatography analysis).

3.5.8 Experimental procedure for synthesis of *N, N-diethyl-4-nitroaniline*

3.5.8.1 Synthesis of N, N-diethyl-4-nitroaniline

An oven dried 100 mL round bottom flask (Rb) with magnetic stirrer was charged with 4-nitroaniline (1a) (138 mg, 1 mmol), potassium carbonate (828 mg, 6 mmol) and ethanol (10 mL). Iodoethane (1550 mg, 10 mmol) was added to this reaction mixture. The reaction mixture containing Rb fitted with a reflux condenser was then

placed in a pre-heated oil bath maintained at a temperature of 60 ^{o}C. The progress of the reaction was monitored by TLC (which was prepared by using silica gel 60 F_{254} (0.25 mm). After 48 h, the reaction mixture was cooled to room temperature and admixed with ethyl acetate (40 mL). The ethyl acetate layer was washed two times with brine solution (2 x 10 mL). The ethyl acetate layer was dried over anhydrous Na_2SO_4 and the solvent was evaporated under reduced pressure. The crude product was purified over a column of silica gel (60-120 mess size) and eluted with hexane/ethyl acetate mixture (97:3) to collect pure *N, N*-diethyl-4-nitroaniline.

3.5.8.2 Characterisation of N, N-diethyl-4-nitroaniline

The isolated compound was confirmed by NMR spectroscopy and mass spectrometry. ^{1}H NMR spectra in $CDCl_3$ with tetramethylsilane as the internal standard in 400 MHz and ^{13}C NMR spectra in $CDCl_3$ with tetramethylsilane as the internal standard in 600 MHz were recorded. Mass spectra were recorded using ESI-MS system.

Table 3-1 Scientific nomenclature of lignocellulosic feedstock

Common name	Class	Order	Family	Genus	Scientific name
Miscanthus	Liliopsida	Cyperales	Poaceae	*Miscanthus*	*Miscanthus sinensis*
Castor	Magnoliopsida	Euphorbiales	Euphorbiaceae	*Ricinus* L.	*Ricinus communis*
Jatropha	Magnoliopsida	Euphorbiales	Euphorbiaceae	*Jatropha* L.	*Jatropha curcas*

Table 3-2 Values for experimental range and levels of independent process variables

Independent variables	Symbols	Range and levels				
		-α	-1	0	1	α
Acid loading % (v/v)	A	0.504	0.91	1.505	2.1	2.505
Solid loading % (w/v)	B	0.977	2	3.5	5	6.022
Autoclave Time (min)	C	14.964	24.1	37.5	50.9	60.036

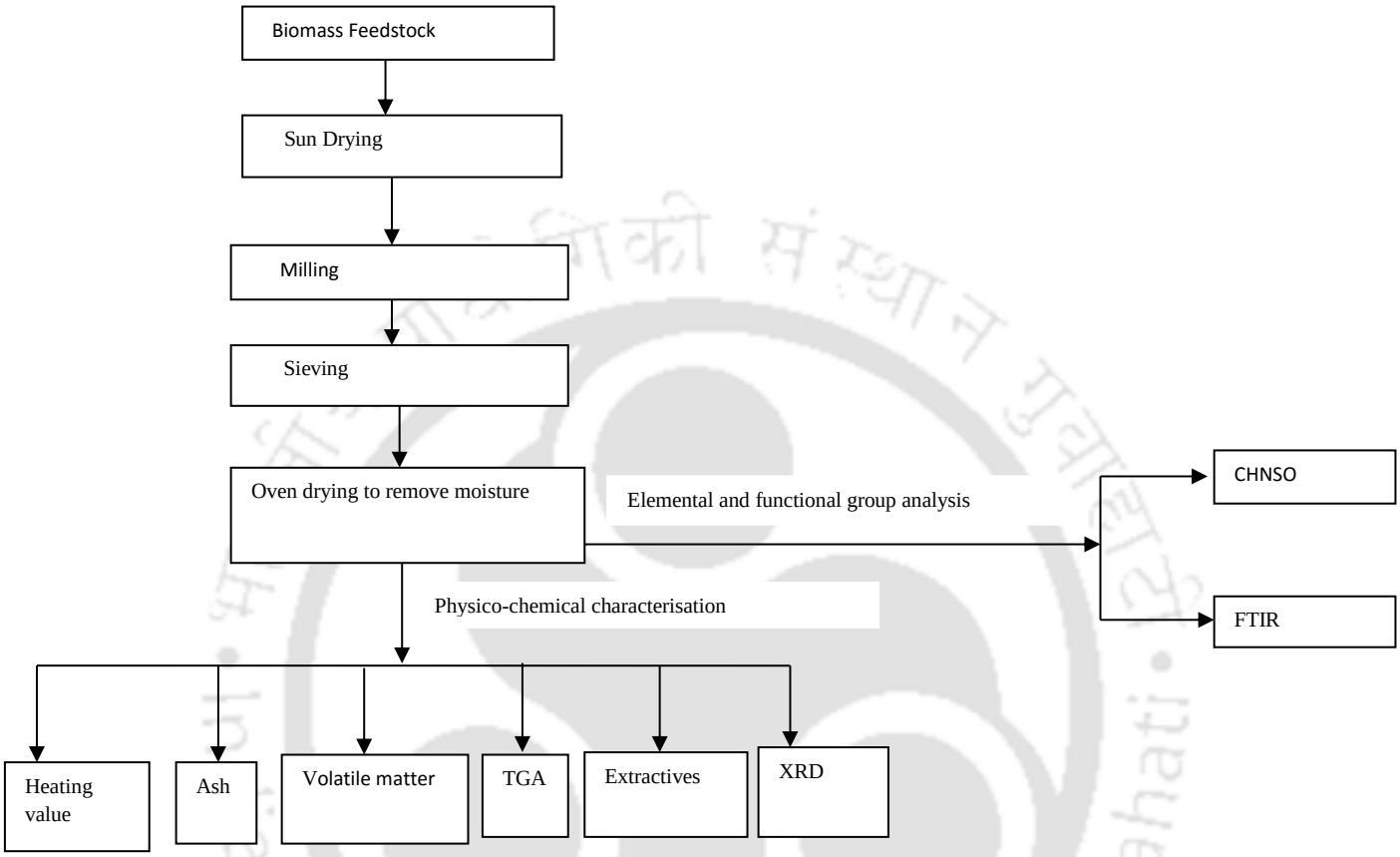

Fig 3-1: Schematic diagram for systematic characterisation of Lignocellulosic biomass

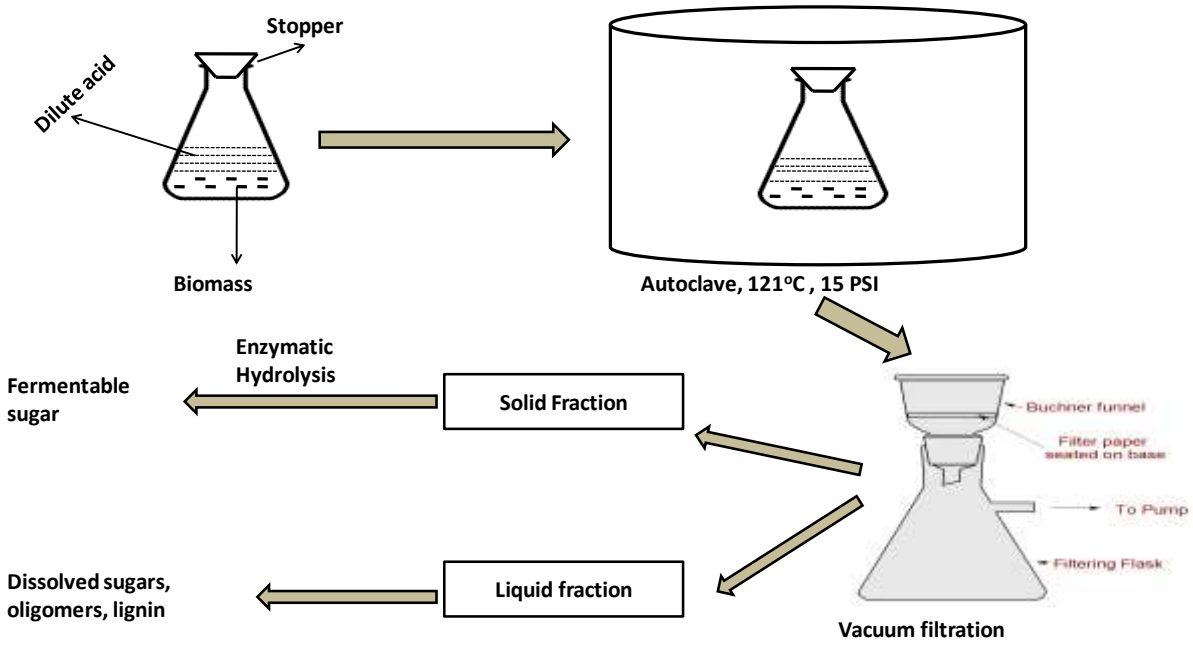

Fig3-2: Methodology for Dilute acid Pretreatment of Miscanthus

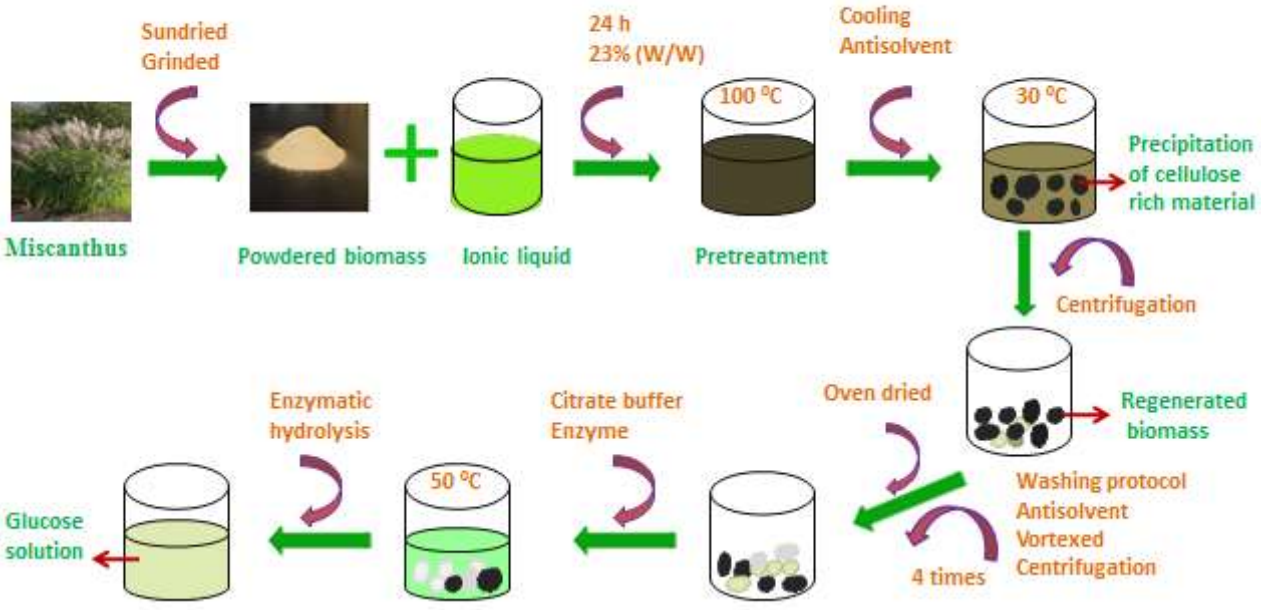

Fig 3-3: Methodology for dissolution of Miscanthus using ILs and regeneration of biomass using different anti-solvents towards fermentable sugar production

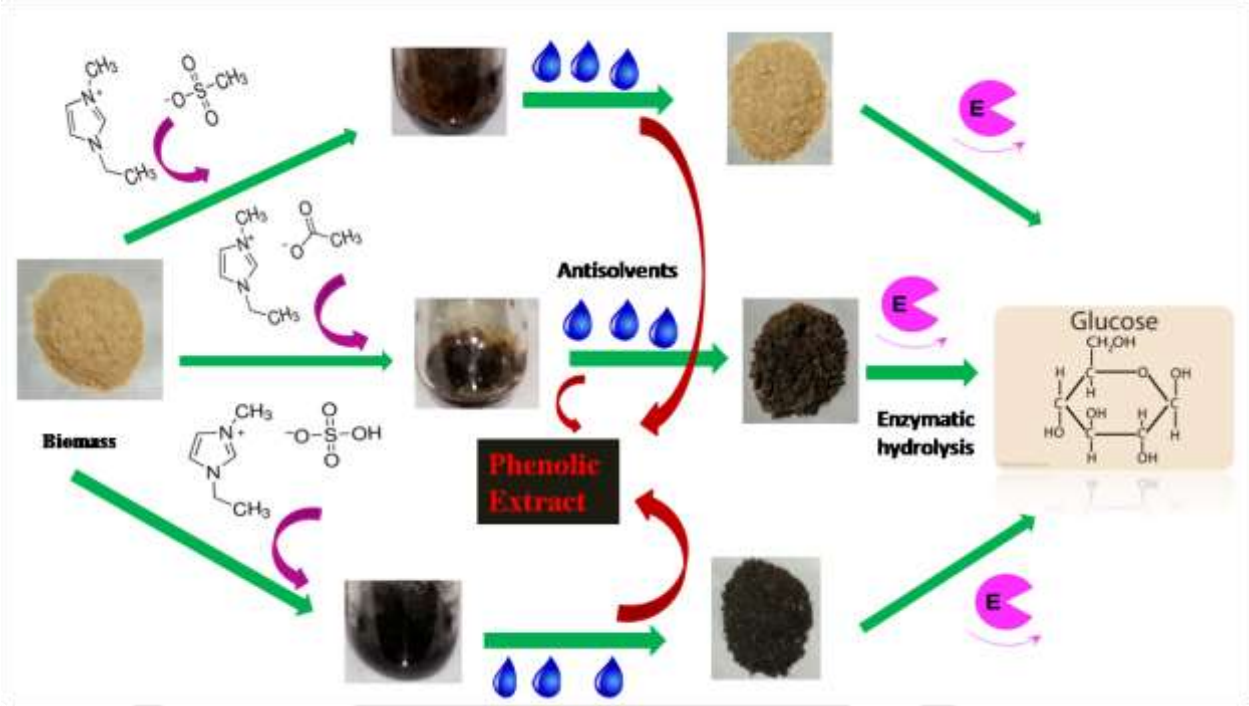

Fig 3-4: Flow chart for dissolution of Miscanthus using ILs and regeneration of biomass using different anti-solvents followed by enzymatic hydrolysis to produce glucose

4 RESULTS AND DISCUSSION

4.1 Characterization of raw materials

The choice of source biomass is governed by the required form of energy, so to get a clear idea, the detail biomass properties towards biofuel production are discussed as follows.

4.1.1 Compositional analysis

Results of compositional analyses for three different lignocellulosic materials were determined and presented in Table 4-1.The quantity of hexane, ethanol and water extracts for three different biomass samples are shown in Table 4-1. Hexane extracts was more for Jatropha, followed by Castor and Miscanthus. So, the non-polar extractive is more in Jatropha. Ethanol extractives represent that Miscanthus contains more polar compounds followed by Castor and Jatropha. Water extractives was more for Jatropha> Miscanthus > Castor. Finally, the total amount of extractive was found to be more for Jatropha > Miscanthus > castor.

Cellulose, hemicellulose and lignin contents for three different biomasses are shown in Table 4-1. Cellulose and hemicellulose content was higher in Miscanthus > Castor > Jatropha. However, lignin content was higher for Jatropha > Micanthus > Castor. The hemicellulose content of Miscanthus was much higher than other two biomasses. The relatively low cellulose and hemicellulose content of Castor and Jatropha compared to that of the Miscanthus, makes Miscanthus more suitable for alcoholic fuel production through biochemical route.

4.1.2 Proximate and ultimate analysis

The proximate and ultimate composition of three lignocellulosic biomasses, i.e., Miscanthus, Castor, and Jatropha are shown in Table 4-2. The volatile matter present in Miscanthus is higher than other two biomasses, whereas the fixed carbon content of Jatropha was higher. Volatile matter and fixed carbon mainly provide information with which the biomass can be ignited and subsequently gasified, or oxidized, depending on how the biomass is to be utilized as an energy source. This type of analysis is also valuable for fuels produced from biomass by biological conversion process [191].

Ash content of Jatropha was higher, i.e., the inorganic material content was higher in Jatropha than Castor and Miscanthus. These inorganic matter content hinder the enzymatic hydrolysis, i.e., saccharification of lignocellulosic biomass [221]. Hence, inorder to reduce ash content, proper washing of lignocellulosic material with water is required to remove the water soluble and loosely adhered inorganic materials using a suitable pre-treatment method.

Moisture content of Castor and Jatropha were similar and higher than Miscanthus, however, the moisture content of all the three biomasses were below 15%. Low moisture content leads to efficient handling, storage and transportation of lignocellulosic biomass [222].

The results obtained for ultimate analysis depicts that carbon, and oxygen are the main components whereas nitrogen and sulphur contents are very low in feedstock which implies that amount of environmental contaminants such as nitrogen oxide (NO_X), hydrogen sulphide, or SO_X emission during the gasification process will be less [185].

4.1.3 Determination of gross calorific value

The calculated calorific value of the Miscanthus, Castor and Jatropha were 20.72 ± 0.2 $mJkg^{-1}$, 17.09 ± 0.2 $mJkg^{-1}$ and 16.33 ± 0.2 $mJkg^{-1}$ respectively. The calorific value is a measure of the energy content, or heating value released when burnt completely. It closely related to the moisture content in biomass and low moisture content can increase the calorific value of lignocellulosic biomass. From above three biomasses, Miscanthus is more suitable for alcoholic fuel production due to its high calorific value.

4.1.4 Thermogravimetric analysis

Thermal decomposition profiles of TGA and DTG of the three biomasses are shown in Figs 4-1 (a) and (b). The TG thermograms of Miscanthus, Castor, and Jatropha showed three weights loss steps, where as their decomposition occurred in two main stages. The first stage of weight loss occurred in the temperature range 40–175 ^{o}C and corresponded to the moisture and other volatile evaporation. Second stage of the decomposition occurred in the temperature range of 175–390 ^{o}C which corresponded to the degradation of structural carbohydrates (hemicellulose and cellulose). The third stage of the decomposition aroused in the range 390–750 ^{o}C mainly due to degradation of cellulose and lignin. Beyond this range, there is no significant loss of weight. Lignin decomposition occurred slowly from ambient temperature to 900 ^{o}C which is explained by Yang etal [137]. The amount of residual char left after 900 ^{o}C for Castor, Jatropha, and Miscanthus are ~21%, ~10%, ~8%, respectively. The TG curves for switch grass, wheatstraw, eastern red cedar and dried distilled grains with soluble given in the literature [223] revealed similar behavior with the TG curves presented here.

The DTG thermogram is representative of the derivative of percentage weight loss per minute. The decomposition profile showed degree of maximum weight loss and its corresponding temperature. Two main peaks were observed for three biomass samples within range 300-310 ^{o}C and 440-480 ^{o}C and information obtained from this study was also useful to estimate approximate amount of cellulose, hemicellulose, and lignin of biomass.

Fig 4-2 shows the values of T-50 and R-50 of sample biomass, from which it is clear that the highest value of R-50 obtained for Miscanthus (0.09 % min^{-1}) followed by Jatropha (0.07 % min^{-1}) and Castor (0.02 % min^{-1}). The T-50 value for Castor was higher than Miscanthus and Jatropha and for three biomasses the values of T-50 ranges from 352-326 ^{o}C. Higher value of R-50 depicts that the biomasses are relatively active at T-50 [224]. Comparative analysis of T-50 and R-50 reveals that higher R-50 value for Miscanthus leads to less T-50 value i.e., more active at this temperature and lower R-50 value for Castor leads to high T-50 value.

4.1.5 X-ray Diffraction (XRD) analysis

Fig 4-3 shows that the X-ray diffraction patterns of Miscanthus, Jatropha and Castor. There are two peaks aroused in the diffraction patterns. The position for prominent peak appeared due to 002 crystalline plane, which varied with biomass: 22.5^{o} for Miscanthus, 22.1^{o} for Jatropha and 22.4^{o} for castor, which is consistent with literatures [225,226]. This peak represents distance between hydrogen-bonded sheets in cellulose I [227]. Another peak aroused at 15.6^{o}, 15.1^{o}, 16.1^{o} for Miscanthus, Jatropha and Castor respectively, which is consistent with the literatures [228,229]. Crystallinity of biomass affects enzymatic digestion of biomass for bioethanol and biohydrogen production, which can be changed by different pre-treatment methods such as thermal,

thermochemical, biochemical, biological etc. The crystallinity index was found to be: Miscanthus (71.73%) followed by Castor (69.4%) and Jatropha (68.94 %), inferred that the crystalline cellulose content was more in Miscanthus than other two lignocellulosic biomasses.

4.1.6 FTIR analysis of raw materials and extractives

The major spectral features of raw biomass and their extracts (hexane, ethanol, water) were studied using FTIR which is shown in Fig 4-4. The absorption peaks were recorded in the 4000–400 cm^{-1} region and major absorption peaks are tabulated in Table 4-3 representing different compounds and bonds associated in these fractions. The raw biomass spectra (Fig 4a) revealed that the broad peak appeared in the range 3797-3012 cm^{-1} due to –OH stretching vibration, and the peak in the region 2800-3012 cm^{-1} due to –CH stretching vibration [185]. An intense peak at 1733 cm^{-1} arouse from the stretching of carbonyls, ketones and esters [187]. The band arouse in the range 1482-1700 cm^{-1} signifying the aromatic ring stretch (mainly due to lignin because protein content of lignocellulosic biomass is insignificant) [185]. The peak arouse at around ~1454, ~1422, ~1320, ~1243 cm^{-1} mainly from lignin, while the peaks around ~1373, 1157, 899 cm^{-1} mostly due to carbohydrates and there was no significant role of lignin [230]. This observation also conclude that lignocellulosic biomass consist of carbohydrates (cellulose, hemicellulose), lignin and extractives. The chemical structure and composition of extractives (hexane, ethanol, and water) will helpful to know the effect of extractives during analysis of structural carbohydrates and lignin, and also for production of green chemicals from extractives. Hence, in order to know the chemical structure and composition of extractives FTIR analysis of extractives carried out.

FTIR spectra of hexane extracts of raw biomasses are shown in Fig 4-4b, a prominent peak at 2850 cm^{-1} and 2920 cm^{-1} originating from aliphatic CH signals due to methylene and methyl functionalities, again bands arouse at 1373-1378 cm^{-1} and 1462 cm^{-1} are also reliable with these functionalities. The strong peak at 1731cm^{-1} represents the carbonyls in esters and/or organic acids [231]. This clearly indicated that mostly aliphatic and nonpolar compounds like wax was extracted during hexane extraction.

Fig 4-4c shows the FTIR spectrum of ethanol extracts of biomasses, obtained after hexane extraction. Ethanol extracts of Castor showed peak at 2851 and 2920 cm^{-1}, whereas in case of Miscanthus peak arouse at 2904 cm^{-1} and for Jatropha, peak arouse at 2900 $cm^{-1}$and there is no peak arouse at around 2850 cm^{-1}, wave number of these band referred to methyl and methylene stretching frequencies. The band at 1056 cm^{-1} and 1504-1508 cm^{-1} correspond to aromatic group [187,231]. From this it is clear that both aliphatic and aromatic, which are mainly polar compounds are extracted during ethanol extraction hence forth the amount of ethanol extractives more than hexane extraction.

Fig 4-4d shows the FTIR spectrum of water extracts of biomasses, obtained after hexane and ethanol extraction respectively. The peak at 879-880 cm^{-1} refers to aromatic hydrogen (C-H) and the peak at 1062-1064 cm^{-1} refers to C–O stretching in aliphatic ether, alcohol and ester [187]. This clearly indicated that during water extraction both aliphatic and aromatic compounds are extracted which remained after hexane and ethanol extraction and are mainly dissolved in water. Due to this it was observed that the biomass having more amounts of ethanol extractives leads to lower amount of water extractive and vice versa.

4.2 Non isothermal kinetic study of raw materials

4.2.1 Effect of temperature and heating rate during thermal degradation

Differential mass loss (DTG) thermograms of thermal decomposition of Miscanthus, Castor and Jatropha at three heating rates of 10, 15 and 20 ^{o}C min^{-1} under nitrogen atmosphere are shown in Fig 4-5(a), Fig 4-5(b), and Fig 4-5(c) respectively. It was found that the first peak show that there was due to an initial loss of moisture from the sample starting at around 25 ^{o}C and continuing up to about 175 ^{o}C. Higher temperature drying (>100 ^{o}C) occurs due to the loss of surface tension bound water of the ground biomass particles (Min, Zhang, & Chen, 2007) [232]. The second peak arouse around 175-380 ^{o}C, which shows mainly decomposition of hemicelluloses. Then next peak was found within 380-570 ^{o}C which showed mainly the decomposition of cellulose. The decomposition of lignin occurred slowly under the whole temperature range from ambient to 900 ^{o}C. It was found that the mass loss rate was higher for hemicelluloses decomposition and lower for lignin decomposition.

The DTG peaks differed in their position and height, because the heating rate was acting as a main factor on thermal decomposition. With increasing the heating rate from 10 to 20 °C min^{-1}, the peak temperature corresponding to the maximum loss of the mass peak also shifted towards a little higher value and also the maximum value of weight loss rate was increased slightly. According to Gao-jin Lv et al. (2010) [233], the heating rate affects the temperature gradient between the outside and the internal parts of the sample. As the heating rate increases, thermal hysteresis increases, which results in DTG curve moving to higher temperature. In case of Miscanthus there was a shoulder peak at 285 °C

which was due to the thermal decomposition of hemicellulose. Similar phenomenon was reported by Varhegyi et al. (1197) [234].

Further the peak heights of the DTG of the Castor, Jatropha and Miscanthus increased with increase in heating rate. According to Zheng and Kozinski (2000), the peak height of the DTG curve is proportional to the biomass reactivity, while the temperature corresponding to peak height is inversely proportional to the reactivity [235].

4.2.2 Kinetic analysis

Thermogravimetric analysis results are elaborated according to Kissinger and Ozawa methods to obtain the activation energy (*E)* and pre-exponential factor (*ln A*). In the first method the activation energy and pre-exponential factor were calculated from eq. **3-10** as described in Chapter 3 (section Kissinger Method). T_m is the peak temperature obtained from Fig 4-5(a), Fig 4-5(b), Fig 4-5(c) for each peak obtained in active pyrolysis zone. ln $\left[\frac{\beta}{T_m{}^2}\right]$ was plotted against 1000/T_m(typical plots shown here, Figs 4-6 (a) and (c) and found to be linear for all the biomass. The resulted linear equations along with the R^2 values are shown in Table 4-4. From these linear equations, the apparent activation energy (*E*) and the pre-exponential factors were calculated and presented in Table 4-5.

In Ozawa method, the activation energy and pre-exponential factor were calculated from eq. 3-12, has described in Chapter 3 (section Ozawa Method). T_m is the peak temperature is obtained from Fig 4-5(a), (b) and (c) for each peak obtained in active pyrolysis zone. Ln β was plotted against 1000/T_m (typical plots shown here, Fig 4-6 (b) and (d)) and found to be linear for all the three biomass. Table 4-6 shows the linear

equations along with the R^2 values. From these linear equations, the apparent activation energy (E) and the pre-exponential factor were calculated and presented in Table 4-7.

In this study, kinetic parameters were calculated separately from two reaction zone as shown in Tables 4-5 and 4-7. It was found that the calculated value of activation energy and pre-exponential factor for all three biomass from Kissinger and Ozawa method do not show much difference, but the fitting degree for Ozawa method was slightly better than the Kissinger method for Miscanthus and Jatropha and same for Castor.

The activation energy for all three biomass for the first reaction zone (568 – 611 K) was found to be within 71.1 and 180.91 kJ mol^{-1} and for second reaction zone (700 – 726 K) it was within 134.86 and 345.6 kJ mol^{-1}. This signifies that in the first reaction zone mainly less thermally stable sugar i.e., hemicelluloses was decomposed and in the second reaction zone more thermally stable sugar i.e., celluloses was decomposed. Further, the activation energy obtained for Miscanthus was lower and Jatropha was higher, which depicts that Miscanthus contains more less stable sugars i.e., hemicellulose than Castor and Jatropha.

4.3 Dilute acid pretreatment of raw Miscanthus

4.3.1 Analysis of effect of parameters through Response Surface Methodology

Dilute acid hydrolysis was evaluated on the basis of the effects of three factors: acid loading (%), treatment time and solid loading (%) as variables for the degradation of carbohydrate and lignin in Miscanthus. In this study dilute sulphuric acid at low concentration (0.5%-2.5%) was used as a catalyst for hemicellulose and lignin solubilisation. Hemicellulose present in biomass is mainly removed through dilute acid

pretreatment and it partially removes lignin. Hence, crystallinity of biomass increases after dilute acid pretreatment as amorphous substances like hemicellulose and lignin are removed. At high crystallinity of dilute acid pretreated biomass, there is less loss of glucose obtained in the filtrate. Hence, crystallinity index (CrI (%)) was taken as one response. For higher yield of bioethanol production through *Saccharomyces cerevisiae* the concentration of hemicellulose should decrease in biomass. Therefore, the concentration of xylose and arabinose present in filtrate after dilute acid hydrolysis (X+A) was taken as another response. The effects of three factors on these responses were investigated using a central composite design (CCD). The experimental value for CrI (%) and (X+A) from different treatment combinations obtained by CCD are presented in Table4-8.

From Table 4-8 it is clear that 0.5% dilute sulphuric acid treatment for 37.5 minutes at 3.5% solid loading gave highest CrI (%). Again Table 4-8 indicated that 0.91% dilute sulphuric acid treatment for 50.9 minutes at 5% solid loading gave highest X+A.

Minitab (16 version) was used for data analysis, analysis of variance (ANOVA), regression coefficients and regression equations. Table 4-9 and 4-10 represents Analysis of Variance for CrI (%) and X+A respectively.

According to Table 4-9, a high F-value (53.00) was obtained, indicating high efficiency of the factors. The P-value (< 0.001), is important to understand the pattern of mutual interactions between the variables and confirmed that the model was statistically significant. The coefficient of variation (R^2) for CrI (%) was 97.95%. The lack of fit test used for testing of model explains p value is 0.259 and it is not significant, which make clear that model appears statistically sound. Analysis of residuals showed no abnormality.

According to Table 4-10, high F-value (94.32) explained high efficiency of the factors and the P-value (< 0.001) demonstrated that the model was statistically significant. Again, the model for X+A did not show any lack of fit and obtained coefficient of variation (R^2) was 98.84%. There was no abnormality during analysis of residuals.

By applying multiple regression analysis to the experimental data, the following polynomial equation was obtained to represent the relationship between the CrI%, acid loading, solid loading and treatment time adequately.

$$Y= 77.258 -1.761\ A+0.586\ S -0.407\ T +0.612\ A^2-1.057\ S^2 -1.801T^2-0.052\ AS -0.532\ AT-0.051\ ST \quad \textbf{4-1}$$

The following polynomial equation was then found using multiple regression analysis to represent the relationship between the X+A (g/L), acid loading, solid loading and treatment time adequately.

$$Y= -13.856+ 5.148\ A+ 5.016\ S+ 0.25\ T -1.138\ A^2 -0.549\ S^2 -0.001\ T^2 -0.04\ AS -0.027\ AT + 0.004\ ST \quad \textbf{4-2}$$

where, A is a coded value of acid loading, S is a coded value of Solid loading and T is a coded value of treatment time. Contour plots or three-dimensional surface plots showing the optimal point can be achieved by solving the above derived polynomial equation using a partially differential equation.

For CrI (%), comparison of the predicted values with the experimentally observed values indicated that these data are in good agreement (Fig4-7). For X+A, obtained in the filtrate indicated that there is reasonable agreement between predicted value and experimental value (Fig 4-8).

The three-dimensional response surface plots demonstrate the effects of independent variables (acid loading, solid loading and treatment time) on the CrI% and X+A shown in Fig 4-9and Fig 4-10 respectively. Three-dimensional response surface plots visualize how the response reacts to changes in the two variables and represents the functional relationship between the response and variables based on the quadratic model equation. To depict the relationship between independent variables and response, one variable should be kept constant while the other two variables were varied at different ranges. The shapes of the response surfaces explain the interaction between different factors.

Fig 4-9 (a) represents the three-dimensional response surface plot of CrI% at a constant solid loading % (3.5) to investigate the effects of acid loading and treatment time on CrI (%). It was found that maximum crystallinity percentage obtained around 0.6% acid loading and 60 minute treatment time. Fig 4-9 (b) shows the effects of acid loading and solid loading at constant treatment time (37.5 min) on CrI%. It was found that maximum crystallinity percentage obtained around 0.6% acid loading and 4.5% solid loading. Fig 4-9 (c) explains the effects of treatment time and solid loading at constant acid loading (1.5%) on the CrI (%). It was found that maximum crystallinity (%) obtained around 3% solid loading and 45 minute treatment time.

The effects of treatment time and acid loading on X+A are shown in Fig 4-10 (a). The maximum X+A was obtained around 2% acid loading and 60 minute treatment time. When solid loading was selected at 3.5% as centre point, the effects of acid loading and solid loading on X+A are shown in Fig 4-10 (b). The maximum X+A was obtained around 4% solid loading and 2.4% acid loading. When treatment time was selected at 37.5 minute as centre point, the effects of treatment time and solid loading on X+A are

shown in Fig 4-10 (c). The maximum X+A was obtained around 4% solid loading and 60 minute treatment time, when acid loading was selected at 1.5% as centre point.

Based on the models, numerical optimisation was carried out with Minitab (version 16) program. Based on maximum goal for CrI (%) and X+A, optimal working conditions and optimum predicted values were obtained and given in Table4-11. The obtained optimal working condition for CrI (%) was, Acid loading % (v/v) = 0.50, Solid loading % (w/v) = 3.98, Treatment Time (min) = 39.09 and the predicted value for this working condition was 82.09. Optimal working condition for X+A was, Acid loading % (v/v) = 1.47, Solid loading % (w/v) = 4.75, Treatment Time (min) = 60.17 and predicted optimum value was 9.61. It was found that optimum value for predicted and experimental are good in agreement.

The composition of filtrate obtained after optimum dilute acid pretreatment working condition for CrI% and X+A are shown in Table 4-12. From this table, it is clear that less amount of glucose was lost for optimum CrI% than optimum X+A. Again less amount of inhibitors (formic acid, acetic acid, furfural, hydroxy methyl furfural) were produced for optimum CrI% than optimum X+A.

4.3.1.2 Compositional analysis of raw and treated biomass

The Miscanthus composition of treated and untreated sample is represented in Table 4-13. Chemical composition of Miscanthus changed after dilute acid pretreatment. There was an increase in percentage of cellulose content in treated biomass sample with comparison to untreated. However, hemi-cellulose and lignin content percentage were reduced. Again, it was found that percentage of cellulose in pretreated Miscanthus (optimised for amount Xylose and Arabinose present in filtrate (X+A) (g/L)) was higher

than pretreated Miscanthus (Optimised for Crystallinity (CrI%)), whereas hemicellulose and lignin content percentage were decreased.

4.3.1.2 X-ray Diffraction (XRD) analysis of untreated and treated biomass

Crystallinity is defined as the fraction of crystalline parts and crystallinity index, was used to describe the percentage of crystalline material in the biomass [206]. XRD analysis (Fig 4-11) showed that the crystallinity index of dilute acid treated Miscanthus was high as compared to the untreated sample. Percentage of crystallinity index for untreated, treated (optimised for amount Xylose and Arabinose present in filtrate (X+A) g/L)) and treated (optimised for crystallinity % (CrI%)) sample was 71.73%, 80.03%, 82% respectively. The results revealed that amorphous part i.e., hemicellulose and lignin removed effectively from treated biomass sample. Percentage of crystallinity index of pretreated biomass (optimised for Crystallinity (CrI%)) was higher in comparison to pretreated biomass (optimised for amount Xylose and Arabinose present in filtrate (X+A) g/L)) because some part of crystalline cellulose hydrolyzed to glucose as glycosidic linkage is susceptible to acid treatment [236]. For which more amount of glucose was present in filtrate of pretreated biomass (Optimised for amount Xylose and Arabinose present in filtrate (X+A) g/L than other pretreated biomass). In case of pretreated biomass having highest crystallinity, imperfect microcrystalline cellulose was hydrolyzed and large perfect cellulose was left.

To determine the crystallite size, the XRD diffractograms were deconvoluted using Gaussian profiles. The crystallite sizes obtained for untreated, treated (optimised for amount Xylose and Arabinose present in filtrate (X+A) g/L)) and treated (optimised for Crystallinity % (CrI%)) sample was 3nm, 3.23 nm and 3.31 nm respectively. This confirms that percentage of crystallinity index increased with increasing crystallite sizes.

4.3.1.3 Thermogravimetric analysis of the raw material and pretreated raw material

The weight loss and derivative (DTG) curves of native and after dilute acid hydrolysis of Miscanthus were shown in Fig 4-12. The thermal stability of treated biomass was improved in comparison to raw biomass. From thermogravimetric analysis (TGA) (Fig 4-12 a), it was found that moisture loss started from room temperature to 105 °C for both treated and raw biomass. Decomposition of hemicellulose and cellulose for raw biomass was focused at temperature of 175- 362 °C with the weight loss of 62%. The effect of dilute sulfuric acid pretreatment contributes to the higher degradation temperature of hemicellulose and cellulose at 185-400 °C. The decomposition temperature was increased due to loss of amorphous hemicellulose and cellulose having imperfect crystalline structure. Degradation of cellulose and lignin of raw biomass was at 360-500 °C whereas degradation of cellulose and lignin of pretreated biomass (CrI%) was at 410- 560 °C and for pretreated biomass (X+A) was at 430-600 °C. The decomposition temperature was increased due to loss of lignin and small amount of cellulose.

In Fig 4-12b, DTG curve represents that the rate of degradation for cellulose and hemicellulose was very high for treated biomass than untreated biomass and peak was shifted towards high temperature. In addition to this narrower peak width suggests a more uniform chemical structure in comparison to untreated biomass. This clearly indicated that there was loss of hemicellulose, and cellulose can be easily degraded at high temperatures. In contrast the rate of degradation of cellulose and lignin of raw biomass was higher than treated biomass but peak was shifted towards high temperature. This happened due to loss of less stable lignin and cellulose. Again the peak arouse for decomposition of cellulose and lignin for pretreated biomass was shifted towards higher

temperature for pretreated biomass (X+A) in comparison to pretreated biomass (CrI %) indicating degradation of backbone of cellulose and lignin.

4.3.1.4 FTIR analysis of the raw material and pretreated raw material

The Fourier transform infrared (FTIR) spectroscopic results of untreated Miscanthus and dilute acid pretreated Miscanthus samples were shown in Fig 4-13. The analysis of samples was based on absorption spectra band for lignocelluloses. The stronger bands of hydrogen bonded (O-H) stretching absorption of cellulose and hemicellulose at 3400 cm^{-1} and C–H stretching of aliphatic (=CH_2 and –CH_3) at 2919 cm^{-1} were found in the pretreated Miscanthus samples compared with untreated Miscanthus. This indicated the removal of lignin from treated biomass. The peaks arouse around 2370 cm^{-1} and 2130 cm^{-1} assigned for glucose ring stretching of cellulose. These two bands are weaker for untreated sample compared with treated samples, indicated the up gradation of cellulose content in treated biomass. The absorbance band of (C=O) of acetyl groups and other carbonyl groups of hemicelluloses at 1740 cm^{-1} were found in untreated Miscanthus became weak in pretreated Miscanthus (CrI%) and almost invisible in pretreated Miscanthus (X+A). This indicated the removal of hemicellulose through dilute acid pretreatment and maximum hemicellulose removed for optimisation condition of (X+A). The weak absorbance peak at 1597 cm^{-1}, 1508 cm^{-1},1420 cm^{-1},1248 cm^{-1} were present in untreated biomass and became weak in treated biomass indicated that there was not complete removal of lignin through dilute acid pretreatment. A prominent and stronger band of (C-O-C) pyranose skeletal vibration at 1050 cm^{-1} and a small stronger band of (C_1- H) deformation with ring vibration and OH bending (which is characteristic of β- glycosidic linkages between glucoses in cellulose) at 900 cm^{-1} were

found in pretreated Miscanthus compared with untreated Miscanthus. This is in reasonable agreement with increase in concentration of cellulose in pretreated biomass.

4.3.1.5 Field Emission Scanning Electron Microscope (FESEM) analysis

The role of various acid pretreatments on the surface morphological ultrastructure was investigated on Miscanthus using FESEM. The surface structure of dilute acid pretreated Miscanthus and untreated Miscanthus was shown in Fig 4-14. Fig 4-14 (a) and (b) presents the FESEM images of untreated Miscanthus. It is clear that the surface of untreated biomass was almost free of trenches and the fibres that make up the structure of biomass were connected very tightly. After acid pretreatment (optimised for maximum CrI%) of biomass, the FESEM image (Fig 4- 14 (c)) presents that many terraces, steps, and kinks on the surface explained that the fibres less tightly connected due to the removal of very reactive amorphous cellulose, solubilisation of hemicellulose and alteration of the structure of lignin. FESEM images of the dilute acid pretreated (optimised for maximum (X+A)) biomass Fig 4-14 (d), presents that terraces, steps, and kinks were almost disappeared, where now numerous different small structures with different shapes observed which explained that the fibres are more less tightly connected than another pretreatment. These structures arouse in the image due to the removal of some part of crystalline cellulose along with amorphous cellulose, hemicellulose and acid soluble lignin. From this it clear that, the dissolution of hemicellulose, acid soluble lignin in the cell wall loosens the structure of the Miscanthus and increasing the available surface area of cellulose for enzymatic hydrolysis.

4.3.2 Enzymatic hydrolysis of pre-treated biomass

In the present study, enzymatic digestibility of dilute acid pretreated Miscanthus was evaluated using cellulase enzyme. Optimum temperature for enzymatic hydrolysis

was found to be 50 °C. However, at 30 °C negligible decrease in sugar yield was observed [237]. Saccharification was carried at 30 °C as this temperature is useful for the SSF process, because high temperature is the limiting factor for yeast growth. The pH 4.8 was optimum, for enzymatic hydrolysis and this pH is also suitable for the SSF process. The performance of the enzymatic hydrolysis was determined by measuring the amount of glucose released from the conversion of cellulose present in biomass at different time interval (Fig 4-15 and Fig 4-16) and this was expressed as the yield of glucose per gram cellulose or per gram biomass (Table 4-14). The optimum reaction time was found to be 72 h, and extending the reaction time to 84 h had no considerable effect on enzymatic hydrolysis.

4.3.2.1 Effect of enzyme concentration on yield of fermentable sugar

To characterize the effects of enzyme (Accelerase®1500) loading on enzymatic hydrolysis of dilute acid pretreated biomass, the reaction was carried out at different enzyme loading (10, 20, 25 FPU/g dry pretreated biomass) with 10% solid loading (Fig 4-15). Accelerase®1500 is a cellulase complex supplemented with exoglucanase, endoglucanase, hemicellulase and β-glucosidase produced from a genetically modified strain of *T. reesei*. In Fig 4-15, CrI represents pretreated biomass obtained at optimised condition for highest crystallinity and (X+A) represents pretreated biomass obtained at optimised condition for highest xylose and arabinose present in liquid fraction after dilute acid pretreatment. Fig 4-15 indicated that more glucose was released at 20 FPU/ g dry biomass enzyme loading i.e. 40.26 g L^{-1} released from CRI and 54.112 g L^{-1} released from (X+A). Table 4-14 summarizes the glucose yield from enzymatic hydrolysis at different condition. From Table 4-14 it is clear that glucose yield was higher for 20 (FPU/g dry biomass) enzymes loading. Again it was found that for (FPU/g dry biomass)

enzyme loading and 10% solid loading, glucose yield was higher for X+A in comparison to CrI i.e 0.68 and 0.51 (g/g cellulose), 0.54 and 0.4 (g/g dry biomass) respectively. Low glucose yields from the enzymatic hydrolysis of CrI can be explained due to the higher lignin and xylan content in comparison to X+A. In addition to this, crystallinity percentage of CrI was little higher than X+A. Generally, the acid-catalyzed reaction decomposes the surrounding xylan, acid-soluble lignin and the cellulose fibers present in raw materials. The removal of xylan and lignin results extensive changes in the structure and accessibility of cellulose and lignin preventing enzyme loss by unproductive binding with enzyme [238]. Crystallinity of lignocellulosic biomass played a major role in limiting hydrolysis in some studies [239,240], whereas other studies have shown that, when all other factors of biomass are similar, the degree of crystallinity has no significant effect on enzymatic hydrolysis [241].

4.3.2.2 Effect of substrate concentration on yield of fermentable sugar

To study the effect of solid loading (dilute acid pretreated Miscanthus) on enzymatic hydrolysis the reaction was carried out at different solid loading (5 and 10 % (w/v)) with 20 (FPU/g dry pretreated biomass) enzyme loading (Fig 4-16). It was found that (Fig 4-16) glucose produced from CrI with different substrate concentrations, i.e. 5%, 10% (w/v) was 24.03 mg mL^{-1} and 40.26 mg mL^{-1} respectively and glucose produced from X+A with different substrate concentrations, i.e. 5%, 10% (w/v) was 54.11 and 31.89 mg mL^{-1}respectively. Table 14, listed glucose yield for CrI and X+A with different substrate concentrations, i.e. 5%, 10% (w/v). It was found that glucose yield via enzymatic hydrolysis was higher for 5% (w/v) substrate concentration in comparison to 10% (w/v) substrate concentration. The cause of decreased cellulose hydrolysis with increased solid concentration can be explained due to mass transfer

limitations or non-productive adsorption of enzymes. Glucose yield via enzymatic hydrolysis at high solid loadings can be increased using an extra pre-treatment step to remove more lignin and therefore minimize the non-specific binding of enzymes with lignin [242].

4.4 Ionic liquids pretreatment and regeneration of raw Miscanthus

4.4.1 Selection of solvents

One of the most important job is to select proper RTILs for the pre-treatment of Miscanthus. Screening is complicated, but to start with, we focused more on the RTIL composition and their effect on sugar yield through enzymatic hydrolysis. An RTIL is a salt that melts below 100 ^{o}C, shows high thermal stability, and negligible vapour pressure. Liquid properties such as viscosities, melting point, polarity, and hydrogen bond basicity are important for the lignocellulosic biomass pre-treatment. These properties of ionic liquids are controlled by the selection of the anion and cation. For this reason, ionic liquids have been termed as "designer solvents" [243]. To understand the effect of anionic part of ionic liquid on the dissolution of Miscanthus, our search narrowed down to three RTILs viz. $[EMIM]^{+}[Ac]^{-}$, $[EMIM]^{+}[MeSO_3]^{-}$ and $[EMIM]^{+}[HSO_4]^{-}$, all of them contain immidazolium cation along with three distinct anions. The structure and solvent properties (i.e., relative density, melting point, flash point and pH) of these three RTILs as specified by the manufacturer Sigma-Aldrich are summarized in the supporting information. From the Table 4-15 it can be seen that the relative density at 25 ^{o}C increased in the following order $[EMIM]^{+}[Ac]^{-}$ $<[EMIM]^{+}[MeSO_3]^{-}<[EMIM]^{+}[HSO_4]^{-}$. $[EMIM]^{+}[HSO_4]^{-}$ is a very thick solvent compared to the other two ILs and the density is in the following order: $[EMIM]^{+}[Ac]^{-}<$

$[EMIM]^+[MeSO_3]^-$<$[EMIM]^+[HSO_4]^-$. Moderate pH value (5.4) and lower thickness of $[EMIM]^+[Ac]^-$ solvent makes it more suitable to handle.

4.4.1.1 Solvent parameters (Kamlet-Taft parameters) measurement of selected Ionic liquids

In this study, relative dissolution capacity of above three RTILs for Miscanthus was evaluated through Kamlet-Taft solvent parameters. The Kamlet-Taft solvatochromic parameters (α, β, π^*) for each RTIL at 100 ^oC are summarized in Table 4-16. From the table, it is clear that the value of β for $[EMIM]^+[Ac]^-$ was higher than $[EMIM]^+[MeSO_3]^-$ and $[EMIM]^+[HSO_4]^-$ and again the value of β for $[EMIM]^+[MeSO_3]^-$ was little higher than $[EMIM]^+[HSO_4]^-$. The π^* value was high for all the three ionic liquids. Reichardt's dye did not produce a signal in $[EMIM]^+[MeSO_3]^-$, so α was not determined for this RTIL and for $[EMIM]^+[HSO_4]^-$, the value of α value was found to be very low, whereas $[EMIM]^+[Ac]^-$ reported a moderate α value.

As the disruption of the inter- and intra-molecular hydrogen bonding in cellulose, hemicellulose and lignin is the key to its dissolution mechanism, thus, a good RTIL for dissolution of biomass is one which contains a strong H-bond acceptor and a moderate H-bond donor [244]. Our results show that large H-bond acceptor capacity and moderate H-bond donor capacity of $[EMIM]^+[Ac]^-$ makes it suitable for cellulose dissolution in Miscanthus than that of $[EMIM]^+[MeSO_3]^-$ and $[EMIM]^+[HSO_4]^-$.

4.4.1.2 Effect of anions on composition of regenerated biomass

As discussed under materials and methods section, 23% of Miscanthus sample pre-treated by RTIL at 100 ^oC for 24 h was cooled to room temperature and precipitated

out using water and water-acetone mixture (1:1 v/v). It was previously reported that the glucan content of the regenerated solid was higher (68%) after [C_2mim][OAc] pre-treatment at 3 wt% biomass loading when compared to that of untreated switch grass (35%) [245]. Further increasing the biomass loading during [C_2mim][OAc] pre-treatment resulted in a monotonic decrease of the relative glucan content in the regenerated solids and an increase in the xylan and lignin content of the recovered biomass [246]. Wang et al. observed that anti-solvents, such as, the addition of dimethyl sulfoxide (DMSO) to water was effective in increasing the cellulose content in regenerated biomass [247]. Table 4-17 presents the effect of anions and anti-solvents on the compositions of regenerated Miscanthus. Table 4-17 confirms that high cellulose with low lignin content increased in the following order $[EMIM]^+[HSO_4]^-$> $[EMIM]^+[MeSO_3]^-$> $[EMIM]^+[Ac]^-$. This behaviour could be explained due to the difference in hydrogen bond basicity (β) of anions present in RTILS at 100 ^oC. It was found that RTIL having lower β value was responsible for higher cellulose with low lignin content and vice versa. Unlike cellulose and lignin, the removal of hemicellulose was possibly due to the hydrolysis of hemicellulose during pre-treatment process instead of dissolution of hemicellulose in ionic liquid [166]. Hemicellulose content of regenerated biomass increased in the following order $[EMIM]^+[HSO_4]^-$ < $[EMIM]^+[MeSO_3]^-$ < $[EMIM]^+[Ac]^-$. This behaviour could be contributed to the efficient removal of lignin at a particular pre-treatment condition. This in turn increased the exposure of hemicellulose to hydrolysis or auto-hydrolysis process since lignin and hemicellulose are closely bound to each other in the biomass matrix.

4.4.1.3 Effect of anti-solvents on the composition of regenerated biomass

Anti-solvent effect was observed when water and acetone-water mixtures were used to precipitate biomass successively and the results are shown in Table 4-17. Regenerated biomass from $[EMIM]^+[Ac]^-$ mixture using water as anti-solvent resulted in high cellulose (47.5%), hemicellulose (22.78%) and lignin (14.7%) content in comparison to acetone-water (1:1, v/v) as anti-solvent. The results confirmed that more cellulose, lignin and hemicellulose were dissolved in the anti-solvent during the regeneration process. It was observed that the hydrogen bonds between ionic liquid and cellulose were disrupted by the addition of anti-solvents and the hydrogen bonds in cellulose-cellulose system were formed again, resulting in the regeneration of the cellulose [175]. It was found that cellulose (48.5%) as well as hemicellulose (21.32%) content increased and lignin content decreased (8%) in the regenerated biomass when $[EMIM]^+[MeSO_3]^-$ ionic liquid was used along with acetone-water (1:1, v/v) as anti-solvent. However, when water was used as anti-solvent for the same ionic liquid, the lignin content in regenerated Miscanthus was found to be higher than acetone-water mixture. Exactly similar trend was noticed for $[EMIM]^+[HSO_4]^-$ pre-treatment along with water and acetone-water mixture as anti-solvents. For $[EMIM]^+[MeSO_3]^-$ and $[EMIM]^+[HSO_4]^-$ system, high cellulose and hemicellulose content of regenerated biomass was probably due to the greater lignin solubilisation in acetone-water (1:1, v/v) anti-solvent. From the above, it was confirmed that acetone-water (1:1, v/v) mixture as anti-solvent was more effective than water for delignification of regenerated Miscanthus.

4.4.1.4 Effect of anion and anti-solvents on dissolution and regeneration of Miscanthus

The dissolution of Miscanthus in three different RTILs was followed by regeneration using water and water-acetone mixture (1:1 v/v). Table 4-18 shows the percentage of mass removed from the original biomass by both water and water-acetone mixture for each RTIL for the same pre-treatment condition. Dissolution of Miscanthus in $[EMIM]^+[Ac]^-$ removed approximately 5.5% mass of the untreated Miscanthus using water as anti-solvent whereas water-acetone mixture removed 7.5% of the original mass. However, in case of other two RTILs, the mass removal was less for water-acetone mixture than that of only water as anti-solvent. Though the exact mechanism for the same is not clear, it may be concluded that some components of the Miscanthus other than cellulose, hemicellulose and lignin were probably dissolved in water-acetone mixture. Further, from Table 4-18, it can be seen that the type of anions had a direct effect on the lignin removal. The lignin removal was in the following order: $[HSO_4]^-$> $[MeSO_3]^-$ > $[Ac]^-$. It can be concluded that the percentage of mass removed was directly depended on the percentage of lignin removed. In other words, greater lignin removal percentages lead to greater mass removal of treated biomass.

4.4.1.5 Effect of anion on the cellulose crystallinity of pretreated Miscanthus

To evaluate the role of anions in the ionic liquid on crystallinity of Miscanthus, the precipitates obtained after 24 h treatment at 100 ^oC followed by washing with anti-solvents and drying were analysed using XRD. The X-ray diffraction patterns of the raw and RTIL treated Miscanthus were illustrated in Fig 4-17a and b. Table 4-19 reports the fermentable sugar yields, saccharification rates, and crystallinity index of Miscanthus treated with IL at 100 ^oC for 24 h. From the Table 4-19, it is clear that crystallinity index

of RTIL treated and untreated Miscanthus decreased in the following order: Untreated>$[EMIM]^+[HSO_4]^-$> $[EMIM]^+[MeSO_3]^-$> $[EMIM]^+[Ac]^-$. In other words, this sharp decrease in crystallinity was due to the $[EMIM]^+[Ac]^-$pre-treatment which confirmed that the regenerated products were highly amorphous. Hence, it was concluded that ionic liquid with highest value of β parameter (in this case $[EMIM]^+[Ac]^-$) was responsible for greater degree decrystallization of Miscanthus.

4.4.1.6 Effect of anti-solvent on the cellulose crystallinity of pretreated Miscanthus

From Fig 4-17a and b, XRD pattern for raw Miscanthus had an intense primary peak at 2θ angle 22.04° corresponds to the (200) plane of crystals, the diffraction peaks of the (110) and (110) planes merged together at 2θ=15.89° and the diffraction peak (004) at 34.68^o was very weak, indicated the characteristic diffraction pattern of crystalline cellulose of native biomass. The crystallinity Index (CrI) of untreated Miscanthus was 71.73%. For regenerated Miscanthus from $[EMIM]^+[Ac]^-$ mixture using water as anti-solvent, the main peak at 22.04^o disappeared and a broad asymmetric peak consisting of a doublet at 20.6^o and 20.9^o appeared. The broad peak at 15.89° disappeared, and new peaks at 12.22^o, 14.8^{o}and 17.87^o appeared whereas the small peak at ~34^o was broadened. A more flat XRD diffraction pattern was obtained for regenerated Miscanthus from $[EMIM]^+[Ac]^-$ mixture using acetone-water (1:1 v/v) as anti-solvent in comparison to water as anti-solvent. In this diffraction pattern the primary peak splitted into two weaker peaks located at 20.21^o and at 21.39^o and other small peaks arouse at 11.87^o, 14.9^{o}and 18.66^o. The small peak at ~34^o was almost disappeared. The changes in diffraction pattern for both regenerated Miscanthus indicated a transformation from cellulose I to cellulose II [248]. A quite flat diffraction pattern was obtained for both regenerated biomass which indicated an amorphous structure [249]. Again CrI of

the regenerated biomass from $[EMIM]^+[Ac]^-$ ILs using water as anti-solvent was 25.5%, whereas CrI of the regenerated biomass from $[EMIM]^+[Ac]^-$ RTIL using water-acetone (1:1, v/v) as anti-solvent was 21.08%. It was hypothesized that, in this reaction system polarity and protic nature of water decreased with addition of acetone, making the reaction medium conducive for further swelling and dissolution of cellulose in water-acetone mixture. For regenerated Miscanthus from $[EMIM]^+[MeSO_3]^-$ mixture using water as anti-solvent and regenerated Miscanthus from $[EMIM]^+[MeSO_3]^-$ mixture using water-acetone as anti-solvent, the primary peak arouse at ~22.04^o and the secondary peak arouse at ~15.89^o. XRD diffraction pattern was more broadened for regenerated biomass through water-acetone anti-solvent in comparison to water anti-solvent. The small peak at ~34.68^o was noticed for water washing regenerated biomass and almost vanished in water-acetone washing regenerated biomass. The CrI obtained for regenerated biomass through water anti-solvent and water-acetone anti-solvent were 54.31% and 50.85% respectively. Thus, it was clear that small amount of cellulose II was present in regenerated biomass after water-acetone washing because of swelling of crystalline cellulose (cellulose I) in this reaction system. XRD pattern for regenerated Miscanthus from $[EMIM]^+[HSO_4]^-$mixture using water anti-solvent and regenerated Miscanthus from $[EMIM]^+[HSO_4]^-$ mixture using water-acetone anti-solvent were found to be similar with untreated Miscanthus. However, there is decrease in the intensities of the (002) diffraction peak as observed for both regenerated biomass in comparison to untreated Miscanthus. The CrI obtained for regenerated biomass after water anti-solvent and water-acetone anti-solvent were 59.92% and 58.01% respectively. In this reaction system there is not much difference in crystallinity because it was hypothesized that, there was swelling of very little amount of crystalline cellulose (cellulose I) in comparison to cellulose II in regenerated biomass from water-acetone anti-solvent.

4.4.1.7 Effect of cellulose content on crystallinity of regenerated biomass

It was observed from Table 4-17 that, cellulose content in pre-treated biomass with three different ILs increased in the following order $[EMIM]^+[HSO_4]^-$> $[EMIM]^+[MeSO_3]^-$> $[EMIM]^+[Ac]^-$. Comparing the cellulose content with CrI data obtained from XRD (Table 4-19), it was found that higher cellulose content lead to higher crystallinity. However, Table 4-19 also confirmed that there is different trend among these three ILs when two different anti-solvents were considered. The CrI obtained for the regenerated biomass treated with $[EMIM]^+[Ac]^-$ using water and water-acetone anti-solvents were 25.5%, and 21.08% respectively. The respected cellulose content for both the anti-solvent regenerated biomass were found to be 47.5% and 40% respectively which indicated that the crystallinity was higher for recovered biomass with high cellulose content as mentioned in the beginning of this section. However, for other two anions based ILs such as $[EMIM]^+[HSO_4]^-$ and $[EMIM]^+[MeSO_3]^-$, it was observed that the higher cellulose content resulted in decreased CrI value for water-acetone anti-solvent in comparison with water anti-solvent (Table 4-19). The decrease in CrI may be attributed to the presence of more amount of hemicelluloses and less amount of lignin. Increase in hemicellulose content has made the biomass more amorphous in nature, thus, the reduced CrI. This result was also supported by the work of Xu et al. who confirmed that more hemicellulose content resulted in a reduced CrI for the biomass studied [203]. From the above discussion, it can be noted that the CrI calculated from XRD data was related to the chemical composition of biomass. In the subsequent section, the crystallinity calculated from FTIR was presented and compared with that obtained from XRD.

4.4.1.8 FTIR analysis

To get more insights in to the effects of ionic liquid pre-treatments, the chemical structure of untreated and ionic liquid treated Miscanthus samples were analyzed using FTIR. The spectra of regenerated Miscanthus from the ionic liquids using different anti-solvents and untreated Miscanthus are presented in Fig 4-18. In Table 4-20, the absorption bands at 897 cm^{-1}, 1056 cm^{-1}, 1160 cm^{-1}, 1235 cm^{-1}, 1318 cm^{-1}, 1372 cm^{-1}, 1457 cm^{-1}, 1508 cm^{-1}, 1733 cm^{-1} and 2918 cm^{-1} are associated with native Miscanthus lignocelluloses. As shown in Fig 4-18 and supporting information, the spectra generated for regenerated samples and untreated Miscanthus were similar, however, some small differences were observed.

The presence of cellulose II and decreased cellulose crystallinity also reduced C-H stretching at 2896 cm^{-1}, where broadening of this band indicated higher amorphous nature of the regenerated cellulose [250]. A broad absorption band at ~2896 cm^{-1}, appeared in the regenerated biomass from $[EMIM]^{+}[Ac]^{-}$ mixture with water as anti-solvent and the regenerated biomass from $[EMIM]^{+}[Ac]^{-}$ mixture with acetone-water mixture (1:1 v/v) as anti-solvent. A small peak arouse at ~2896 cm^{-1} in the untreated biomass and regenerated biomass from other two ILs with different anti-solvents, suggested the presence of more amorphous cellulose in $[EMIM]^{+}[Ac]^{-}$ treated biomass. The almost disappearance of absorption band at 1457 cm^{-1} in RTIL treated biomass suggested the removal of lignin in regenerated biomass. A strong peak at 1733 cm^{-1} described the presence of C=O in xylan acetates (hemicelluloses) in untreated and RTIL treated Miscanthus [251].

The absorbance band at around 1420 – 1430 cm^{-1} is associated with the amount of the crystalline structure of the cellulose, while the band at 898 cm^{-1} is sensitive to the

amount of the amorphous region in cellulose [252]. Using the FTIR data, LOI was calculated which is related to the existence of cellulose I and its conversion to amorphous cellulose or cellulose II. Higher LOI values indicate the higher degree of crystallinity (more ordered cellulose structure) [253]. Table 4-19 reported the LOI values of treated and untreated Miscanthus. LOI showed higher value for untreated Miscanthus (0.75) compared to the regenerated material using the three ILs. These results indicate that the IL treatment of Miscanthus promote the conversion of cellulose I to cellulose II or amorphous cellulose. The LOI values of RTIL treated and untreated Miscanthus is in the following order: Untreated > $[EMIM]^+[HSO_4]^-$> $[EMIM]^+[MeSO_3]^-$> $[EMIM]^+[Ac]^-$ This sharp decrease in LOI was due to the $[EMIM]^+[Ac]^-$ pre-treatment which confirmed that the regenerated products contained higher amount of cellulose II or amorphous cellulose. It was also concluded from XRD data that the regenerated Miscanthus from $[EMIM]^+[Ac]^-$ has lowest crystallinity and products were highly amorphous.

The LOI obtained for untreated Miscanthus (*Miscanthus sinensis)* is in good agreement with reported LOI for *Miscanthus giganteus* and wheat straw [254]. The LOI of $[EMIM]^+[Ac]^-$ treated Miscanthus using water as anti-solvent was higher (0.47) in comparison to acetone-water as anti-solvent (0.44). The same trend was also observed for the regenerated samples using the other two ILs, $[EMIM]^+[MeSO_3]^-$ and $[EMIM]^+[HSO_4]^-$ for the same two anti-solvents. From this discussion it can be concluded that regenerated samples using water as anti-solvent contained more cellulose chains in a highly organized form than the regenerated samples using water-acetone as anti-solvent. XRD data also correlated well with this observation.

Again among the three ionic liquids studied, $[EMIM]^+[HSO_4]^-$ is more acidic. The acidity of RTILS decreased in the following order $[EMIM]^+[HSO_4]^-$> $[EMIM]^+[Ac]^-$> $[EMIM]^+[MeSO_3]^-$. The pH of three RTILs is given in the Table 4-15.

The effect of IL acidity can be confirmed from that fact that $[EMIM]^+[Ac]^-$ having moderate acidity (pH = 5.4) was the best in terms of reducing Miscanthus crystallinity as well as low LOI. The other two ILs, $[EMIM]^+[HSO_4]^-$ (pH=1.0) and $[EMIM]^+[MeSO_3]^-$ (pH=6.5) have lesser effect on reduction of cellulose crystallinity and LOI values than $[EMIM]^+$ $[Ac]^-$. However, type of biomass and pre-treatment conditions highly affect the crystallinity of treated biomass [253].

4.4.2 Saccharification of treated and untreated Miscanthus

4.4.2.1 Effect of anion on the saccharification rate and glucose yield of pre-treated Miscanthus through enzymatic hydrolysis

In the present study, glucose release rate and glucose yield were used to evaluate the enzyme digestibility performance of RTIL treated and untreated Miscanthus. Enzymatic hydrolysis of Miscanthus treated with the ionic liquids was carried out to produce reducing sugars (mainly glucose) using commercial cellulase enzyme. From Fig4-19a, it was clear that the rate of enzymatic hydrolysis of regenerated Miscanthus was highest for 24 h of process and then decreased. Fig4-19b showed that the maximum yield of glucose was obtained at 96 h of enzymatic hydrolysis of regenerated Miscanthus from $[EMIM]^+[Ac]^-$ mixture. Similarly, the maximum yield of glucose for $[EMIM]^+[MeSO_3]^-$ and $[EMIM]^+[HSO_4]^-$ treated RTIL was obtained at 108 h of enzymatic hydrolysis. The maximum yield of glucose for untreated Miscanthus was also obtained at 108 h. Table4-19 showed that the rate of enzymatic hydrolysis of regenerated Miscanthus was improved significantly after the treatment with RTIL $[EMIM]^+[Ac]^-$ followed by $[EMIM]^+[MeSO_3]^-$ and $[EMIM]^+[HSO_4]^-$. The amount of glucose liberated from RTIL treated and untreated Miscanthus decreased in the following order: $[EMIM]^+[Ac]^- > [EMIM]^+[MeSO_3]^- > [EMIM]^+[HSO_4]^-$ > Untreated.

4.4.2.2 Effect of anti-solvent on the saccharification rate and glucose yield of pretreated Miscanthus through enzymatic hydrolysis

IL treated biomass that was regenerated from reaction mixture using anti-solvent was washed for five times with the same anti-solvent followed by drying and enzymatic hydrolysis. Fig 4-19a showed that enzymatic hydrolysis rate was lower for regenerated Miscanthus using water as anti-solvent in comparison to acetone-water mixture (1:1 v/v). Fig 4-19b presented that glucose yield through enzymatic hydrolysis was lower for regenerated Miscanthus using water as anti-solvent in comparison to acetone-water mixture (1:1 v/v). However, the exact mechanism of this hydrolysis was not clear. Probably acetone-water mixture as anti-solvent washed away more inhibitors and lignin from regenerated Miscanthus generated after IL treatment of biomass.

4.4.2.3 Effect of Lignin removal on enzymatic hydrolysis

Fig 4-21 represents that almost lignin removal from the Miscanthus was observed after treatment with $[EMIM]^+[HSO_4]^-$ followed by $[EMIM]^+[MeSO_3]^-$ and $[EMIM]^+[Ac]^-$. However, the highest cellulose digestibilities and glucose yield were obtained for $[EMIM]^+[Ac]^-$ treated biomass followed by $[EMIM]^+[MeSO_3]^-$ and $[EMIM]^+[HSO_4]^-$. It is well known that lignin plays an inhibitory role for limiting cellulose hydrolysis; however, in the present study there is a mismatch of lignin removal with respect to cellulose digestibilities and glucose yield. This means that at highest lignin removal, the cellulose digestibilities as well as glucose yield was not the highest. This suggests that the enzymatic saccharification was being inhibited, perhaps by incomplete removal of the inhibitors as well as affected by other factors such as cellulose structure, crystallinity and amount of hemicellulose present in the regenerated biomass.

4.4.2.4 Effect of cellulose structure and crystallinity on enzymatic hydrolysis

The effect of cellulose structure and crystallinity on enzymatic cellulose hydrolysis was evaluated. Recent studies show that Cellulose II is thermodynamically more stable than cellulose I, however cellulose II is more readily digested than cellulose I because vander Waals interaction between hydrogen-bonded sheets in cellulose I is stronger than that in cellulose II and this acts as a main factor to resist the hydrolysis by cellulose [19]. The transformation of cellulose I form to cellulose II form was observed in regenerated biomass with $[EMIM]^+[Ac]^-$ mixture. The crystallinity of this regenerated biomass was drastically decreased. However, untreated Miscanthus and pre-treated samples with $[EMIM]^+[MeSO_3]^-$ and $[EMIM]^+[HSO_4]^-$ ionic liquids showed similar diffractograms, somewhat decreased crystallinity indicated that small amount of cellulose II was present and the remaining cellulose allomorph was not at all altered by the above ionic liquids treatment. It was noted that the saccharification efficiency was significantly enhanced and high cellulose conversion and high hydrolysis rate were observed for decreased crystallinity and increased amount of cellulose II content present in biomass. This result indicated that cellulose structure and crystallinity should be considered in order to obtain the best cellulose digestibility.

4.4.2.5 Effect of acidity of ILs on compositional changes of Miscanthus and enzymatic digestibility

Table 4-17 depicted that extensive delignification obtained with highly acidic (pH 1.0) ionic liquid $[EMIM]^+[HSO_4]^-$. Removal of hemicellulose was also more effective and cellulose content significantly increased with this highly acidic ionic liquid, however, this resulted in very low glucose yield through saccharification. The lower glucose yield even less than that of untreated Miscanthus could be attributed to the

formation of various inhibitors during pre-treatment. Pre-treatment of Miscanthus with $[EMIM]^+[MeSO_3]^-$ (pH 6.5), resulted in delignification of biomass, however the hemicellulose and cellulose content increased. The glucose yield from this pre-treated biomass was little higher than glucose yield from untreated biomass as well as $[EMIM]^+[HSO_4]^-$ treated biomass. Miscanthus treated with $[EMIM]^+[Ac]^-$ having moderate acidic nature (pH = 5.4), resulted in partial delignification along with increased hemicellulose content. The cellulose content was not changed significantly, however, it lead to very high glucose yield. This may be due to the production of more amorphous cellulose with almost no inhibitors during pre-treatment. Thus, it can be concluded that highly acidic as well as mild acidic ionic liquids are not good solvents for increasing glucose yield whereas moderate acidic ionic liquid was found to be efficient for glucose yield.

4.4.2.6 Effect of different parameters on compositional changes of Miscanthus and enzymatic digestibility

A comprehensive relation between composition of pre-treated biomass and its crystallinity percentage is shown in Fig 4-20. Lower lignin removal, higher hemicellulose content and lower cellulose content resulted in lower crystallinity percentage and vice versa. Fig 4-21, represents the compositional changes of RTIL pre-treated biomass associated with the glucose yield. It seems that only at 40% cellulose, 22% hemicellulose and ~ 50% lignin removed the pre-treated biomass resulted in higher glucose yield (0.98 g/g of cellulose) as well as saccharification rate. In contrast, the treated biomass with 53.1% of cellulose, 6% hemicellulose content and ~ 71% lignin removal lead to lower glucose yield (0.43 g/g of cellulose) and saccharification rate. From Fig 4-22, it is clear that glucose yield increased when crystallinity of treated biomass decreased and the highest glucose yield was obtained at lowest crystallinity of

the treated biomass. Furthermore, β value of three RTILs indicated that pre-treated biomass with RTIL having higher β value resulted in lower lignin removal, lower cellulose content and higher hemicellulose content and vice versa (Fig 4-23). This ultimately led to lower crystallinity percentage and higher glucose yield (Fig 4-24 and 4-25). The parameter β correlated well with reduction of crystallinity as well as enzymatic digestibility of pre-treated Miscanthus. From above discussion, it was concluded that cellulose digestibility can be affected by β value of RTILs, crystallinity percentage, lignin/hemicellulose/cellulose content as well as properties of the reaction mixture.

4.4.3 Synthesis of N, N-diethyl-4-nitroaniline

Due to high cost and unavailability of *N, N-diethyl-4-nitroaniline*, it was necessary to synthesize it along with a need to develop a method that employs simple, mild as well as environmentally benign conditions. 4-Nitroaniline having an electron-withdrawing group such as $–NO_2$ gave a lesser yield of the product. To improve the possible yield of the desired product, different reaction parameters such as reagent quantity, solvent and temperature were screened which is shown in Table 4-21. It was found that the yield of the reactions increased with polar protic solvent (C_2H_5OH) and higher reaction temperature.

Herein, we report a facile, mild, and environmentally benign N, N-dialkylation of 4-nitroaniline using iodoethane (C_2H_5I) as the alkylation partner and an inorganic base e.g., K_2CO_3 in polar protic solvent such as ethanol (EtOH) under heating at a temperature of 80 ^oC (Scheme1).

Due to the presence of electron withdrawing group in 4-nitroaniline makes it weak nucleophile for which it needs polar protic solvent to solvate the anion of iodoethane properly and gave better yield in the presence of ethanol. Spectral data and spectra of (^1H

NMR,^{13}C NMR and Mass spectra) of *N, N-diethyl-4-nitroaniline* are given in supporting Information.

4.4.3.1 Spectral data of N, N-Diethyl-4-nitroaniline

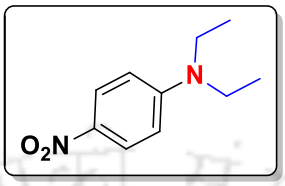

^{1}H NMR (400 MHz, $CDCl_3$): δ (ppm) 1.23 (t, 6H, J = 7.2Hz), 3.45 (q, 4H, J = 7.2Hz), 6.57 (d, 2H, J = 9.2Hz), 8.10 (d, 2H, J = 9.6Hz); ^{13}C NMR (150 MHz, $CDCl_3$): δ (ppm) 12.6, 45.2, 110.0, 126.7, 136.5, 152.4; HRMS (ESI): calcd. for $C_{10}H_{14}N_2O_2$ (MH^+) 195.1134; found 195.1160. ^{1}H NMR and ^{13}C NMR spectra were shown in Figure 4-26 and Fig 4-27. Mass spectra was represented in Fig 4-28.

4.5 Comparison of dilute acid pretreatment and ionic liquid pretreatment

Saccharification results showed that the yield of glucose was higher for the 5% pretreated Miscanthus at 20 (FPU/g dry biomass) enzymes loading. The yield of glucose from enzymatic hydrolysis of the pretreated biomass obtained at optimum condition for maximum xylose and arabinose present in liquid fraction of dilute acid hydrolysis of Miscanthus was higher than another optimum condition for dilute acid pretreatment of biomass because of lower lignin, hemicellulose content and little lower crystallinity. The amount of glucose liberated from IL treated and untreated Miscanthus decreased in the following order, $[EMIM]^+[Ac]^-$ treated > $[EMIM]^+[MeSO_3]^-$ treated > $[EMIM]^+[HSO_4]^-$ treated > Untreated. Table 4-21 showed that the yield of glucose was 0.81 (g/g cellulose) for the 5% pretreated biomass (X+A) at 20 (FPU/g dry biomass) enzymes loading and it

was found that sugar yield was 0.98 (g/g of cellulose) for ($[EMIM]^+[Ac]^-$) treatment. It was thus confirmed that ionic liquid based pre-treatment of Miscanthus resulted in higher glucose yield than that of dilute acid base pre-treatment.

Table 4-1 Extractives (g) present in 100 g lignocellulosic biomass

Name of the Biomass	Hexane Extract	Ethanol Extract	Water Extract	Total Extract	Cellulose	Hemicellulose	Lignin
Miscanthus	1.62	11.38	4.62	17.62	43.34	13.63	26.29
Castor	3.9	5.12	3.02	12.04	42.07	9.72	21.18
Jatropha	5.3	3.2	10.82	19.32	40	7.81	29.6

Table 4-2 Proximate analysis, Ultimate analysis of Lignocellulosic Biomass

Name of the Biomass	Proximate analysis				Ultimate Analysis				
	Moisture (%)	Ash (%)	Volatile (%)	Fixed Carbon (%)	Carbon (%)	Hydrogen (%)	Nitrogen (%)	Sulphur (%)	Oxygen (%)
Miscanthus	10.8	5.49	76.16	7.55	53.94	3.49	1.15	0.81	40.61
Castor	12	5.56	76	6.44	38.26	1.25	4.21	0.58	55.7
Jatropha	12.01	9.1	68.93	9.96	43.22	1.90	3.66	0.11	51.11

Table 4-3 Wave number of FTIR absorption bands for functional groups of lignocellulosic biomass samples and their extractives

Wave number(cm^{-1})	Band assignment
Lignocellulosic biomass	
~3345	OH stretching
2910-2935	CH stretching of aliphatic structure
~1732	C=O in ketone, ester, carboxylic acid, un-conjugated Xylan
~1650	OH deformation vibration of adsorbed water and C=O stretching vibration
~1632	C=C in benzene stretching ring
1500-1600	Aromatic ring stretching in lignin
~1456	C-H Asymmetric bending of CH_3 and methoxy groups present in lignin
~1422	Aromatic skeletal combine with C-H in-plane deforming and stretching
1373	Aliphatic C-H stretching in methyl and phenol
~1323	C-H_2 wagging vibration in cellulose and C1-O vibrations in S derivatives
~1245	C-O stretching vibration in lignin, Aryl-alkyl ether linkage
~1160	C-O-C asymmetric stretching vibration in cellulose I and cellulose II
~1108	O-H association band in C-OH, cellulose and hemicellulose
~1065	C-O stretching and C-O vibration in cellulose and hemicellulose
~900	C1 vibration in cellulose and hemicellulose
~ 670	C-OH out of plane bending in cellulose
Extractives	
2800-3000	Methylene and methyl stretching frequencies
1650-1800	Carbonyls in esters and/or organic acids
1350-1500	Stretching vibrations of the CH_2 and CH_3 groups

Table 4-4 Equations obtained by applying Kissinger formula

	For first degradation zone			For second degradation zone		
Biomass	TR (K)	Equation	R^2	Temp. range (K)	Equation	R^2
Miscanthus	584-611	Y=-8.552x+4.199	0.988	700-721	Y=-16.22x +12.35	0.998
Castor	575-585	Y=-24.75x +32.62	0.990	717-726	Y=-40.46x +45.58	0.997
Jatropha	568-579	Y=-21.74x +27.89	0.972	715-724	Y= -42.29 +48.28	0.974

Table 4-5 Kinetic parameters from Kissinger method

	For first degradation zone			For second degradation zone		
Biomass	TR (K)	E_a, KJ mol^{-1}	ln A, min^{-1}	Temp. range (K)	E_a, KJ mol^{-1}	ln A, min^{-1}
Miscanthus	584-611	71.1	13.25	700-721	134.86	22.04
Castor	575-585	205.78	42.74	717-726	336.40	56.19
Jatropha	568-579	180.76	37.88	715-724	351.62	58.93

Table 4-6 Equations obtained by applying Ozawa formula

	For first degradation zone			For second degradation zone		
Biomass	TR (K)	Equation	R^2	Temp. range (K)	Equation	R^2
Miscanthus	584-611	Y=-9.747x +18.98	0.991	700-721	Y= -17.64x + 27.48	0.998
Castor	575-585	Y=-25.91x +47.34	0.990	717-726	Y= -41.90x +60.75	0.997
Jatropha	568-579	Y=-22.89x +42.60	0.975	715-724	Y= -43.73x +63.44	0.975

Table 4-7 Kinetic parameters from Ozawa method

	For first degradation zone			For second degradation zone		
Biomass	TR (K)	E_a,KJ mol^{-1}	ln A,min^{-1}	Temp. range (K)	E_a,KJ mol^{-1}	ln A,min^{-1}
Miscanthus	584-611	77.03	15.18	700-721	139.42	23.08
Castor	575-585	204.78	35.65	717-726	331.157	55.48
Jatropha	568-579	180.91	37.94	715-724	345.62	58.13

Table 4-8 The central composite design employed for three independent variables

No of runs	Independent variables (coded values)			Response	
	Acid loading % (v/v)	Solid loading % (w/v)	Treatment Time (Min)	CrI %	X+A (g/L)
1	-1	-1	-1	76.1	2.39
2	1	-1	-1	73.55	3.21
3	-1	1	-1	77	6.03
4	1	1	-1	75.12	7.06
5	-1	-1	1	76.3	4.9
6	1	-1	1	72.5	5.23
7	-1	1	1	77.873	9.23
8	1	1	1	72.99	9.06
9	-1.68	0	0	82	5.69
10	1.68	0	0	75.5	7.31
11	0	-1.68	0	73	1.08
12	0	1.68	0	75.06	7.2
13	0	0	-1.68	72.95	4.88
14	0	0	1.68	70.9	8.50
15	0	0	0	77.98	7.93
16	0	0	0	77.1	7.4
17	0	0	0	77	7.3
18	0	0	0	76.95	8.04
19	0	0	0	77	7.97
20	0	0	0	77.6	8.00

Table 4-9 Analysis of variance of CrI % and its influential factors

Source	Sum of Squares	Degree of freedom	Mean Square	F- value	P- value
Model	120.68	9	13.41	53.00	0.000 **Significant**
Residual	2.53	10	0.25		
Lack-of-Fit	1.64	5	0.33	1.84	0.259 **Insignificant**
Pure Error	0.89	5	0.18	---	---
Total	123.21	19	---	---	---
R^2	97.95%	---	---	---	---

Table 4-10 Analysis of variance of X+A and its influential factors

Source	Sum of Squares	Degree of freedom	Mean Square	F- value	P- value
Model	93.37	9	10.37	94.32	0.000 **Significant**
Residual	1.10	10	0.11		
Lack-of-Fit	0.54	5	0.11	0.98	0.508 **Insignificant**
Pure Error	0.55	5	0.11	---	---
Total	94.47	19	----	----	---
R^2	98.84%	---	---	---	---

Table4-11 Experimental validity test for the optimised values predicted by the statistical analysis for Miscanthus

Biomass	Optimum Crystallinity %		Optimum X+A (g/L)	
	Predicted	Experimental	Predicted	Experimental
Miscanthus	82.09	82	9.61	9.23

Table 4-12 Composition of filtrate obtained from Optimum Crystallinity % and Optimum X+A (g/L)

Miscanthus	Glucose (g/L)	Xylose+Arabinose (g/L)	Formic acid (g/L)	Acetic acid (g/L)	Furfural (g/L)	Hydroxy Methyl Furfural (g/L)
Optimum Crystallinity%	0.75	3.97	0.06	1.05	0.01	0.01
Optimum X+A (g/L)	2.12	9.61	0.08	2.16	0.09	0.04

Table 4-13 Composition for treated and untreated Miscanthus

Biomass	Cellulose (%)	Hemicellulose (%)	Lignin (%)
Miscanthus	43.34	13.63	26.29
Pretreated Miscanthus (Optimised for crystallinity % (CRI %))	65.8	7.8	16.1
Pretreated Miscanthus (Optimised for amount Xylose and Arabinose present in filtrate (X+A) g/L)	79.1	2.9	10.3

Table 4-14 Yield of glucose from enzymatic hydrolysis of dilute acid pretreated Miscanthus

Experimental condition for enzymatic hydrolysis	Glucose yield (g/g cellulose)	Glucose yield (g/g dry pretreated biomass)
CrI (10%) 10 FPU	0.45	0.36
X+A (10%) 10 FPU	0.58	0.46
CrI (10%) 20 FPU	0.51	0.40
X+A (10%) 20 FPU	0.68	0.54
CrI (10%) 25 FPU	0.48	0.38
X+A(10%) 25 FPU	0.65	0.51
CrI (5%) 20 FPU	0.64	0.48
X+A (5%) 20 FPU	0.81	0.74

Table 4-15 Structure, Relative density, melting point and flash point of ionic liquids

IL	Structure of IL	Relative density	Melting point	Flash point	pH
([EMIM]$^+$[Ac]$^-$),97%	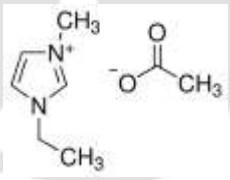	1.027 g/cm^3 at 25 °C	> 30 °C	164 °C	5.4
([EMIM]$^+$[MeSO$_3$]$^-$),≥95%	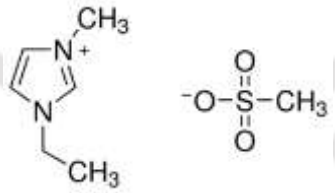	1.247 g/cm^3 at 25 °C	33 °C	286 °C	6.5
([EMIM]$^+$[HSO$_4$]$^-$),95%	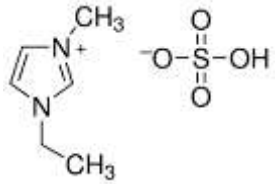	1.367g/cm^3 at 25 °C	NA	NA	1

Table 4-16 Kamlet–Taft parameters (α, β, and π*) measured at 100 °C

Solvent	Kamlet–Taft parameters measured at 100 °C		
	α	β	π^*
$[EMIM]^+[Ac]^-$	0.40	1.13	1.02
$[EMIM]^+[MeSO_3]^-$	NA	0.69	1.20
$[EMIM]^+[HSO_4]^-$	0.085	0.68	1.20

Table 4-17 Summary of % of Cellulose, hemicellulose, lignin present in untreated and RTIL-treated biomass

Pre-treatment Solvent (IL)	Anti- Solvent	Pretreatment and regeneration scheme for biomass (Miscanthus)	Biomass recovery (%)	Cellulose (%)	Hemicellulose (%)	Lignin (%)
None	None	Untreated	100	43.3	13.6	26.3
$[EMIM]^+[Ac]^-$	Water	AC_WW	94.5	47.5	22.8	14.7
$[EMIM]^+[Ac]^-$	Water-acetone (1:1, v/v)	AC_HA	92.5	40	22	13.3
$[EMIM]^+[MeSO_3]^-$	Water	MS_WW	86.7	47.7	20.0	9.4
$[EMIM]^+[MeSO_3]^-$	Water-acetone (1:1, v/v)	MS_HA	89.7	48.5	21.3	8.0
$[EMIM]^+[HSO_4]^-$	Water	HS_WW	67.7	53.1	5.8	7.5
$[EMIM]^+[HSO_4]^-$	Water-acetone (1:1, v/v)	HS_HA	68.8	57.2	11.6	5.6

Note: Miscanthus was treated with different ILs at particular pre-treatment condition i.e. 100 °C for 24 h and was then regenerated from reaction mixture using two different anti-solvents (water and water-acetone mixture).

Table 4-18 Percentages of mass and lignin removed after pre-treatment with three different ILs at 100 ^{o}C for 24 h followed by regeneration of Miscanthus

Pretreatment and regeneration scheme for biomass (Miscanthus)	Mass removal (%)	Lignin removal (%)
AC_WW	5.5	44.1
AC_HA	7.5	49.3
MS_WW	13.3	64.2
MS_HA	10.3	69.6
HS_WW	32.3	71.5
HS_HA	31.5	78.7

Table 4-19 Summary of fermentable sugar yields, saccharification rates, and crystallinity index of Miscanthus treated with IL at 100 ^{o}C for 24h

Pretreatment and regeneration scheme for biomass (Miscanthus)	Crystallinity Index (%)	LOI	Maximum glucose yield (g/ g cellulose)	saccharification rate (mg $ml^{-1}h^{-1}$) at maximum yield
Untreated	71.7	0.75	0.51	0.27
AC_WW	25.5	0.47	0.91	0.47
AC_HA	21.1	0.44	0.98	0.50
MS_WW	54.3	0.57	0.53	0.24
MS_HA	50.9	0.52	0.59	0.27
HS_WW	59.9	0.66	0.43	0.20
HS_HA	58.0	0.64	0.47	0.22

Table 4-20 Assignments of absorption bands of untreated Miscanthus in Fourier transform–infrared spectra

Group frequency, Wave number (cm^{-1})	Band assignments
898	C-H deformation Vibration in cellulose
1056	C-O stretching in cellulose and hemicellulose
1160	C-O-C vibration in cellulose and hemicellulose
1235	Syringyl ring breathing and C-O stretch in lignin and xylan
1318	Vibrations associated with cellulose
1372	C-H deformation in cellulose and hemicelluloses
1457	C-H deformation; asymmetric bending in $-CH_3$ and and methoxy ($-OCH_3$) groups present in lignin
1508	C = C-C Aromatic skeletal stretching in lignin
1733	C=O in xylan acetates (hemicelluloses)
2918	C–H stretching in cellulose

Table 4-20 Screening of reaction condition

Entry	Basic (equiv.)	Solvent	Alkylhalide (equiv.)	Temp (°C)	Yield (%)
1	K_2CO_3 (6)	Acetonitrile	Iodo-ethane (10)	60	20
2	K_2CO_3 (6)	Ethanol	Iodo-ethane (10)	80	32

Table 4-21 Comparison of dilute acid pretreatment and ionic liquid pretreatment for Miscanthus at its optimal condition

Optimal conditions for different treatment	Cellulose (%)	Hemicellulose (%)	Lignin (%)	CrI (%)	Maximum glucose yield (g/ g of cellulose)
X+A	79.1	2.9	10.3	80.03	0.81
AC_HA	40	22	13.3	21.1	0.98

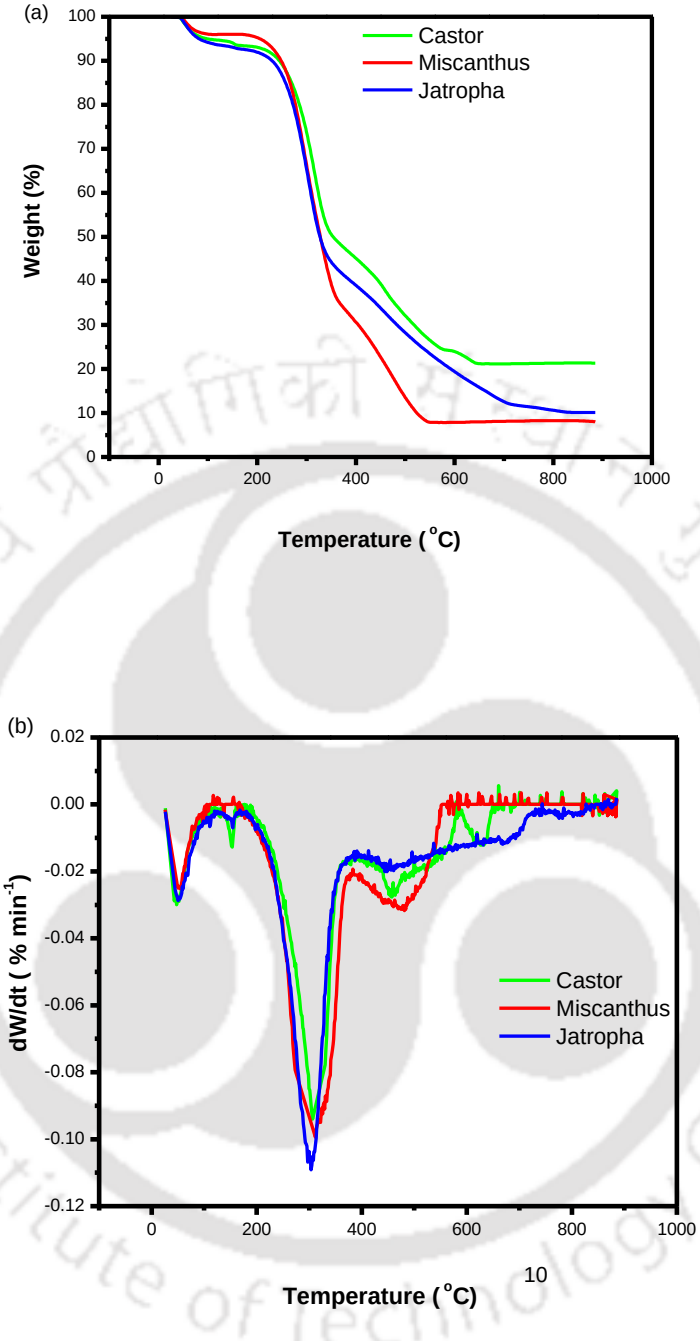

Fig 4-1: (a) TGA and (b) DTG thermograms of raw biomasses

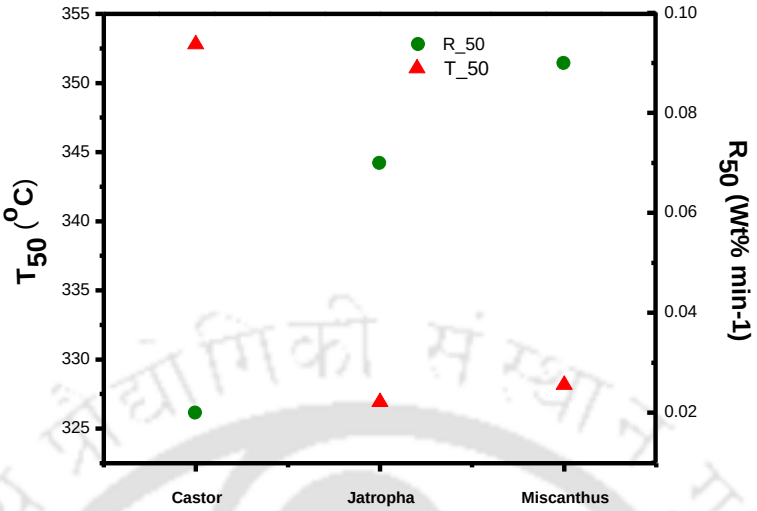

Fig 4-2: T-50 and R-50 values of raw biomasses

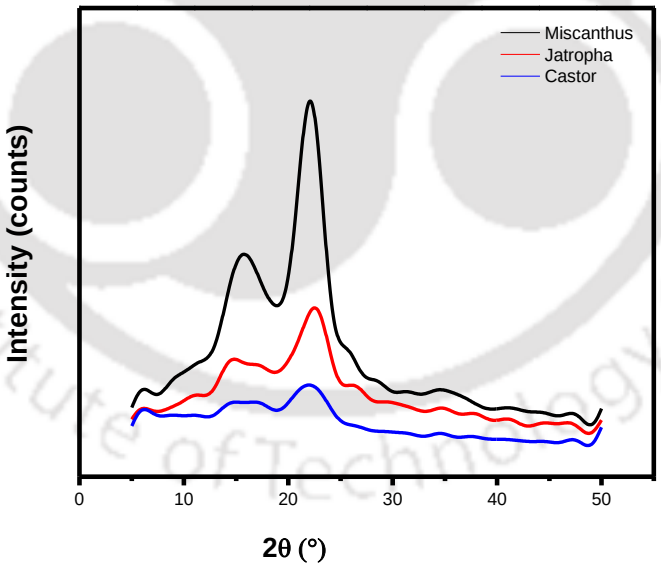

Fig 4-3: XRD analysis of raw biomasses

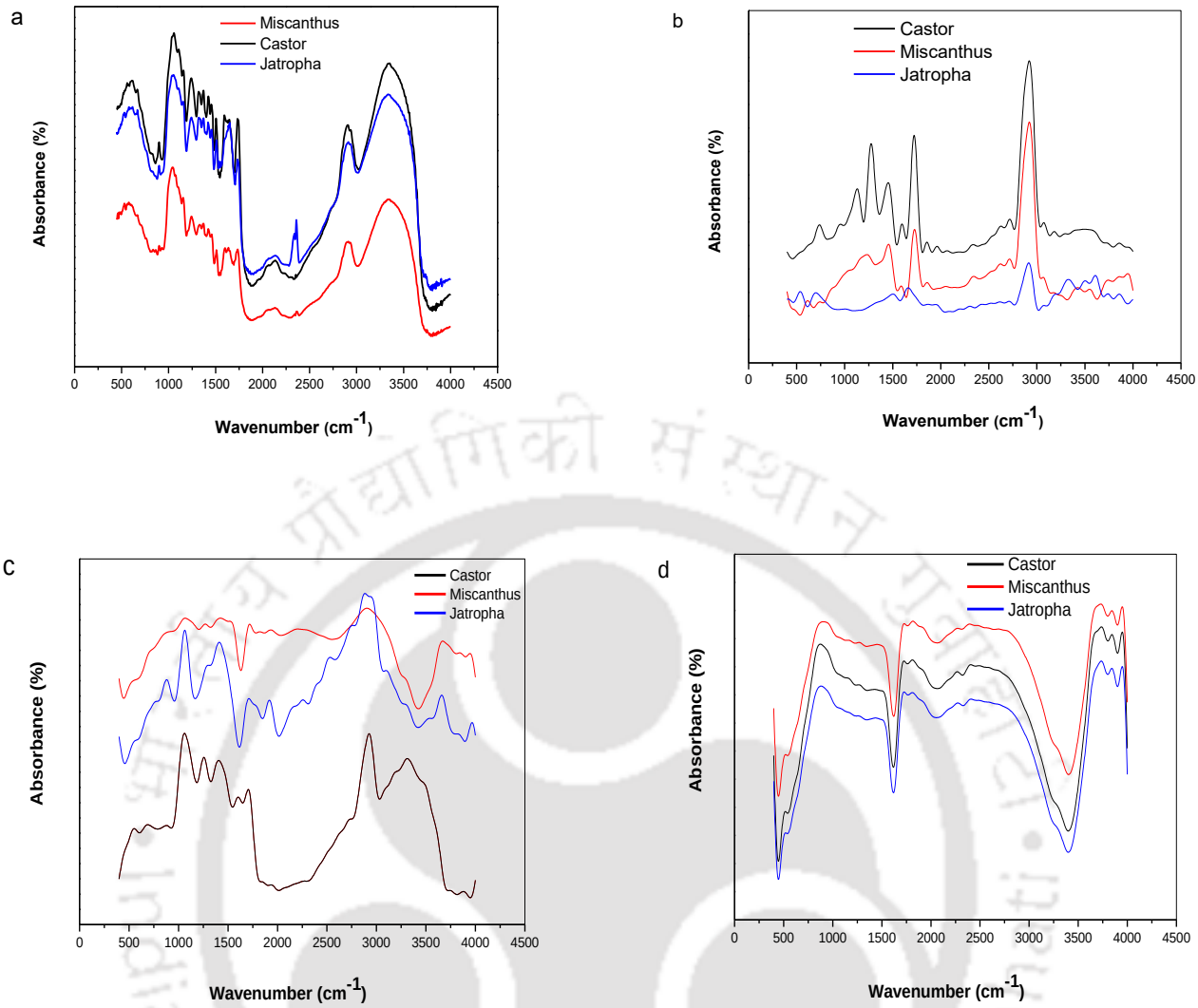

Fig 4-4: (a) FTIR spectra of different raw biomass (b) FTIR spectra of hexane extractives of different raw biomass (c) FTIR spectra of ethanol extractives of different biomass obtained after hexane extraction (d) FTIR spectra of water extractives of different biomass obtained after ethanol extraction.

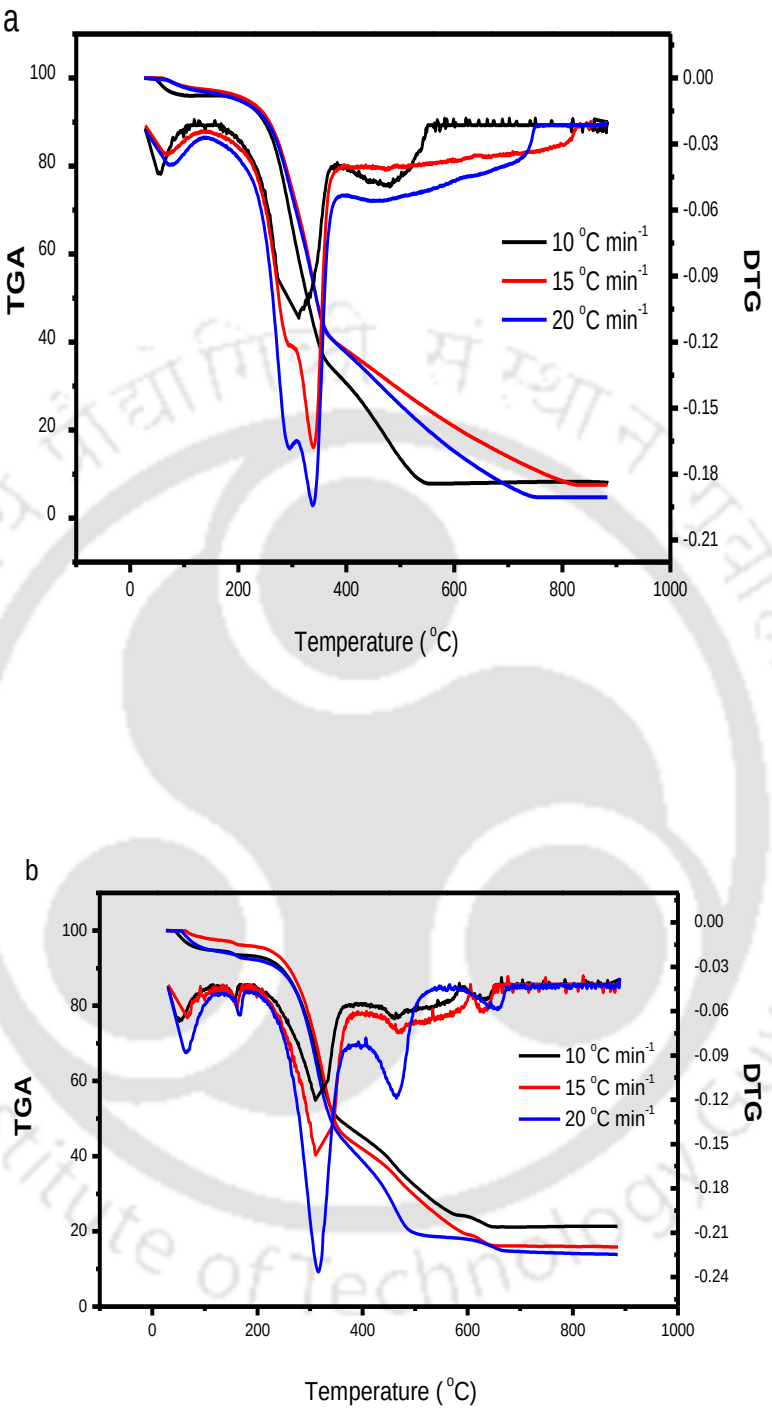

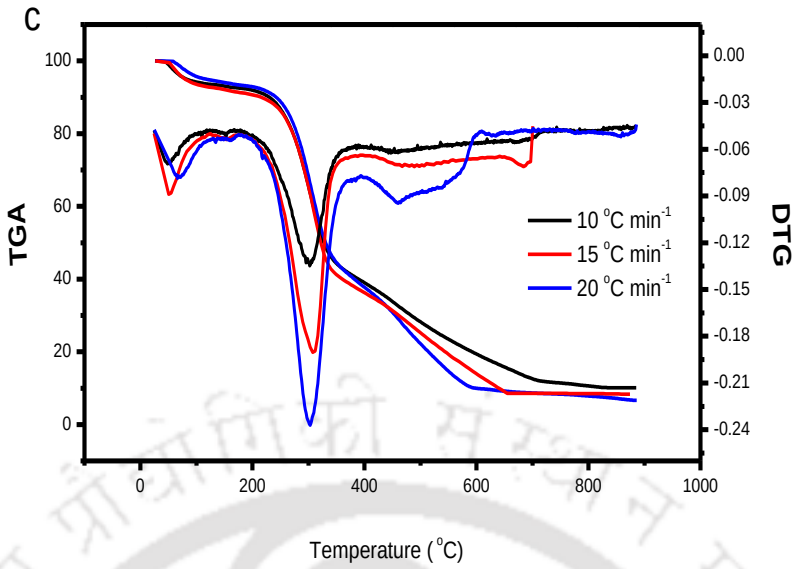

Fig 4- 5: TGA &DTG thermograms of (a) Miscanthus; (b) Castor; (c) Jatropha

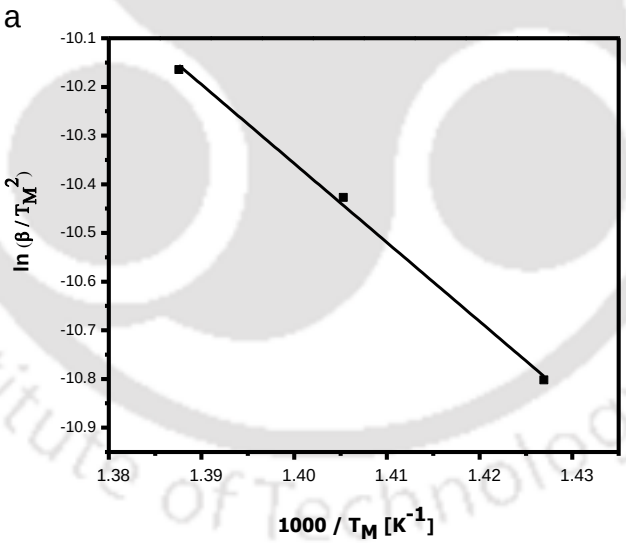

Fig 4-6: (a) Linear plot of Kissinger method for Miscanthus in 700-721K Temperature range (TR)

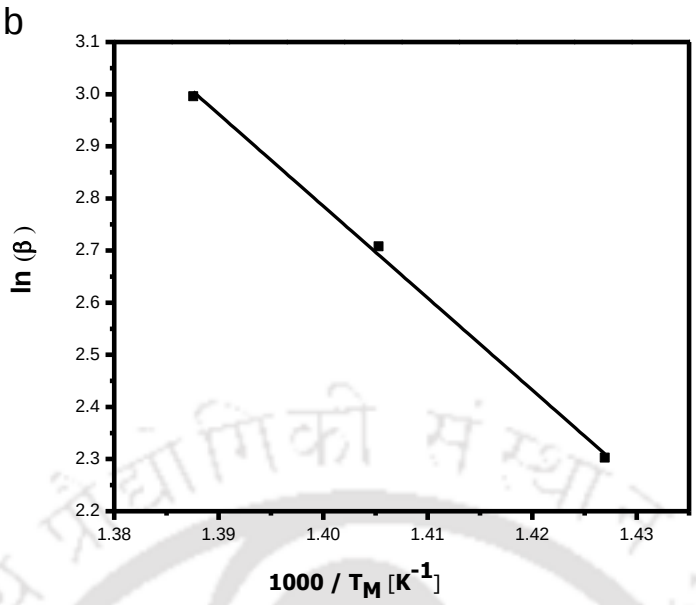

Fig 4-6: (b) Linear plot of Ozawa method for Miscanthus in 700-721K K Temperature range (TR)

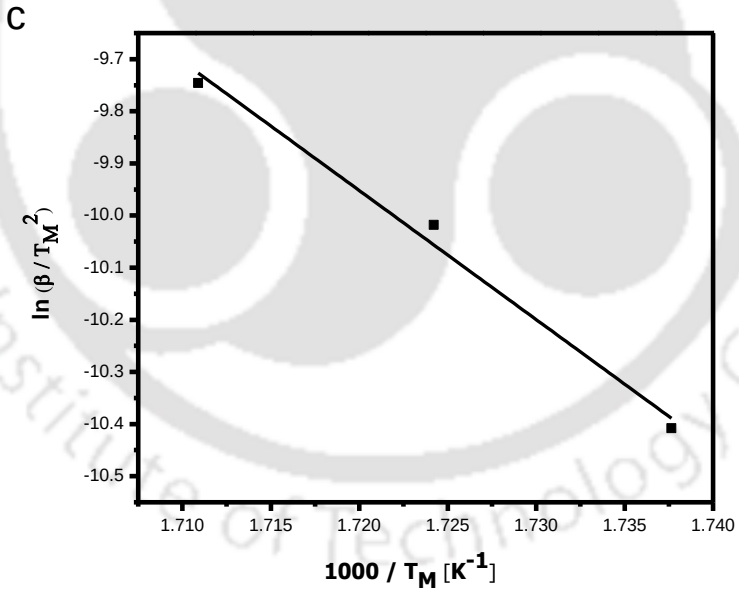

Fig 4-6: (c) Linear plot of Kissinger method for Castor in 575-585 K Temperature range (TR)

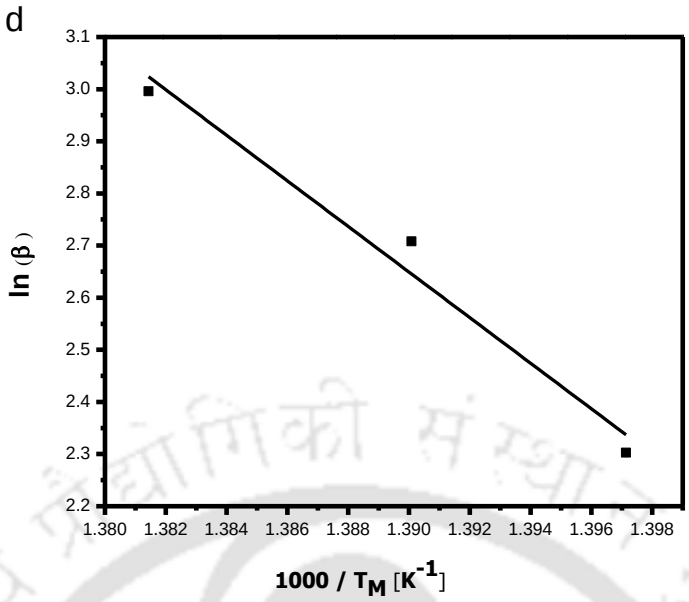

Fig 4-6: (d) Linear plot of Ozawa method for Jatropha in 715-724 K Temperature range (TR)

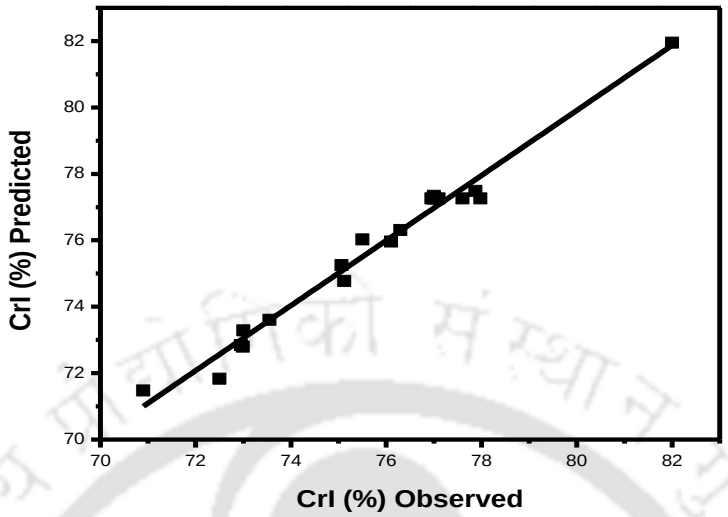

Fig 4-7: Observed vs. predicted values for CrI (%) of the solid fractions obtained after dilute acid pretreatment of Miscanthus

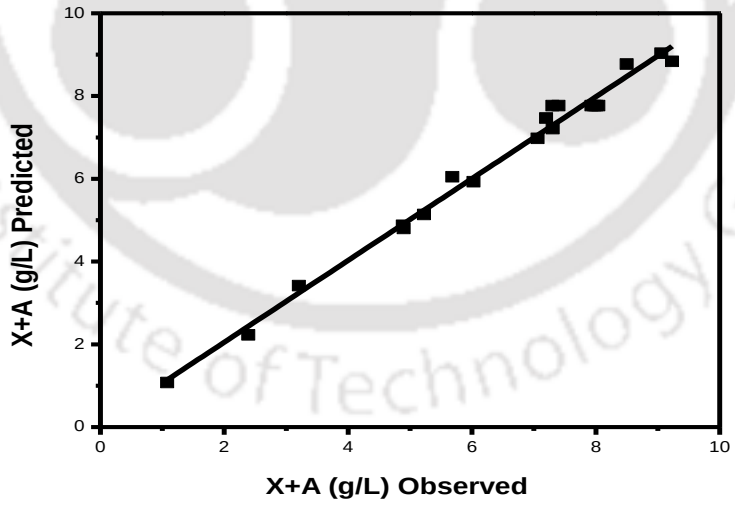

Fig 4-8: Observed vs. predicted values for X+A (g/L) present in the liquid fractions obtained after dilute acid pretreatment of Miscanthus

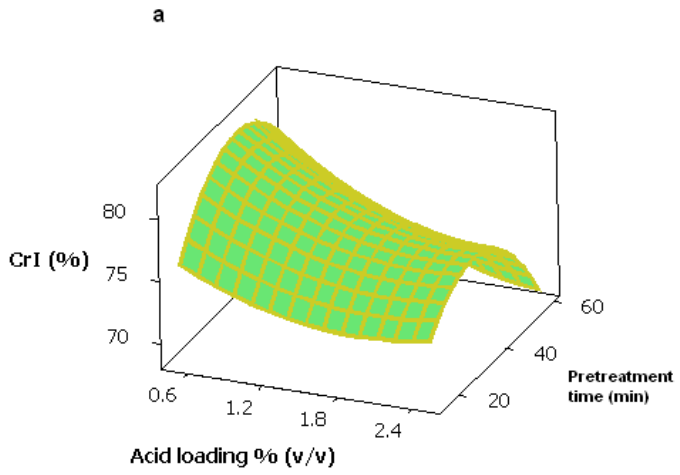

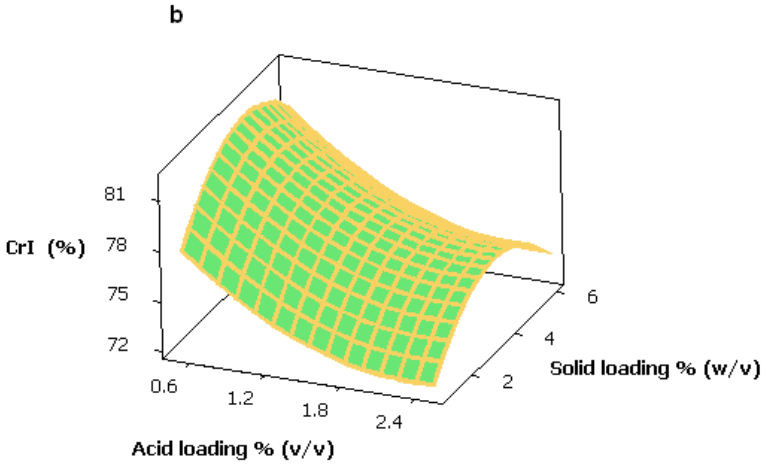

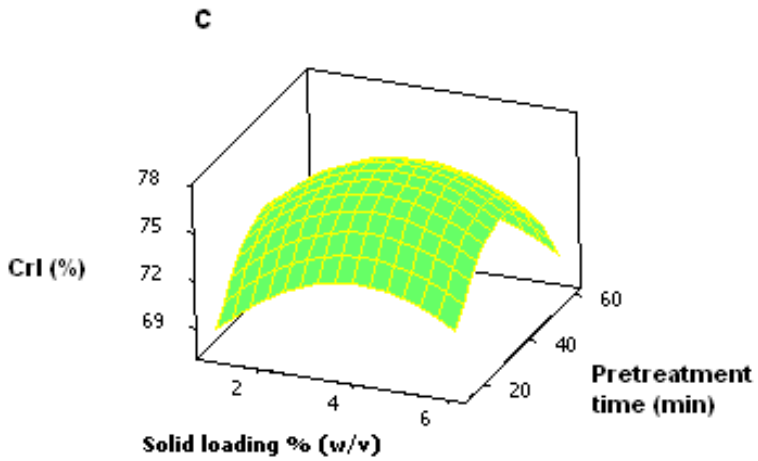

Fig 4-9: Response surface plots of the effect of each factor on CrI % of pretreated Miscanthus (a) Effects of treatment time and acid loading at constant solid loading (b) Effects of acid loading and solid loading at constant treatment time (c) Effects of treatment time and solid loading at constant acid loading on the CrI%.

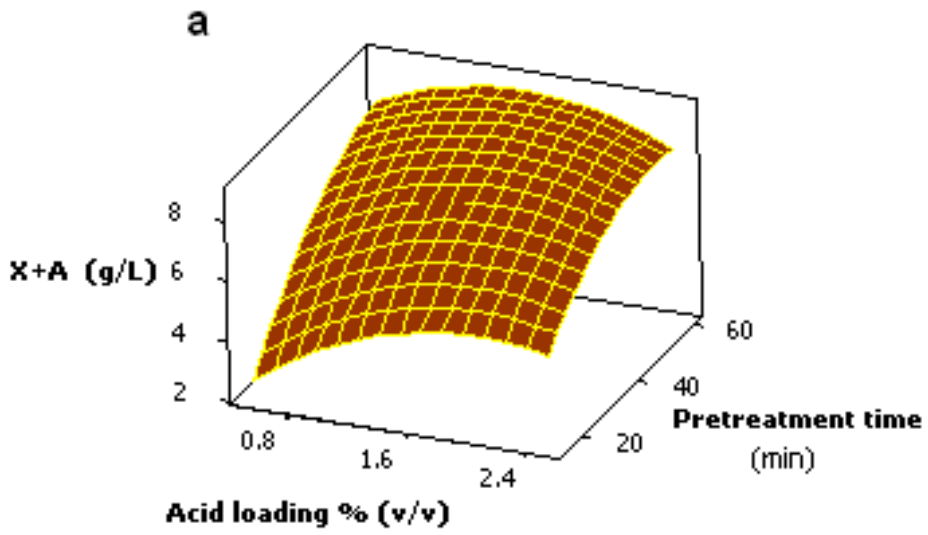

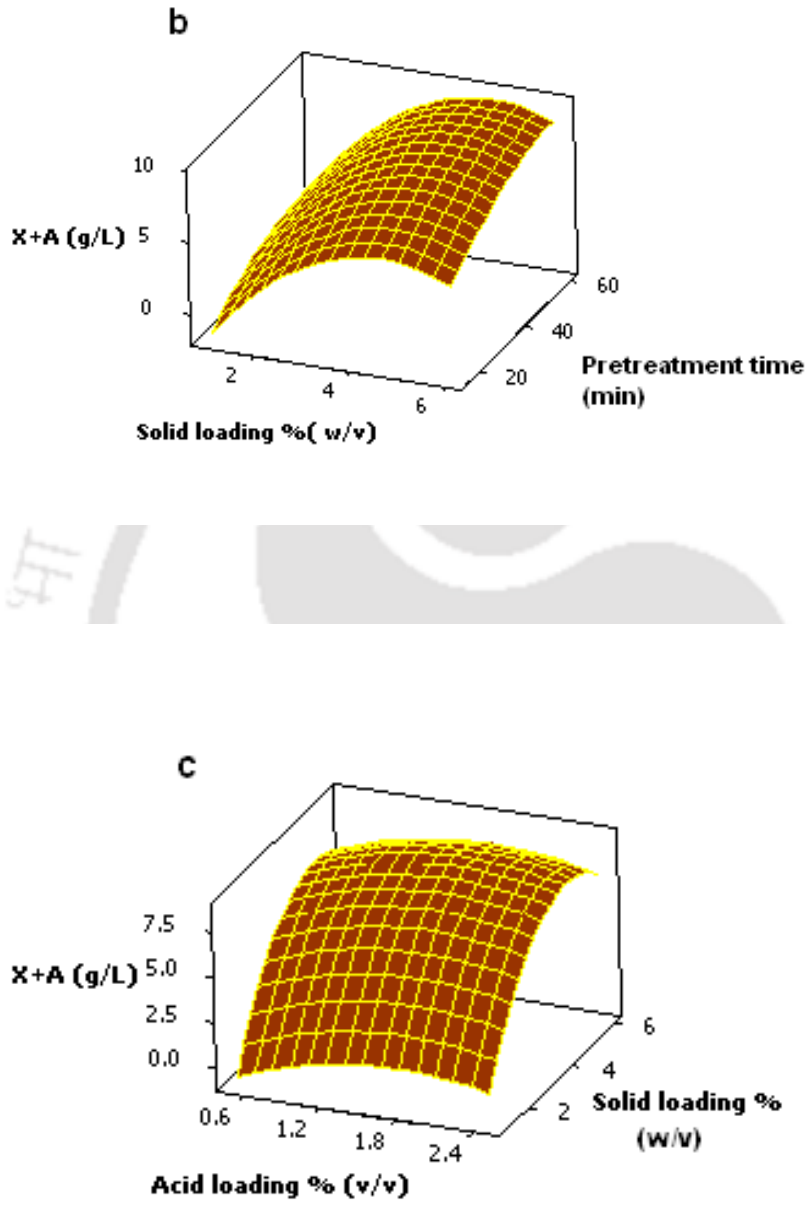

Fig 4-10: Response surface plots of the effect of each factor on (X+A) (g/L) present in filtrate obtained after dilute acid pretreatment of Miscanthus (a) Effects of treatment time and acid loading at constant solid loading (b) Effects of acid loading and solid loading at constant treatment time (c) Effects of treatment time and solid loading at constant acid loading on (X+A).

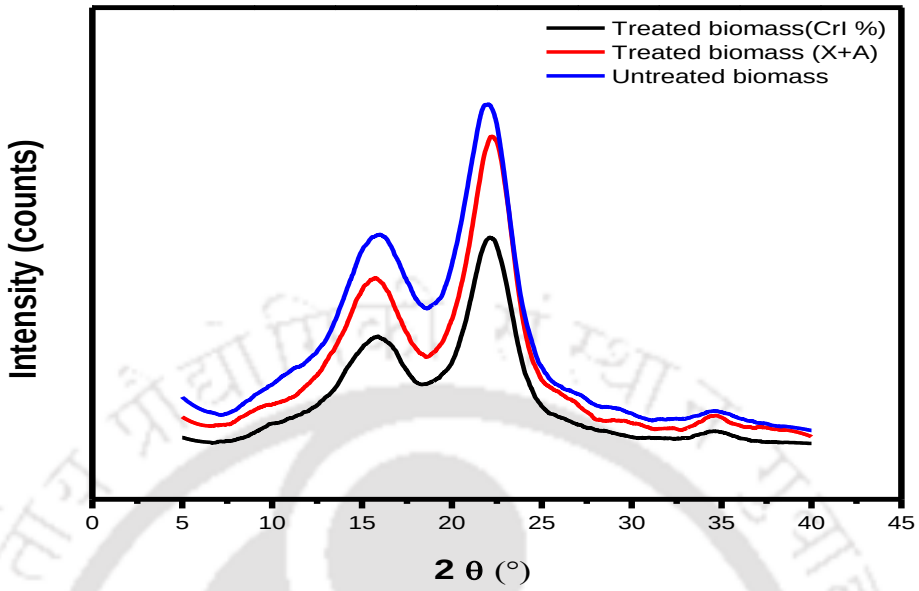

Fig 4-11: XRD analysis of dilute acid treated and raw Miscanthus

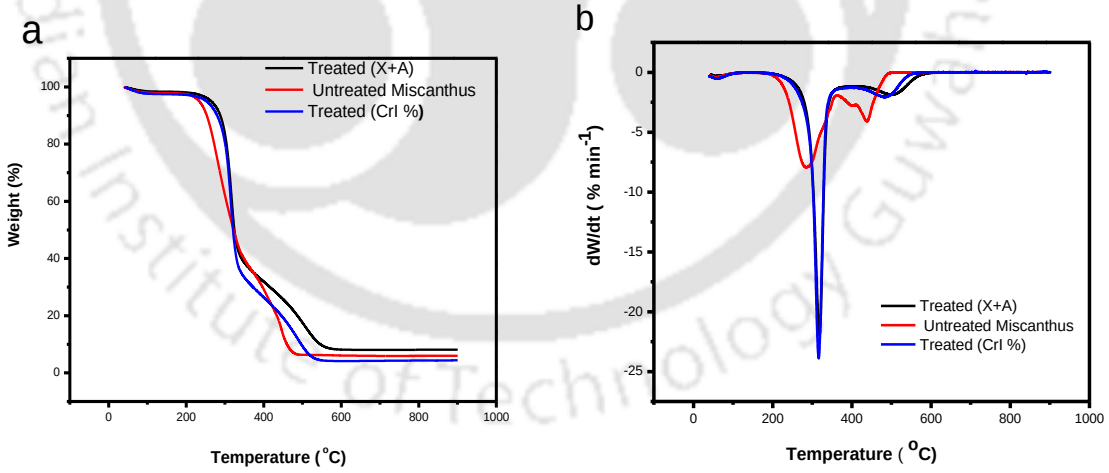

Fig 4-12: (a) Thermogravimetric curves and (b) Differential thermogravimetric curves for dilute acid treated and raw Miscanthus.

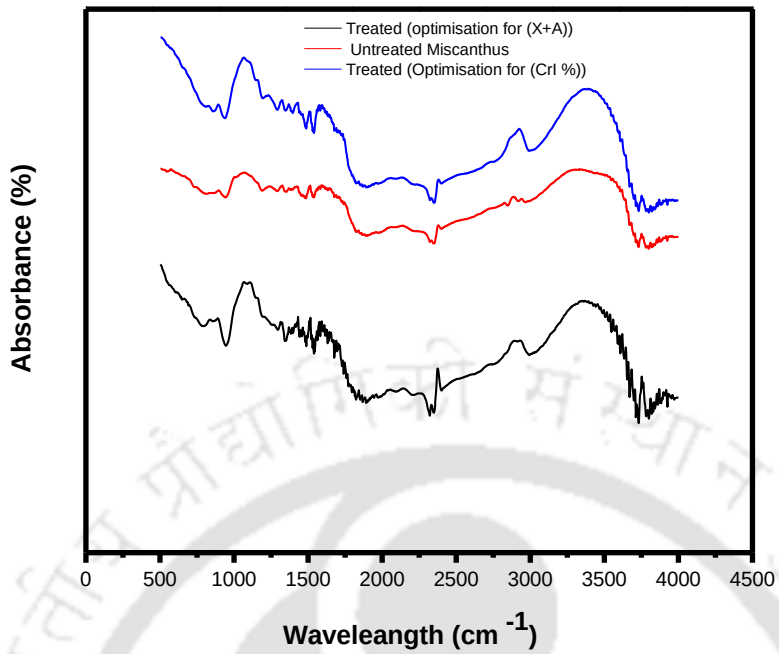

Fig 4-13: FTIR spectra of untreated Miscanthus and dilute acid treated Miscanthus samples.

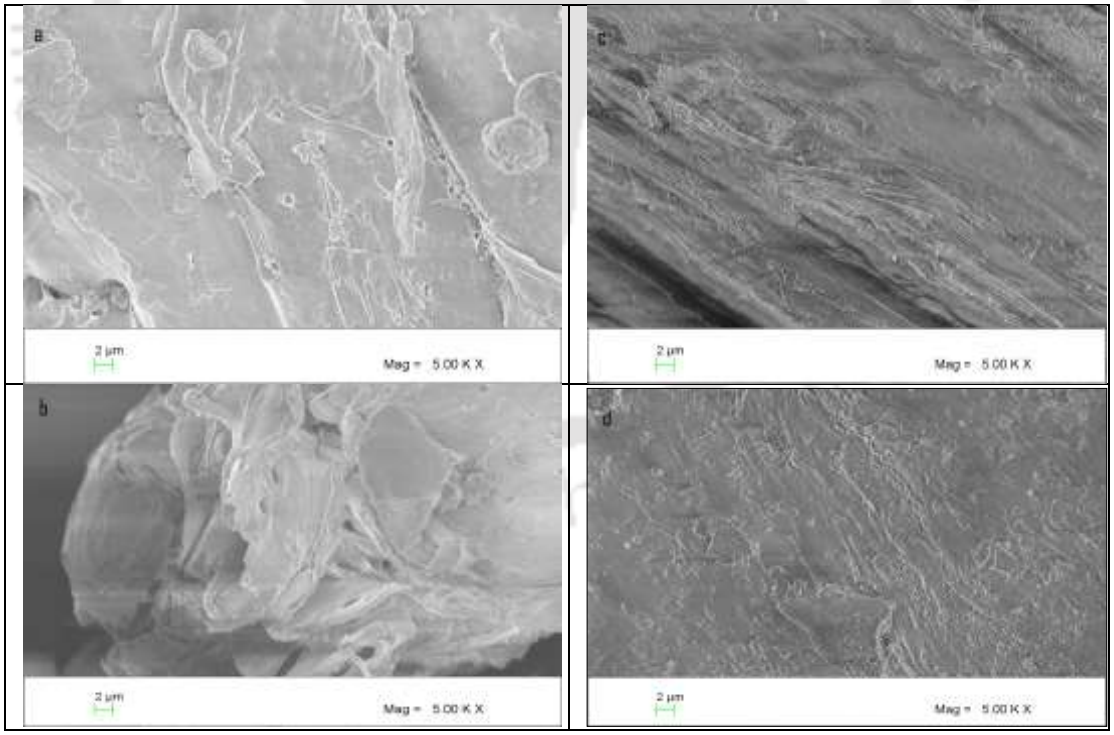

Fig 4-14: FESEM images of untreated Miscanthusand dilute acid treated Miscanthus,**(a)** and **(b)** FE-SEM images of untreated Miscanthus, (c) FESEM images of dilute acid treated (optimised for maximum CRI%) Miscanthus, (d) FESEM images of dilute acid treated (Optimised for maximum (X+A)) Miscanthus

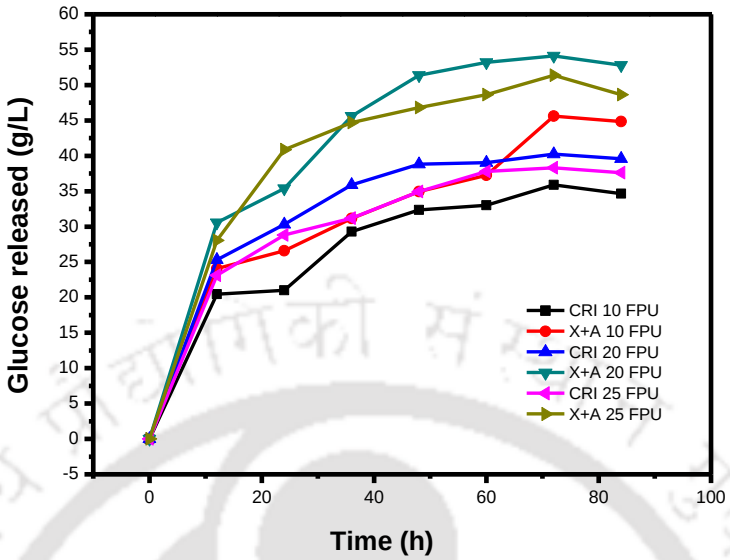

Fig 4-15: The effects of different enzyme loadings (10, 20, 25 FPU/ g dry pretreated biomass) with fixed (10%dilute acid treated biomass) solid loading,on glucose release (g/L).

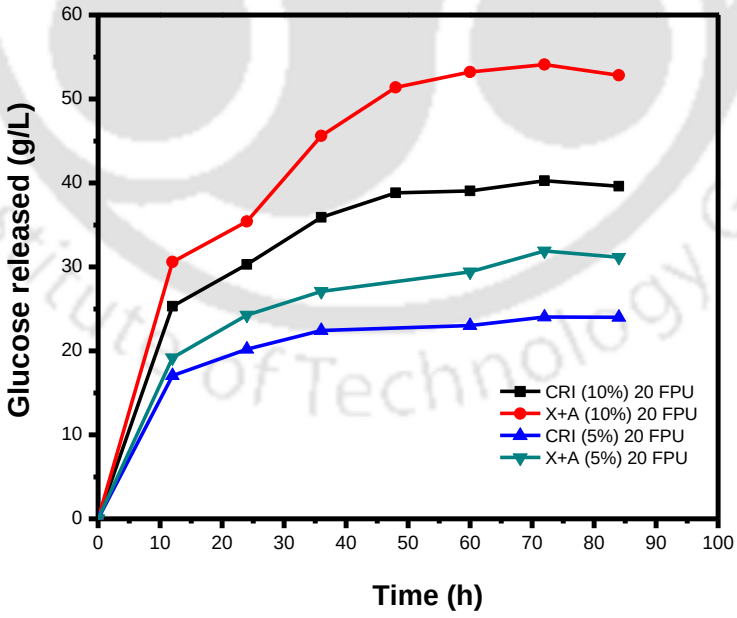

Fig 4-16: The effects of different solid loadings (5%, 10% dilute acid treated biomass) with fixed (20FPU/ g dry pretreated biomass enzyme loading) enzyme loading, on glucose release (g/L)

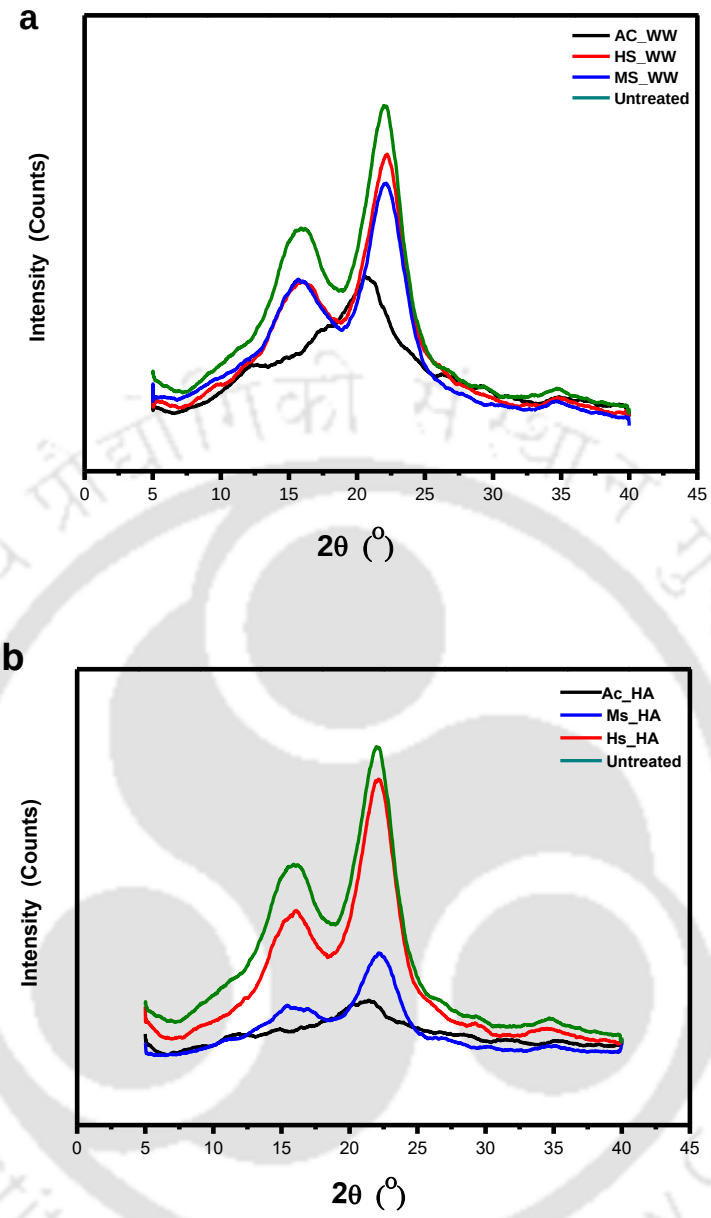

Fig 4-17: (a) XRD Analysis of untreated and regenerated Miscanthus using water anti-solvent (WW) and (b) XRD Analysis of untreated and regenerated Miscanthus using acetone water mixture anti-solvent (HA)

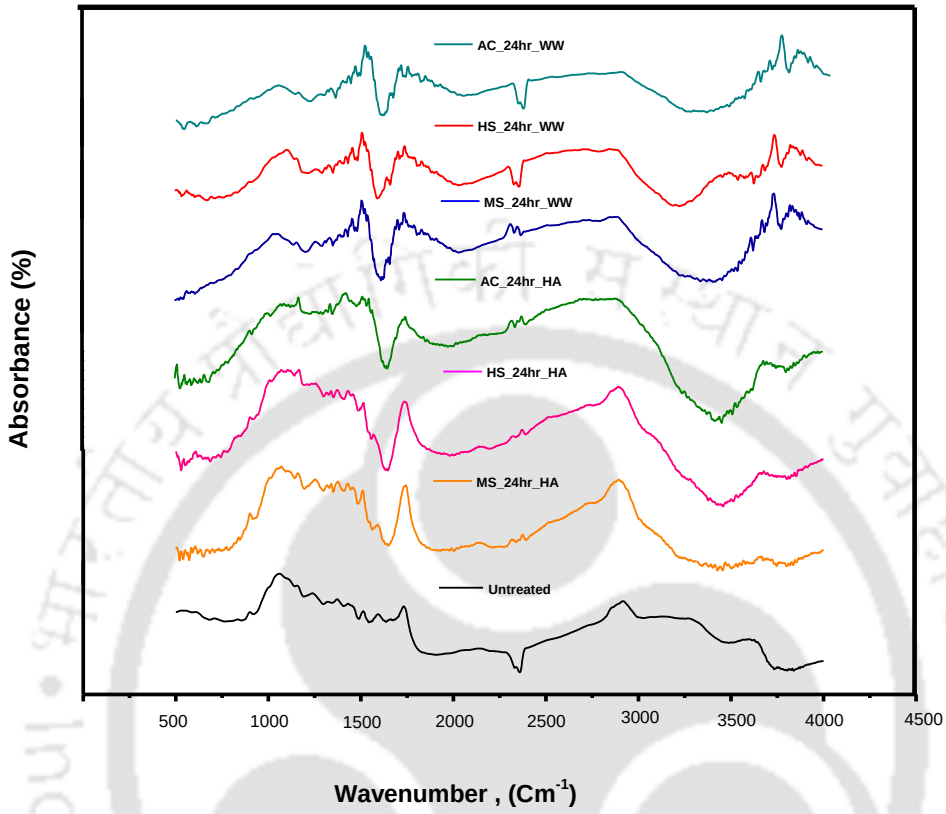

Fig 4-18: Fourier transform–infrared spectra of untreated and ionic liquid treated Miscanthus

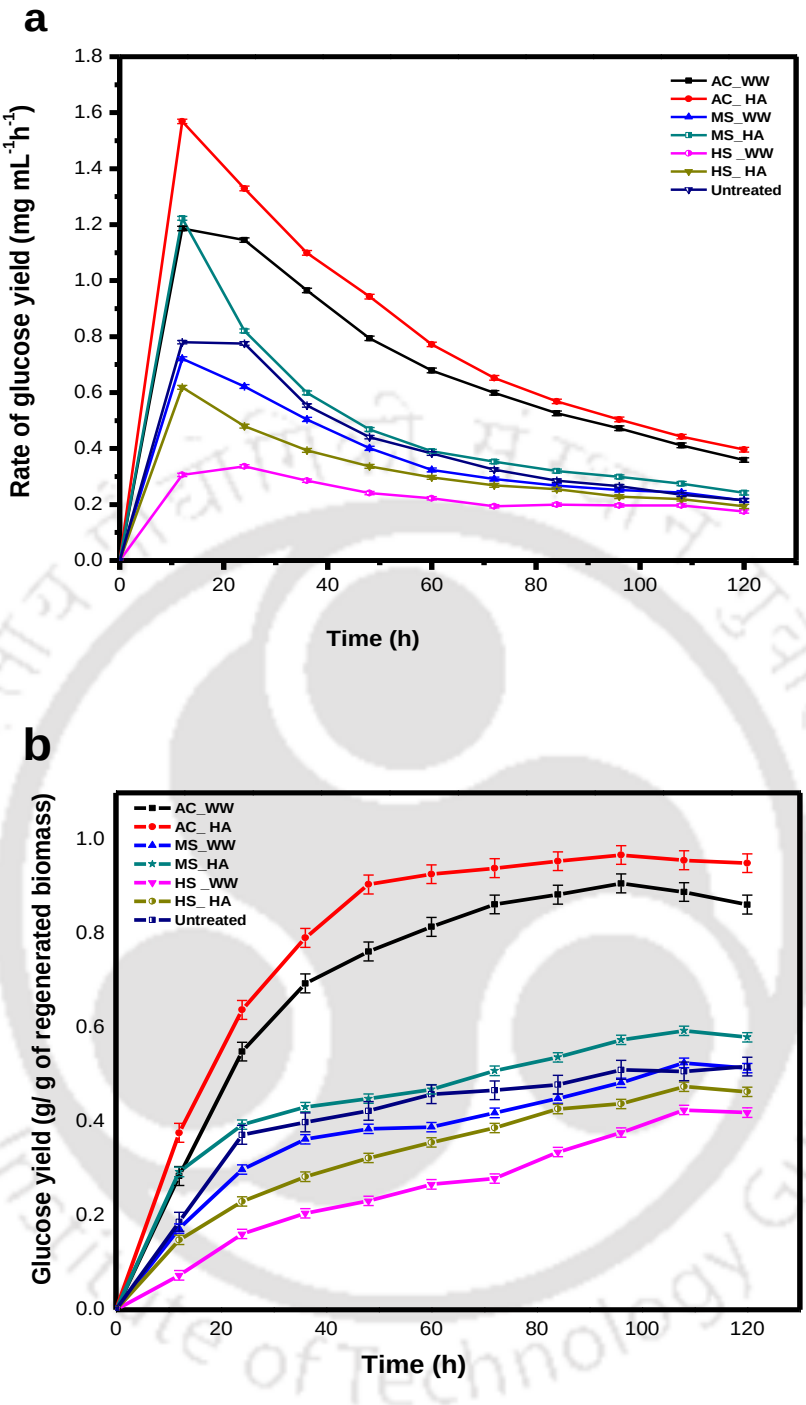

Fig 4-19: (a) Enzymatic hydrolysis rate for regenerated Miscanthus using different anti-solventsand untreated biomass and (b) Glucose yield through enzymatic hydrolysis for regenerated Miscanthus using different anti- solvents and untreated biomass

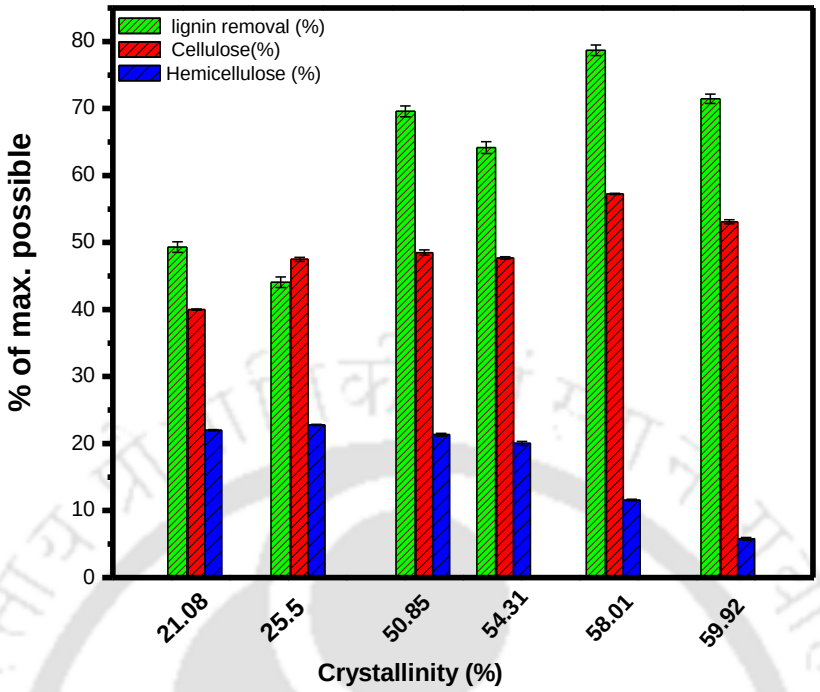

Fig 4-20: Effect of lignin removal (%), cellulose (%) and hemicellulose (%) on crystallinity of treated Miscanthus and effect of antisolvent on crystallinity.

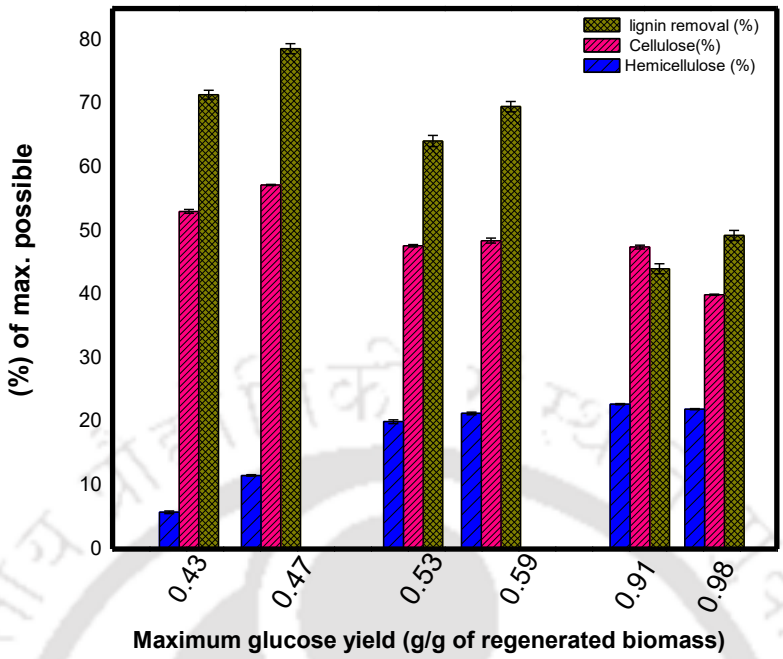

Fig 4-21: Effect of lignin removal (%), cellulose (%) and hemicellulose (%) present in treated Miscanthus on maximum glucose yield and effect of anti-solvent on glucose yield

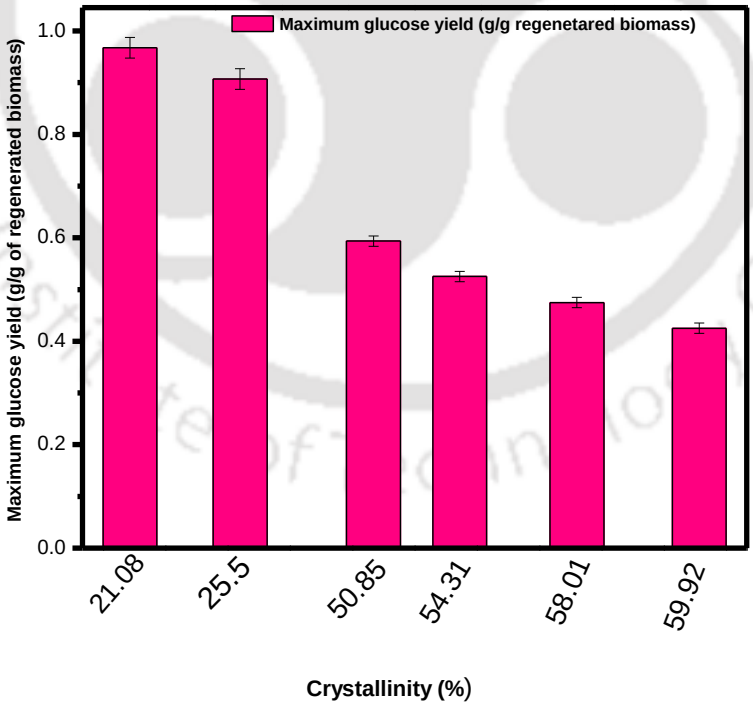

Fig 4-22: Effect of crystallinity and anti-solvent on maximum glucose yield

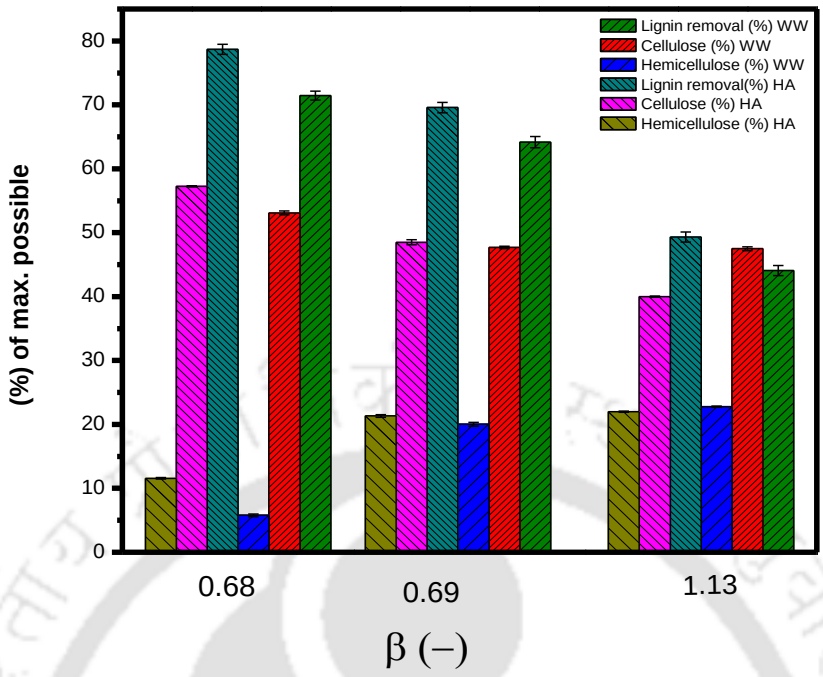

Fig 4-23: Effect of beta parameter on chemical composition of treated Miscanthus and effect of anti-solvent on chemical composition of Miscanthus

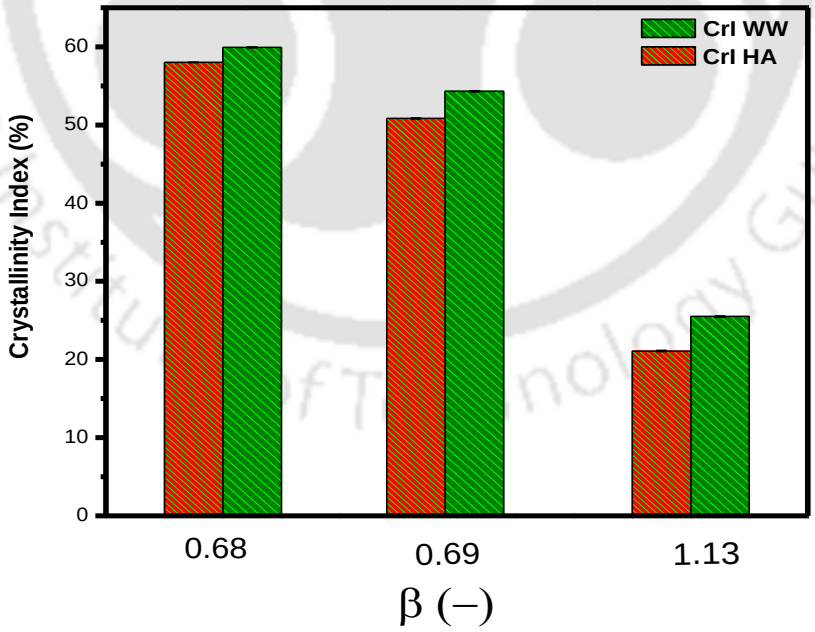

Fig 4-24: Effect of beta parameter on CRI of treated Miscanthus and effect of anti-solvent on CRI of treated Miscanthus

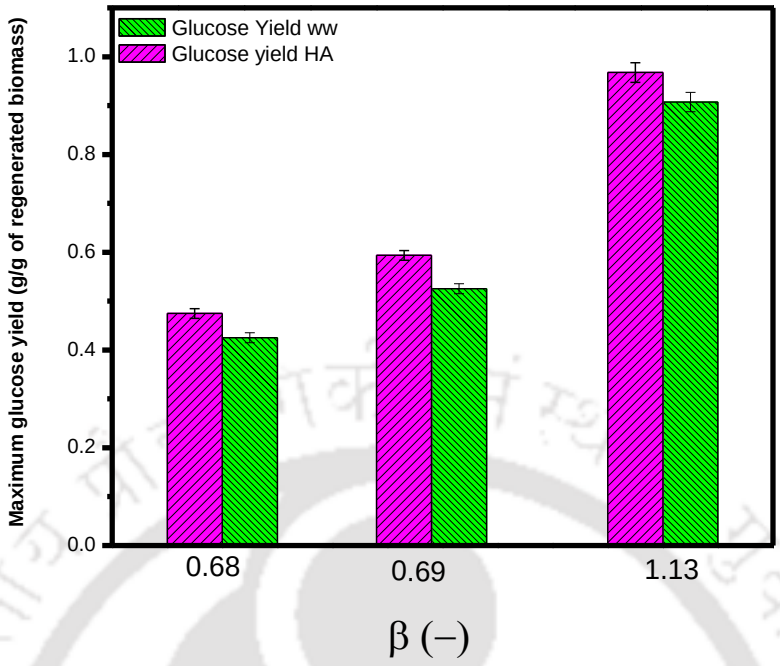

Fig 4-25: Effect of beta parameter on glucose yield and effect of anti-solvent

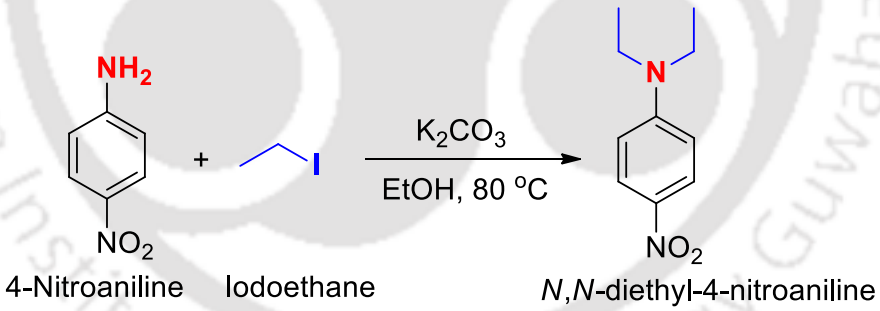

Scheme1: Synthesis of *N*, *N*-diethyl-4-nitroaniline, Yield = 32%

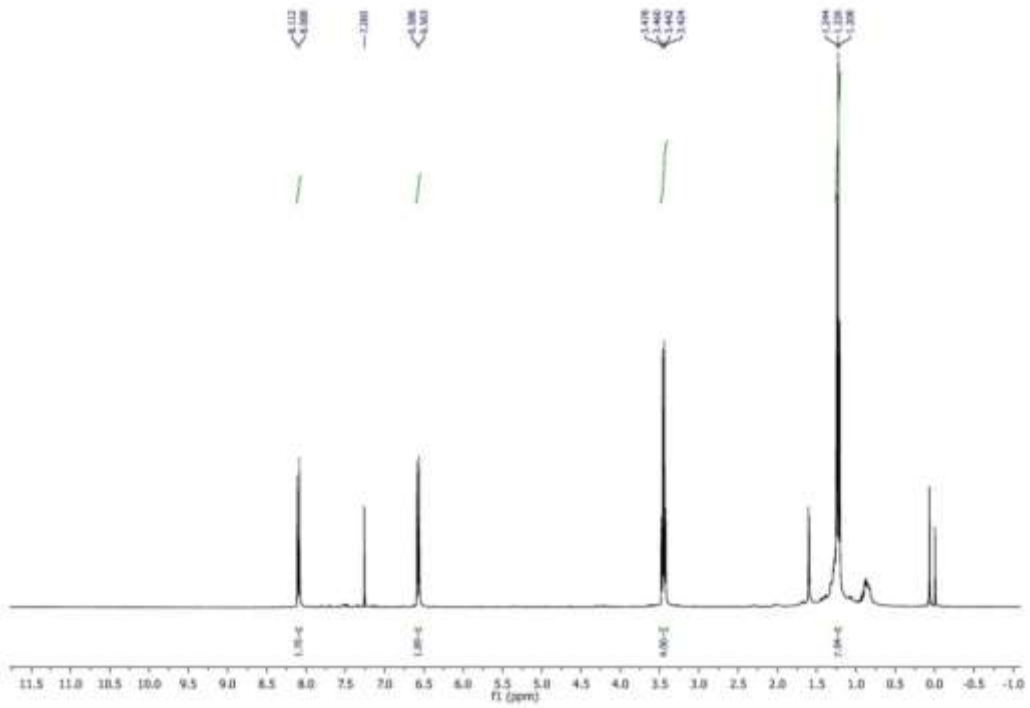

Fig4-26: *N*, *N*-Diethyl-4-nitroaniline: ^{1}H NMR (400 MHz, $CDCl_3$) spectra

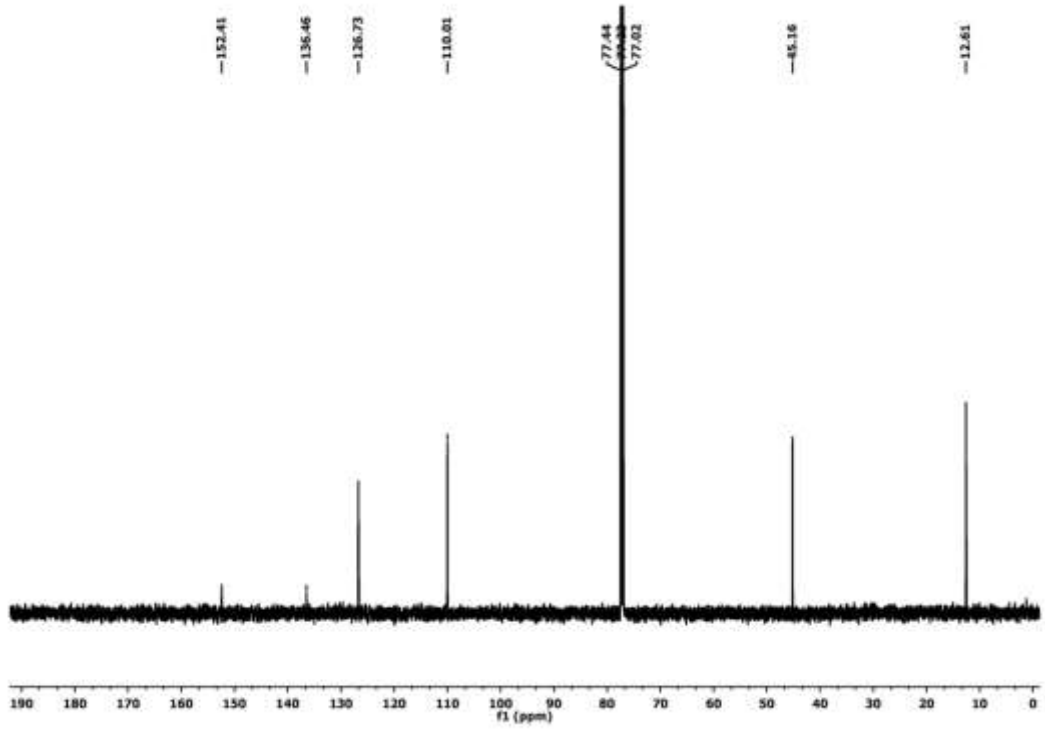

Fig 4-27: *N*, *N*-Diethyl-4-nitroaniline: ^{13}C NMR (150 MHz, $CDCl_3$) spectra

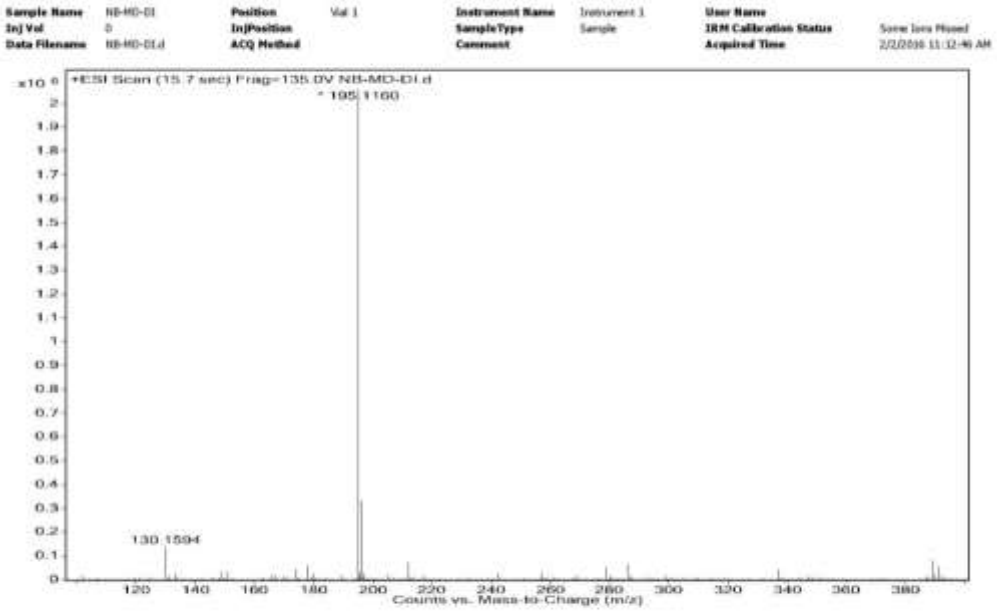

Fig 4-28: Mass spectra of *N*, *N*-Diethyl-4-nitroaniline

5 CONCLUSIONS AND FUTURE SCOPE

5.1 Concluding Remarks

The production and use of bioenergy is being considered as a way to help diminish climate change, which is economically viable. In order to choose or develop energy conversion processes for lignocellulosic biomass, it is necessary to understand its composition, physical and chemical properties. The physico-chemical characterization of Castor, Jatropha, and Miscanthus, which are available in plenty in north-east India, showed that they could be used as a source for bioenergy through gasification, thermal, and biochemical routes. The cellulose content of three biomasses is 40%-44% and was much higher than hemicellulose and lignin, which make them more suitable for cellulosic ethanol production. The chemical composition of structural carbohydrates, lignin and extractives were studied through FTIR. However, Miscanthus was found to be the best cellulosic ethanol source among the tested three biomass because of higher cellulose and hemicellulose content. The higher cellulose content of Miscanthus is also sup-ported by higher carbon content obtained from ultimate analysis (CHNSO) and higher crystallinity obtained from XRD analysis. Thermal decomposition study of Miscanthus, Castor, Jatropha shows that there was an initial loss of moisture from the samples started at around 25 ^{o}C and continued up to about 175 ^{o}C. The decomposition of hemicelluloses and cellulose occurred at around 175–380 ^{o}C and 380–570 ^{o}C, respectively. The decomposition of lignin happened slowly under the entire temperature range from ambient to 900 ^{o}C. For all the three biomass, the DTG peaks differed in their

position and height, because the heating rate acted as the main factor on thermal decomposition. With increasing the heating rate from 10 to 20 ^{o}C min^{-1}, the peak temperature corresponding to the maximum loss of the mass also shifted towards a little higher value. The maximum value of rate of weight loss was increased slightly. Further peak height was increased with increase in heating rate. The activation energy and pre-exponential factor for all three biomass from Kissinger and Ozawa method could not show much difference, but the fitting degree for Ozawa method was better than the Kissinger method for Miscanthus and Jatropha whereas the fitting degree was same for Castor. Calculation of activation energy separately from two reaction zones gave the clear idea that hemicelluloses decomposed first followed by cellulose. The estimation of kinetic parameters of lignocellulosic biomasses is useful for design and optimization of chemical processes such as pretreatment, gasification, and pyrolysis of biomass.

Pretreatment of lignocellulosic biomass is the major bottleneck for fermentable sugar production towards bio-ethanol production. Hence extensive research is needed for optimization of existing pretreatment technology and development of new pre-treatment technology for biomass fractionation to improve process economics and competitiveness of bio-ethanol. Based on the characterization study, it was found that Msicanthus was the most suitable biomass for conversion into bioethanol. Optimization of dilute acid pretreatment of Miscanthus was performed by RSM. Dilute sulphuric acid pre-treatment was effective in solubilising hemicellulose in the biomass. The optimum crystallinity for cellulose in the solid fraction of the acid pretreatment of Miscanthus was achieved with an Acid loading %(v/v) = 0.50, Solid loading %(w/v) = 3.98, Treatment Time (min)= 39.09. These conditions inevitably resulted in lower amount of glucose and inhibitors along with good amount of pentose sugar in liquid fraction. The cellulose amount present in solid fraction, upgraded from 43.34% to 65.8%. The reaction

condition for optimum concentration for xylose and arabinose present in liquid fraction was achieved with an Acid loading %(v/v) = 1.47, Solid loading %(w/v) = 4.75, Treatment Time (min)= 60.17. These conditions inevitably resulted in higher amount of glucose and inhibitors in liquid fraction whereas the cellulose amount present in solid fraction, upgraded from 43.34% to 79.1%. More lignin was removed from solid fraction in second optimisation in comparison to first optimisation for dilute acid treatment of Miscanthus.

Thermogravimetric analysis, XRD, FTIR and FESEM analysis were performed for raw and dilute acid pretreated Miscanthus in order to confirm changes after dilute acid pretreatment. The measured crystallinity index percentage for untreated, treated (optimised for amount xylose and arabinose present in filtrate (X+A) g/L) and treated (optimised for Crystalinity % (CRI %)) sample was 71.73%, 80.03% , 82% respectvily.

Optimum enzyme concentration obtained for enzymatic hydrolysis of pretreated biomass obtained was 20 (FPU/ g dry pretreated biomass). The optimum substrate concentration (pretreated biomass) for enzymatic hydrolysis was 5% (w/v). The yield of glucose from enzymatic hydrolysis of the pretreated biomass obtained at optimum condition for maximum xylose and arabinose present in liquid fraction of dilute acid hydrolysis of Miscanthus was higher than another optimum condition for dilute acid pretreatment of biomass because of lower lignin, hemicellulose content and lower crystallinity.

In the present work, three different ionic liquids i.e., $[EMIM]^+[Ac]^-$, $[EMIM]^+[MeSO_3]^-$, $[EMIM]^+[HSO_4]^-$ having fixed Imidazolium cation and variable anions were used for the pre-treatment of Miscanthus. Two different anti-solvents were used i.e., water and water-acetone mixture (1:1 v/v) for regeneration of the treated

Miscanthus from IL mixture. Among these three RTILs, the RTIL with acetate anion partially solubilised cellulose and lignin, converted cellulose I to cellulose II, drastically decreased the cellulose crystallinity, increased the cellulose accessibility and in combination greatly affected the enzymatic digestibility. IL with hydrogen sulphate anion solubilized almost entire amount of lignin present in Miscanthus, partially removed hemicellulose, enriched cellulose content, partially decreased crystallinity and resulted in poor enzymatic digestibility. IL with methanesulfonate anion partially solubilised lignin and hemicellulose, enriched cellulose content, decreased crystallinity and resulted in less enzymatic digestibility. It was found that glucose yield from treated and untreated biomass followed the following order:$[EMIM]^+[Ac]^-$ treated > $[EMIM]^+[MeSO_3]^-$ treated > untreated biomass > $[EMIM]^+[HSO_4]^-$ treated. Again, it was observed that glucose yield increased when water-acetone mixture (1:1 v/v) was used to regenerate the biomass in comparison with water as the anti-solvent. The hydrogen bond basicity (β value) which signified the ability to disrupt the inter- and intra-molecular hydrogen bonding in cellulose, hemicellulose and lignin co-related well with crystallinity index, lignin removal and glucose yield. Hence, β value of RTILs is very useful for selection of suitable RTILs for biomass dissolution. *N, N-diethyl-4-nitroaniline* was used to calculate the β parameter. To get better yield of *N, N-diethyl-4-nitroaniline,* the synthesis process was optimised and optimum yield obtained with polar protic solvent (C_2H_5OH) and higher reaction temperature. The acidity of the ILs also affected the glucose yield and it was found that RTIL with moderate acidity resulted in more glucose yield. The results of the present study will help future researchers to choose ILs as well as anti-solvents for pre-treatment as well as enzymatic digestibility of biomass. Preliminary experiments on ethanol production via shake flask along with estimation of fuel properties have shown us promising results to move forward to the

next stage and we hope to come up with substantial results very soon in order to demonstrate the commercial viability of these selected biomass.

5.2 Future Scope

- Synthesize of low cost, highly efficient ionic liquids for lignocellulose pretreatment.
- Recovery and reuse of ionic liquids.
- Strong analysis of impact of ionic liquid cations and anions on pre-treatment and fractionation of biomass.
- Integrated systems approach should be developed.

6 References

1. About the Energy Mix, (accessed July 3, 2015) http://www.planete-energies.com/en/medias/close/about-energy-mix.
2. U.S. Energy Information Administration. U.S. Department of Energy. International Energy Outlook 2016, (accessed May 11, 2016). https://www.eia.gov/outlooks/ieo/pdf/0484(2016).pdf.
3. National Research Council. (2010). *Liquid transportation fuels from coal and biomass: technological status, costs, and environmental impacts*. National Academies Press.
4. Wi, S. G., Cho, E. J., Lee, D. S., Lee, S. J., Lee, Y. J., & Bae, H. J. (2015). Lignocellulose conversion for biofuel: a new pretreatment greatly improves downstream biocatalytic hydrolysis of various lignocellulosic materials. *Biotechnology for Biofuels*, *8*(1), 228.
5. Cen, Y. P., Turpin, D. H., & Layzell, D. B. (2001). Whole-plant gas exchange and reductive biosynthesis in white lupin. *Plant Physiology*, *126*(4), 1555-1565.
6. Kuhad, R. C., & Singh, A. (1993). Lignocellulose biotechnology: current and future prospects. *Critical Reviews in Biotechnology*, *13*(2), 151-172.
7. Duffy, M. D., & Nanhou, V. Y. (2002). Switchgrass Production in Iowa: Economic Analysis. *Especial publication for Cahriton Valley resource Conservation District. Iowa State University Extension publication*, 18.
8. Rentizelas, A. A., Tolis, A. J., & Tatsiopoulos, I. P. (2009). Logistics issues of biomass: the storage problem and the multi-biomass supply chain. *Renewable and Sustainable Energy Reviews*, *13*(4), 887-894.
9. Caputo, A. C., Palumbo, M., Pelagagge, P. M., & Scacchia, F. (2005). Economics of biomass energy utilization in combustion and gasification plants: effects of logistic variables. *Biomass and Bioenergy*, *28*(1), 35-51.
10. Bajpai, P. (2016). *Pretreatment of lignocellulosic biomass for biofuel production*. Springer.
11. O'sullivan, A. C. (1997). Cellulose: the structure slowly unravels. *Cellulose*, *4*(3), 173-207.

12. Klemm, D., Heublein, B., Fink, H. P., & Bohn, A. (2005). Cellulose: fascinating biopolymer and sustainable raw material. *Angewandte Chemie International Edition*, *44*(22), 3358-3393.
13. Nishiyama, Y., Sugiyama, J., Chanzy, H., & Langan, P. (2003). Crystal structure and hydrogen bonding system in cellulose Iα from synchrotron X-ray and neutron fiber diffraction. *Journal of the American Chemical Society*, *125*(47), 14300-14306.
14. Wada, M., Heux, L., Isogai, A., Nishiyama, Y., Chanzy, H., & Sugiyama, J. (2001). Improved structural data of cellulose IIII prepared in supercritical ammonia. *Macromolecules*, *34*(5), 1237-1243.
15. Wada, M., Chanzy, H., Nishiyama, Y., & Langan, P. (2004). Cellulose IIII crystal structure and hydrogen bonding by synchrotron X-ray and neutron fiber diffraction. *Macromolecules*, *37*(23), 8548-8555.
16. Wada, M., Heux, L., & Sugiyama, J. (2004). Polymorphism of cellulose I family: reinvestigation of cellulose IVI. *Biomacromolecules*, *5*(4), 1385-1391.
17. Newman, R. H. (2008). Simulation of X-ray diffractograms relevant to the purported polymorphs cellulose IVI and IVII. *Cellulose*, *15*(6), 769.
18. Horikawa, Y., Konakahara, N., Imai, T., Kentaro, A., Kobayashi, Y., & Sugiyama, J. (2013). The structural changes in crystalline cellulose and effects on enzymatic digestibility. *Polymer Degradation and Stability*, *98*(11), 2351-2356.
19. Wada, M., Ike, M., & Tokuyasu, K. (2010). Enzymatic hydrolysis of cellulose I is greatly accelerated via its conversion to the cellulose II hydrate form. *Polymer Degradation and Stability*, *95*(4), 543-548.
20. Fengel, D. (1971, January). Ideas on the ultrastructural organization of the cell wall components. In *Journal of Polymer Science: Polymer Symposia* (Vol. 36, No. 1, pp. 383-392). Wiley Subscription Services, Inc., A Wiley Company.
21. Agbor, V. B., Cicek, N., Sparling, R., Berlin, A., & Levin, D. B. (2011). Biomass pretreatment: fundamentals toward application. *Biotechnology advances*, *29*(6), 675-685.
22. Beily, P. (1993). Biochemical aspects of the production of microbial hemicellulose. *Hemicellulose and Hemicellulases. Portland Press, London*, 29-51.
23. Scheller, H. V., & Ulvskov, P. (2010). Annual Review of Plant Biology. *Hemicelluloses*, *61*, 263-289.

24. Peng, F., Ren, J. L., Xu, F., & Sun, R. C. (2011). Chemicals from hemicelluloses: A review. In *Sustainable production of fuels, chemicals, and fibers from forest biomass* (pp. 219-259). American Chemical Society.
25. Sun, R. (2010). *Cereal straw as a resource for sustainable biomaterials and biofuels: chemistry, extractives, lignins, hemicelluloses and cellulose*. Elsevier.
26. Ragauskas, A. J., Beckham, G. T., Biddy, M. J., Chandra, R., Chen, F., Davis, M. F., ... & Langan, P. (2014). Lignin valorization: improving lignin processing in the biorefinery. *Science*, *344*(6185), 1246843.
27. Calvo-Flores, F. G., & Dobado, J. A. (2010). Lignin as renewable raw material. *Chem Sus Chem*, *3*(11), 1227-1235.
28. Boerjan, W., Ralph, J., & Baucher, M. (2003). Lignin biosynthesis. *Annual Review of Plant Biology*, *54*(1), 519-546.
29. Guo, F., Shi, W., Sun, W., Li, X., Wang, F., Zhao, J., & Qu, Y. (2014). Differences in the adsorption of enzymes onto lignins from diverse types of lignocellulosic biomass and the underlying mechanism. *Biotechnology for Biofuels*, *7*(1), 38.
30. Buranov, A. U., & Mazza, G. (2008). Lignin in straw of herbaceous crops. *Industrial Crops and Products*, *28*(3), 237-259.
31. Mussatto, S. I., & Teixeira, J. A. (2010). Lignocellulose as raw material in fermentation processes. *Current Research, Technology and Education Topics in Applied Microbiology and Microbial Biotechnology (Méndez-Vilas, A., Ed.)*, *2*, 897-907.
32. Martinez, J. A., Szeto, P. L., & Stewart, T. M. (2017). The Relationship between Structural Parameters and Mechanical Properties of Cactus Spines.
33. Xiao, C., & Anderson, C. T. (2013). Roles of pectin in biomass yield and processing for biofuels. *Frontiers in Plant Science*, *4*.
34. Dash, M., Venkata Dasu, V., & Mohanty, K. (2015). Physico-chemical characterization of Miscanthus, Castor, and Jatropha towards biofuel production. *Journal of Renewable and Sustainable Energy*, *7*(4), 043124.
35. Alriksson, B. (2009). *Ethanol from lignocellulose: Management of by-products of hydrolysis* (Doctoral dissertation, Karlstad University).
36. Rowell, R. M., Pettersen, R., Han, J. S., Rowell, J. S., & Tshabalala, M. A. (2005). Cell wall chemistry. *Handbook of Wood Chemistry and Wood Composites*, *2*.

37. Faulon, J. L., Carlson, G. A., & Hatcher, P. G. (1994). A three-dimensional model for lignocellulose from gymnospermous wood. *Organic Geochemistry, 21*(12), 1169-1179.
38. Harmsen, P. F. H., Huijgen, W., Bermudez, L., & Bakker, R. (2010). *Literature review of physical and chemical pretreatment processes for lignocellulosic biomass* (No. 1184). Wageningen UR Food & Biobased Research.
39. Iiyama, K., Lam, T. B. T., & Stone, B. A. (1994). Covalent cross-links in the cell wall. *Plant physiology*, *104*(2), 315.
40. Toikka, M., Sipilä, J., Teleman, A., & Brunow, G. (1998). Lignin–carbohydrate model compounds. Formation of lignin–methyl arabinoside and lignin–methyl galactoside benzyl ethers via quinone methide intermediates. *Journal of the Chemical Society, Perkin Transactions 1*, (22), 3813-3818.
41. Sun, J. X., Sun, X. F., Sun, R. C., Fowler, P., & Baird, M. S. (2003). Inhomogeneities in the chemical structure of sugarcane bagasse lignin. *Journal of Agricultural and Food Chemistry*, *51*(23), 6719-6725.
42. Houghton, J., Weatherwax, S., & Ferrell, J. (2006). *Breaking the biological barriers to cellulosic ethanol: a joint research agenda* (No. DOE/SC--0095). EERE Publication and Product Library.
43. Brandt, A., Gräsvik, J., Hallett, J. P., & Welton, T. (2013). Deconstruction of lignocellulosic biomass with ionic liquids. *Green Chemistry*, *15*(3), 550-583.
44. Nigam, P. S., & Singh, A. (2011). Production of liquid biofuels from renewable resources. *Progress in Energy and Combustion Science*, *37*(1), 52-68.
45. Tan, K. T., Lee, K. T., & Mohamed, A. R. (2008). Role of energy policy in renewable energy accomplishment: The case of second-generation bioethanol. *Energy Policy*, *36*(9), 3360-3365.
46. Accelerating Industry Innovation (2012). Ethanol Industry Outlook. Renewable Fuels Association. http://ethanolrfa.3cdn.net/d4ad995ffb7ae8fbfe_1vm62ypzd.pdf
47. Fenton, P., & Carlsson, H. (2010). *Bioethanol for sustainable transport: results and recommendations from the European BEST project*. Environment Health Administration, City of Stockholm. https://web.archive.org/web/20100930040041/http://www.eve.es/ecomovil/pdf/BEST_FinalReport.pdf

48. Balat, M., Balat, H., & Öz, C. (2008). Progress in bioethanol processing. *Progress in Energy and Combustion Science*, *34*(5), 551-573.
49. Kumar, D., & Murthy, G. S. (2011). Impact of pretreatment and downstream processing technologies on economics and energy in cellulosic ethanol production. *Biotechnology for biofuels*, *4*(1), 27.
50. Yang, B., & Wyman, C. E. (2008). Pretreatment: the key to unlocking low-cost cellulosic ethanol. *Biofuels, Bioproducts and Biorefining*, *2*(1), 26-40.
51. Brodeur, G., Yau, E., Badal, K., Collier, J., Ramachandran, K. B., & Ramakrishnan, S. (2011). Chemical and physicochemical pretreatment of lignocellulosic biomass: a review. *Enzyme Research*, *2011*.
52. Ethanol in India - information and useful links (2017). http://www.ethanolindia.net/
53. Prasad, S., Singh, A., Jain, N., & Joshi, H. C. (2007). Ethanol production from sweet sorghum syrup for utilization as automotive fuel in India. *Energy & Fuels*, *21*(4), 2415-2420.
54. Sukumaran, R. K., Surender, V. J., Sindhu, R., Binod, P., Janu, K. U., Sajna, K. V., Rajasree, K. P., & Pandey, A. (2010). Lignocellulosic ethanol in India: prospects, challenges and feedstock availability. *Bioresource Technology*, *101*(13), 4826-4833.
55. Gonsalves, J. B. (2006). An assessment of the biofuels industry in India. *Geneva: Unctad*. http://unctad.org/en/docs/ditcted20066_en.pdf
56. Wyman, C. E. (1995). *Ethanol production from lignocellulosic biomass* (No. CONF-950336--). American Society of Mechanical Engineers, New York, NY (United States).
57. Agricultural statistics at a glance (2014). *Directorate of Economics and Statistics. Dept. of Agric. and Co-operation. Ministry of Agriculture, Government of India*. http://eands.dacnet.nic.in/PDF/Agricultural-Statistics-At-Glance2014.pdf
58. Nguyen, Q. A., & Saddler, J. N. (1991). An integrated model for the technical and economic evaluation of an enzymatic biomass conversion process. *Bioresource Technology*, *35*(3), 275-282.
59. Abbasi, T., & Abbasi, S. A. (2010). Biomass energy and the environmental impacts associated with its production and utilization. *Renewable and Sustainable Energy Reviews*, *14*(3), 919-937.

60. Joshi, P., Sharma, N., & Manab Sarma, P. (2016). Assessment of biomass potential and current status of bio-fuels and bioenergy production in India. *Current Biochemical Engineering*, *3*(1), 4-15.
61. MNRE Annual Report (2015). Overview of biomass power sector in India. *Ministry of new and Renewable energy, Government of India*. http://biomasspower.gov.in/About-us-3-Biomass%20Energy%20scenario-4.php
62. Kumar, A., Kumar, N., Baredar, P., & Shukla, A. (2015). A review on biomass energy resources, potential, conversion and policy in India. *Renewable and Sustainable Energy Reviews*, *45*, 530-539.
63. Sukumaran, R. K., Mathew, A. K., Kumar, M. K., Abraham, A., Chistopher, M., & Sankar, M. (2017). First-and Second-Generation Ethanol in India: A Comprehensive Overview on Feedstock Availability, Composition, and Potential Conversion Yields. In *Sustainable Biofuels Development in India* (pp. 223-246). Springer International Publishing.
64. Agarwal, A. K., Pandey, A., Gupta, A. K., Aggarwal, S. K., & Kushari, A. (Eds.). (2014). *Novel combustion concepts for sustainable energy development*. Springer.
65. Chandel, A. K., & Sukumaran, R. K. (2017). *Sustainable Biofuels Development in India*. Springer International Pu.
66. Chung, J. H., & Kim, D. S. (2012). Miscanthus as a potential bioenergy crop in East Asia. *Journal of Crop Science and Biotechnology*, *15*(2), 65-77.
67. Walsh, M., & Jones, M. (Eds.). (2013). *Miscanthus: for energy and fibre*. Routledge.
68. Brosse, N., Dufour, A., Meng, X., Sun, Q., & Ragauskas, A. (2012). Miscanthus: a fast-growing crop for biofuels and chemicals production. *Biofuels, Bioproducts and Biorefining*, *6*(5), 580-598.
69. Ricinus communis, (2007). http://www.jatrophabiodiesel.org/castor/about-plant.php
70. Castor Bean, (2011). http://www.ibuzzle.com/articles/castor-bean.html
71. Jena, J., & Gupta, A. K. (2012). Ricinus communis Linn: a phytopharmacological review. *International Journal of Pharmacy and Pharmaceutical Sciences*, *4*(4), 25-29.
72. Openshaw, K. (2000). A review of Jatropha curcas: an oil plant of unfulfilled promise. *Biomass and Bioenergy*, *19*(1), 1-15.

73. Canilha, L., Chandel, A. K., Suzane dos Santos Milessi, T., Antunes, F. A. F., Luiz da Costa Freitas, W., das Graças Almeida Felipe, M., & da Silva, S. S. (2012). Bioconversion of sugarcane biomass into ethanol: an overview about composition, pretreatment methods, detoxification of hydrolysates, enzymatic saccharification, and ethanol fermentation. *BioMed Research International*, *2012*.
74. Limayem, A., & Ricke, S. C. (2012). Lignocellulosic biomass for bioethanol production: current perspectives, potential issues and future prospects. *Progress in Energy and Combustion Science*, *38*(4), 449-467.
75. Kumar, A. K., & Sharma, S. (2017). Recent updates on different methods of pretreatment of lignocellulosic feedstocks: a review. *Bioresources and Bioprocessing*, *4*(1), 7.
76. Himmel, M. E., Baker, J. O., & Overend, R. P. (1994). *Enzymatic conversion of biomass for fuels production* (pp. 292-324). Washington, DC: American Chemical Society.
77. Gírio, F. M., Fonseca, C., Carvalheiro, F., Duarte, L. C., Marques, S., & Bogel-Łukasik, R. (2010). Hemicelluloses for fuel ethanol: a review. *Bioresource Technology*, *101*(13), 4775-4800.
78. Chan, E. S., Rudravaram, R., Narasu, M. L., Rao, L. V., & Ravindra, P. (2007). Economics and environmental impact of bioethanol production technologies: an appraisal. *Biotechnology and Molecular Biology Reviews*, *2*(1), 14-32.
79. Larsson, S., Palmqvist, E., Hahn-Hägerdal, B., Tengborg, C., Stenberg, K., Zacchi, G., & Nilvebrant, N. O. (1999). The generation of fermentation inhibitors during dilute acid hydrolysis of softwood. *Enzyme and Microbial Technology*, *24*(3), 151-159.
80. Kanchanalai, P., Temani, G., Kawajiri, Y., & Realff, M. J. (2016). Reaction kinetics of concentrated-acid hydrolysis for cellulose and hemicellulose and effect of crystallinity. *Bioresources*, *11*(1), 1672-1689.
81. Akpinar, O., Erdogan, K., Bakir, U., & Yilmaz, L. (2010). Comparison of acid and enzymatic hydrolysis of tobacco stalk xylan for preparation of xylooligosaccharides. *LWT-Food Science and Technology*, *43*(1), 119-125.
82. Du, B., Sharma, L. N., Becker, C., Chen, S. F., Mowery, R. A., van Walsum, G. P., & Chambliss, C. K. (2010). Effect of varying feedstock–pretreatment chemistry combinations on the formation and accumulation of potentially

inhibitory degradation products in biomass hydrolysates. *Biotechnology and Bioengineering*, *107*(3), 430-440.

83. Jönsson, L. J., Alriksson, B., & Nilvebrant, N. O. (2013). Bioconversion of lignocellulose: inhibitors and detoxification. *Biotechnology for Biofuels*, *6*(1), 16.
84. Berlin, A., Balakshin, M., Gilkes, N., Kadla, J., Maximenko, V., Kubo, S., & Saddler, J. (2006). Inhibition of cellulase, xylanase and β-glucosidase activities by softwood lignin preparations. *Journal of biotechnology*, *125*(2), 198-209.
85. Ximenes, E., Kim, Y., Mosier, N., Dien, B., & Ladisch, M. (2011). Deactivation of cellulases by phenols. *Enzyme and Microbial Technology*, *48*(1), 54-60.
86. Zaldivar, J., & Ingram, L. O. (1999). Effect of organic acids on the growth and fermentation of ethanologenic Escherichia coli LY01. *Biotechnology and Bioengineering*, *66*(4), 203-210.
87. Takahashi, C. M., Takahashi, D. F., Carvalhal, M. L., & Alterthum, F. (1999). Effects of acetate on the growth and fermentation performance of Escherichia coli KO11. *Applied Biochemistry and Biotechnology*, *81*(3), 193-203.
88. Imai, T., & Ohno, T. (1995). The relationship between viability and intracellular pH in the yeast Saccharomyces cerevisiae. *Applied and Environmental Microbiology*, *61*(10), 3604-3608.
89. Mussatto, S. I., & Roberto, I. C. (2004). Alternatives for detoxification of diluted-acid lignocellulosic hydrolyzates for use in fermentative processes: a review. *Bioresource Technology*, *93*(1), 1-10.
90. Larsson, S., Cassland, P., & Jönsson, L. J. (2001). Development of a Saccharomyces cerevisiae strain with enhanced resistance to phenolic fermentation inhibitors in lignocellulose hydrolysates by heterologous expression of laccase. *Applied and Environmental Microbiology*, *67*(3), 1163-1170.
91. Galbe, M., & Zacchi, G. (2002). A review of the production of ethanol from softwood. *Applied Microbiology and Biotechnology*, *59*(6), 618-628.
92. Kumar, A., Singh, L. K., & Ghosh, S. (2009). Bioconversion of lignocellulosic fraction of water-hyacinth (Eichhornia crassipes) hemicellulose acid hydrolysate to ethanol by Pichia stipitis. *Bioresource Technology*, *100*(13), 3293-3297.
93. Dien, B. S., Cotta, M. A., & Jeffries, T. W. (2003). Bacteria engineered for fuel ethanol production: current status. *Applied Microbiology and Biotechnology*, *63*(3), 258-266.

94. Azhar, S. H. M., Abdulla, R., Jambo, S. A., Marbawi, H., Gansau, J. A., Faik, A. A. M., & Rodrigues, K. F. (2017). Yeasts in sustainable bioethanol production: A review. *Biochemistry and Biophysics Reports*, *10*, 52-61.
95. Mussatto, S. I., Machado, E. M., Carneiro, L. M., & Teixeira, J. A. (2012). Sugars metabolism and ethanol production by different yeast strains from coffee industry wastes hydrolysates. *Applied Energy*, *92*, 763-768.
96. Yanase, S., Hasunuma, T., Yamada, R., Tanaka, T., Ogino, C., Fukuda, H., & Kondo, A. (2010). Direct ethanol production from cellulosic materials at high temperature using the thermotolerant yeast Kluyveromyces marxianus displaying cellulolytic enzymes. *Applied Microbiology and Biotechnology*, *88*(1), 381-388.
97. Singh, A., Bajar, S., & Bishnoi, N. R. (2014). Enzymatic hydrolysis of microwave alkali pretreated rice husk for ethanol production by Saccharomyces cerevisiae, Scheffersomyces stipitis and their co-culture. *Fuel*, *116*, 699-702.
98. Karagöz, P., & Özkan, M. (2014). Ethanol production from wheat straw by Saccharomyces cerevisiae and Scheffersomyces stipitis co-culture in batch and continuous system. *Bioresource Technology*, *158*, 286-293.
99. Zabed, H., Sahu, J. N., Suely, A., Boyce, A. N., & Faruq, G. (2017). Bioethanol production from renewable sources: Current perspectives and technological progress. *Renewable and Sustainable Energy Reviews*, 71, 475-501.
100. Liu, Z. H., Qin, L., Zhu, J. Q., Li, B. Z., & Yuan, Y. J. (2014). Simultaneous saccharification and fermentation of steam-exploded corn stover at high glucan loading and high temperature. *Biotechnology for Biofuels*, *7*(1), 167.
101. Van Zyl, W. H., Lynd, L. R., den Haan, R., & McBride, J. E. (2007). Consolidated bioprocessing for bioethanol production using Saccharomyces cerevisiae. In *Biofuels* (pp. 205-235). Springer Berlin Heidelberg.
102. Sharma, N., Kalra, K. L., Oberoi, H. S., & Bansal, S. (2007). Optimization of fermentation parameters for production of ethanol from kinnow waste and banana peels by simultaneous saccharification and fermentation. *Indian Journal of Microbiology*, *47*(4), 310-316.
103. Adaganti, S. Y., Yaliwal, V. S., Kulkarni, B. M., Desai, G. P., & Banapurmath, N. R. (2014). Factors affecting bioethanol production from lignocellulosic biomass (Calliandra calothyrsus). *Waste and Biomass Valorization*, *5*(6), 963-971.

104. Duff, S. J., & Murray, W. D. (1996). Bioconversion of forest products industry waste cellulosics to fuel ethanol: a review. *Bioresource Technology*, *55*(1), 1-33.
105. Bui, S., Verykios, X., & Mutharasan, R. (1985). In situ removal of ethanol from fermentation broths. 1. Selective adsorption characteristics. *Industrial & Engineering Chemistry Process Design and Development*, *24*(4), 1209-1213.
106. De Filippi, R. P., & Moses, J. M. (1982, January). Extraction of organics from aqueous solutions using critical-fluid carbon dioxide. In *Biotechnol. Bioeng. Symp.;(United States)* (Vol. 12, No. CONF-820580-). Critical Fluid Systems, Inc., Cambridge, MA.
107. Leeper, S. A., & Wankat, P. C. (1982). Gasohol production by extraction of ethanol from water using gasoline as solvent. *Industrial & Engineering Chemistry Process Design and Development*, *21*(2), 331-334.
108. Carton, A., Benito, G. G., Rey, J. A., & de La Fuente, M. (1998). Selection of adsorbents to be used in an ethanol fermentation process. Adsorption isotherms and kinetics. *Bioresource Technology*, *66*(1), 75-78.
109. Bowen, T. C., Meier, R. G., & Vane, L. M. (2007). Stability of MFI zeolite-filled PDMS membranes during pervaporative ethanol recovery from aqueous mixtures containing acetic acid. *Journal of Membrane Science*, *298*(1), 117-125.
110. Lynd, L. R. (1996). Overview and evaluation of fuel ethanol from cellulosic biomass: technology, economics, the environment, and policy. *Annual Review of Energy and the Environment*, *21*(1), 403-465.
111. Mosier, N., Wyman, C., Dale, B., Elander, R., Lee, Y. Y., Holtzapple, M., & Ladisch, M. (2005). Features of promising technologies for pretreatment of lignocellulosic biomass. *Bioresource Technology*, *96*(6), 673-686.
112. Chen, H., Liu, J., Chang, X., Chen, D., Xue, Y., Liu, P., Lin, H., & Han, S. (2017). A review on the pretreatment of lignocellulose for high-value chemicals. *Fuel Processing Technology*, *160*, 196-206.
113. Wyman, C. E., Dale, B. E., Elander, R. T., Holtzapple, M., Ladisch, M. R., & Lee, Y. Y. (2005). Coordinated development of leading biomass pretreatment technologies. *Bioresource Technology*, *96*(18), 1959-1966.
114. Chiaramonti, D., Prussi, M., Ferrero, S., Oriani, L., Ottonello, P., Torre, P., & Cherchi, F. (2012). Review of pretreatment processes for lignocellulosic ethanol production, and development of an innovative method. *Biomass and Bioenergy*, *46*, 25-35.

115. Zhang, K., Pei, Z., & Wang, D. (2016). Organic solvent pretreatment of lignocellulosic biomass for biofuels and biochemicals: a review. *Bioresource Technology*, *199*, 21-33.

116. Mood, S. H., Golfeshan, A. H., Tabatabaei, M., Jouzani, G. S., Najafi, G. H., Gholami, M., & Ardjmand, M. (2013). Lignocellulosic biomass to bioethanol, a comprehensive review with a focus on pretreatment. *Renewable and Sustainable Energy Reviews*, *27*, 77-93.

117. Sun, Y., & Cheng, J. (2002). Hydrolysis of lignocellulosic materials for ethanol production: a review. *Bioresource Technology*, *83*(1), 1-11.

118. Behera, S., Arora, R., Nandhagopal, N., & Kumar, S. (2014). Importance of chemical pretreatment for bioconversion of lignocellulosic biomass. *Renewable and Sustainable Energy Reviews*, *36*, 91-106.

119. Kurian, J. K., Nair, G. R., Hussain, A., & Raghavan, G. V. (2013). Feedstocks, logistics and pre-treatment processes for sustainable lignocellulosic biorefineries: A comprehensive review. *Renewable and Sustainable Energy Reviews*, *25*, 205-219.

120. Swatloski, R. P., Spear, S. K., Holbrey, J. D., & Rogers, R. D. (2002, August). Ionic liquids: New solvents for non-derivitized cellulose dissolution. In *Abstracts of papers of the American Chemical Society* (vol. 224, pp. u622-u622). 1155 16th ST, NW, Washington, DC 20036 USA: Amer Chemical Soc.

121. Zhu, J. Y., Pan, X., & Zalesny, R. S. (2010). Pretreatment of woody biomass for biofuel production: energy efficiency, technologies, and recalcitrance. *Applied Microbiology and Biotechnology*, *87*(3), 847-857.

122. Zheng, Y., Pan, Z., & Zhang, R. (2009). Overview of biomass pretreatment for cellulosic ethanol production. *International Journal of Agricultural and Biological Engineering*, *2*(3), 51-68.

123. Singh, P., Suman, A., Tiwari, P., Arya, N., Gaur, A., & Shrivastava, A. K. (2008). Biological pretreatment of sugarcane trash for its conversion to fermentable sugars. *World Journal of Microbiology and Biotechnology*, *24*(5), 667-673.

124. Sánchez, C. (2009). Lignocellulosic residues: biodegradation and bioconversion by fungi. *Biotechnology Advances*, *27*(2), 185-194.

125. Wan, C., & Li, Y. (2012). Fungal pretreatment of lignocellulosic biomass. *Biotechnology Advances*, *30*(6), 1447-1457.

126. Keller, F. A., Hamilton, J. E., & Nguyen, Q. A. (2003). Microbial pretreatment of biomass. *Applied Biochemistry and Biotechnology*, *105*(1-3), 27.

127. Rouches, E., Zhou, S., Steyer, J. P., & Carrere, H. (2016). White-Rot Fungi pretreatment of lignocellulosic biomass for anaerobic digestion: Impact of glucose supplementation. *Process Biochemistry*, *51*(11), 1784-1792.

128. Martínez, P. M., Bakker, R., Harmsen, P., Gruppen, H., & Kabel, M. (2015). Importance of acid or alkali concentration on the removal of xylan and lignin for enzymatic cellulose hydrolysis. *Industrial Crops and Products*, *64*, 88-96.

129. Sun, X., Sun, X., & Zhang, F. (2016). Combined pretreatment of lignocellulosic biomass by solid base (calcined Na_2SiO_3) and ionic liquid for enhanced enzymatic saccharification. *RSC Advances*, *6*(101), 99455-99466.

130. Chen, H., & Qiu, W. (2010). Key technologies for bioethanol production from lignocellulose. *Biotechnology Advances*, *28*(5), 556-562.

131. Misson, M., Haron, R., Kamaroddin, M. F. A., & Amin, N. A. S. (2009). Pretreatment of empty palm fruit bunch for production of chemicals via catalytic pyrolysis. *Bioresource Technology*, *100*(11), 2867-2873.

132. Mullen, C. A., & Boateng, A. A. (2008). Chemical composition of bio-oils produced by fast pyrolysis of two energy crops. *Energy & fuels*, *22*(3), 2104-2109.

133. Bridgwater, A. V. (2012). Review of fast pyrolysis of biomass and product upgrading. *Biomass and Bioenergy*, *38*, 68-94.

134. Luque, L., Oudenhoven, S., Westerhof, R., Rossum, G., Berruti, F., Kersten, S., & Rehmann, L. (2016). Comparison of ethanol production from corn cobs and switchgrass following a pyrolysis-based biorefinery approach. *Biotechnology for Biofuels*, *9*(1), 242.

135. Wang, Y., Song, H., Peng, L., Zhang, Q., & Yao, S. (2014). Recent developments in the catalytic conversion of cellulose. *Biotechnology & Biotechnological Equipment*, *28*(6), 981-988.

136. Fahmi, R., Bridgwater, A. V., Darvell, L. I., Jones, J. M., Yates, N., Thain, S., & Donnison, I. S. (2007). The effect of alkali metals on combustion and pyrolysis of Lolium and Festuca grasses, switchgrass and willow. *Fuel*, *86*(10), 1560-1569.

137. Yang, H., Yan, R., Chen, H., Lee, D. H., & Zheng, C. (2007). Characteristics of hemicellulose, cellulose and lignin pyrolysis. *Fuel*, *86*(12), 1781-1788.

138. Simon, P. (2004). Isoconversional methods fundamentals meaning and application. *Journal of Thermal Analysis and Calorimetry*, *76*(1), 123- 132.

139. Sbirrazzuoli, N., Vincent, L., Mija, A., & Guigo, N. (2009). Integral, differential and advanced isoconversional methods: complex mechanisms and isothermal predicted conversion–time curves. *Chemometrics and Intelligent Laboratory Systems*, *96*(2), 219-226.

140. Khawam, A. (2007). *Application of solid-state kinetics to desolvation reactions* (Doctoral dissertation, The University of Iowa).

141. Opfermann, J. R., Kaisersberger, E., & Flammersheim, H. J. (2002). Model-free analysis of thermoanalytical data-advantages and limitations. *Thermochimica Acta*, *391*(1), 119-127.

142. Pisharath, S., & Ang, H. G. (2007). Thermal decomposition kinetics of a mixture of energetic polymer and nitramine oxidizer. *Thermochimica Acta*, *459*(1), 26-33.

143. Chowlu, A. C. K., Reddy, P. K., & Ghoshal, A. K. (2009). Pyrolytic decomposition and model-free kinetics analysis of mixture of polypropylene (PP) and low-density polyethylene (LDPE). *Thermochimica Acta*, *485*(1), 20-25.

144. Jeguirim, M., & Trouvé, G. (2009). Pyrolysis characteristics and kinetics of Arundo donax using thermogravimetric analysis. *Bioresource Technology*, *100*(17), 4026-4031.

145. Rogers, R. N. (2008). *A chemist's perspective on the Shroud of Turin*. Barrie M. Schwortz.

146. Aslanzadeh, S., Berg, A., Taherzadeh, M. J., & Horváth, I. S. (2014). Biogas production from N-methylmorpholine-N-oxide (NMMO) pretreated forest residues. *Applied Biochemistry and Biotechnology*, *172*(6), 2998-3008.

147. Geddes, C. C., Peterson, J. J., Roslander, C., Zacchi, G., Mullinnix, M. T., Shanmugam, K. T., & Ingram, L. O. (2010). Optimizing the saccharification of sugar cane bagasse using dilute phosphoric acid followed by fungal cellulases. *Bioresource Technology*, *101*(6), 1851-1857.

148. Iranmahboob, J., Nadim, F., & Monemi, S. (2002). Optimizing acid-hydrolysis: a critical step for production of ethanol from mixed wood chips. *Biomass and Bioenergy*, *22*(5), 401-404.

149. Chaturvedi, V., & Verma, P. (2013). An overview of key pretreatment processes employed for bioconversion of lignocellulosic biomass into biofuels and value added products. *3 Biotech*, *3*(5), 415-431.

150. Guha, S. K., Kobayashi, H., & Fukuoka, A. (2010). Conversion of cellulose to sugars. *Thermochemical Conversion of Biomass to Liquid Fuels and Chemicals*, *1*, 344-364.

151. Shahbazi, A., & Zhang, B. (2010). Dilute and concentrated acid hydrolysis of lignocellulosic biomass. In *Elsevier Inc.*.

152. Moe, S. T., Janga, K. K., Hertzberg, T., Hägg, M. B., Øyaas, K., & Dyrset, N. (2012). Saccharification of lignocellulosic biomass for biofuel and biorefinery applications–a renaissance for the concentrated acid hydrolysis?. *Energy Procedia*, *20*, 50-58.

153. Wijaya, Y. P., Putra, R. D. D., Widyaya, V. T., Ha, J. M., Suh, D. J., & Kim, C. S. (2014). Comparative study on two-step concentrated acid hydrolysis for the extraction of sugars from lignocellulosic biomass. *Bioresource Technology*, *164*, 221-231.

154. Sun, Y., & Cheng, J. J. (2005). Dilute acid pretreatment of rye straw and bermudagrass for ethanol production. *Bioresource Technology*, *96*(14), 1599-1606.

155. Kim, K. H., Tucker, M., & Nguyen, Q. (2005). Conversion of bark-rich biomass mixture into fermentable sugar by two-stage dilute acid-catalyzed hydrolysis. *Bioresource Technology*, *96*(11), 1249-1255.

156. Franco, H., Teixeira Mendonca, R., Marcato, P. D., Duran, N., Freer, J., & Baeza, J. (2011). Diluted acid pretreatment of Pinus radiata for bioethanol production using immobilized Saccharomyces cerevisiae IR2-9 in a simultaneous saccharification and fermentation process. *Journal of the Chilean Chemical Society*, *56*(4), 901-906.

157. Wang, G. S., Lee, J. W., Zhu, J. Y., & Jeffries, T. W. (2011). Dilute acid pretreatment of corncob for efficient sugar production. *Applied Biochemistry and Biotechnology*, *163*(5), 658-668.

158. Kootstra, A. M. J., Beeftink, H. H., Scott, E. L., & Sanders, J. P. (2009). Comparison of dilute mineral and organic acid pretreatment for enzymatic hydrolysis of wheat straw. *Biochemical Engineering Journal*, *46*(2), 126-131.

159. Kim, S. B., Lee, J. H., Oh, K. K., Lee, S. J., Lee, J. Y., Kim, J. S., & Kim, S. W. (2011). Dilute acid pretreatment of barley straw and its saccharification and fermentation. *Biotechnology and Bioprocess Engineering*, *16*(4), 725-732.

160. Bezerra, M. A., Santelli, R. E., Oliveira, E. P., Villar, L. S., & Escaleira, L. A. (2008). Response surface methodology (RSM) as a tool for optimization in analytical chemistry. *Talanta*, *76*(5), 965-977.
161. Liyana-Pathirana, C., & Shahidi, F. (2005). Optimization of extraction of phenolic compounds from wheat using response surface methodology. *Food Chemistry*, *93*(1), 47-56.
162. Sasmal, S., Goud, V. V., & Mohanty, K. (2011). Optimisation of the acid catalysed pretreatment of areca nut husk fibre using the Taguchi design method. *Biosystems Engineering*, *110*(4), 465-472.
163. Sasmal, S., Goud, V. V., & Mohanty, K. (2013). Dilute Sulfuric Acid Pretreatment of Bon Bogori (Ziziphus rugosus): Proselyte to Amorphous Biomass for Biofuel Production. *Journal of Bioprocess Engineering and Biorefinery*, *2*(3), 225-229.
164. Ogura, K., Ninomiya, K., Takahashi, K., Ogino, C., & Kondo, A. (2014). Pretreatment of Japanese cedar by ionic liquid solutions in combination with acid and metal ion and its application to high solid loading. *Biotechnology for Biofuels*, *7*(1), 120.
165. Gale, E., Wirawan, R. H., Silveira, R. L., Pereira, C. S., Johns, M. A., Skaf, M. S., & Scott, J. L. (2016). Directed discovery of greener cosolvents: New cosolvents for use in ionic liquid based organic electrolyte solutions for cellulose dissolution. *ACS Sustainable Chemistry & Engineering*, *4*(11), 6200-6207.
166. Tan, H. T., & Lee, K. T. (2012). Understanding the impact of ionic liquid pretreatment on biomass and enzymatic hydrolysis. *Chemical Engineering Journal*, *183*, 448-458.
167. Doherty, T. V., Mora-Pale, M., Foley, S. E., Linhardt, R. J., & Dordick, J. S. (2010). Ionic liquid solvent properties as predictors of lignocellulose pretreatment efficacy. *Green Chemistry*, *12*(11), 1967-1975.
168. Swatloski, R. P., Spear, S. K., Holbrey, J. D., & Rogers, R. D. (2002). Dissolution of cellose with ionic liquids. *Journal of the American chemical society*, *124*(18), 4974-4975.
169. Zakrzewska, M. E., Bogel-Łukasik, E., & Bogel-Łukasik, R. (2010). Solubility of carbohydrates in ionic liquids. *Energy & Fuels*, *24*(2), 737-745.

170. da Costa Lopes, A. M., João, K. G., Bogel-Łukasik, E., Roseiro, L. B., & Bogel-Łukasik, R. (2013). Pretreatment and fractionation of wheat straw using various ionic liquids. *Journal of agricultural and food chemistry*, *61*(33), 7874-7882.

171. da Costa Lopes, A. M., João, K. G., Rubik, D. F., Bogel-Łukasik, E., Duarte, L. C., Andreaus, J., & Bogel-Łukasik, R. (2013). Pre-treatment of lignocellulosic biomass using ionic liquids: wheat straw fractionation. *Bioresource Technology*, *142*, 198-208.

172. da Silva, S. P. M., da Costa Lopes, A. M., Roseiro, L. B., & Bogel-Łukasik, R. (2013). Novel pre-treatment and fractionation method for lignocellulosic biomass using ionic liquids. *RSC Advances*, *3*(36), 16040-16050.

173. Carvalho, A. V., da Costa Lopes, A. M., & Bogel-Łukasik, R. (2015). Relevance of the acidic 1-butyl-3-methylimidazolium hydrogen sulphate ionic liquid in the selective catalysis of the biomass hemicellulose fraction. *RSC Advances*, *5*(58), 47153-47164.

174. Verdía, P., Brandt, A., Hallett, J. P., Ray, M. J., & Welton, T. (2014). Fractionation of lignocellulosic biomass with the ionic liquid 1-butylimidazolium hydrogen sulfate. *Green Chemistry*, *16*(3), 1617-1627.

175. Hassan, E. S. R., Mutelet, F., Moïse, J. C., & Brosse, N. (2015). Pretreatment of miscanthus using 1, 3-dimethyl-imidazolium methyl phosphonate (DMIMMPh) ionic liquid for glucose recovery and ethanol production. *RSC Advances*, *5*(75), 61455-61464.

176. Socha, A. M., Parthasarathi, R., Shi, J., Pattathil, S., Whyte, D., Bergeron, M., ... & Hahn, M. G. (2014). Efficient biomass pretreatment using ionic liquids derived from lignin and hemicellulose. *Proceedings of the National Academy of Sciences*, *111*(35), E3587-E3595.

177. Li, Y., Liu, X., Zhang, Y., Jiang, K., Wang, J., & Zhang, S. (2017). Why Only Ionic Liquids with Unsaturated Heterocyclic Cations Can Dissolve Cellulose: A Simulation Study. *ACS Sustainable Chemistry & Engineering*, *5*(4), 3417-3428.

178. Huo, F., Liu, Z., & Wang, W. (2013). Cosolvent or antisolvent? A molecular view of the interface between ionic liquids and cellulose upon addition of another molecular solvent. *The Journal of Physical Chemistry B*, *117*(39), 11780-11792.

179. Xie, H., Kilpeläinen, I., King, A., Leskinen, T., Järvi, P., & Argyropoulos, D. S. (2010). Opportunities with wood dissolved in ionic liquids. In *Cellulose solvents:*

For analysis, shaping and chemical modification (pp. 343-363). American Chemical Society.

180. Fort, D. A., Remsing, R. C., Swatloski, R. P., Moyna, P., Moyna, G., & Rogers, R. D. (2007). Can ionic liquids dissolve wood? Processing and analysis of lignocellulosic materials with 1-n-butyl-3-methylimidazolium chloride. *Green Chemistry*, *9*(1), 63-69.
181. Sun, N., Rahman, M., Qin, Y., Maxim, M. L., Rodríguez, H., & Rogers, R. D. (2009). Complete dissolution and partial delignification of wood in the ionic liquid 1-ethyl-3-methylimidazolium acetate. *Green Chemistry*, *11*(5), 646-655.
182. Viell, J., & Marquardt, W. (2011). Disintegration and dissolution kinetics of wood chips in ionic liquids. *Holzforschung*, *65*(4), 519-525.
183. Dibble, D. C., Li, C., Sun, L., George, A., Cheng, A., Çetinkol, Ö. P., ... & Simmons, B. A. (2011). A facile method for the recovery of ionic liquid and lignin from biomass pretreatment. *Green Chemistry*, *13*(11), 3255-3264.
184. Sartori, T., Tibolla, H., Prigol, E., Colla, L. M., Costa, J. A. V., & Bertolin, T. E. (2015). Enzymatic saccharification of lignocellulosic residues by cellulases obtained from solid state fermentation using Trichoderma viride. *BioMed Research International*, *2015*.
185. Sasmal, S., Goud, V. V., & Mohanty, K. (2012). Characterization of biomasses available in the region of North-East India for production of biofuels. *Biomass and Bioenergy*, *45*, 212-220.
186. Fengel, D., & Wegener, G. (Eds.). (1983). *Wood: chemistry, ultrastructure, reactions*. Walter de Gruyter.
187. Nanda, S., Mohanty, P., Pant, K. K., Naik, S., Kozinski, J. A., & Dalai, A. K. (2013). Characterization of North American lignocellulosic biomass and biochars in terms of their candidacy for alternate renewable fuels. *Bioenergy Research*, *6*(2), 663-677.
188. Naik, S., Goud, V. V., Rout, P. K., Jacobson, K., & Dalai, A. K. (2010). Characterization of Canadian biomass for alternative renewable biofuel. *Renewable energy*, *35*(8), 1624-1631.
189. Sluiter, A., Ruiz, R., Scarlata, C., Sluiter, J., & Templeton, D. (2008). Determination of extractives in biomass. *Laboratory Analytical Procedure (LAP)*. Technical Report No.NREL/TP-510-42619.

190. Sluiter, A., Hames, B., Ruiz, R., Scarlata, C., Sluiter, J., Templeton, D., & Crocker, D. (2008). Determination of structural carbohydrates and lignin in biomass. *Laboratory analytical procedure*, *1617*, 1-16. http://www.nrel.gov/biomass/analytical_procedures.html

191. McKendry, P. (2002). Energy production from biomass (part 1): overview of biomass. *Bioresource Technology*, *83*(1), 37-46.

192. García, R., Pizarro, C., Lavín, A. G., & Bueno, J. L. (2012). Characterization of Spanish biomass wastes for energy use. *Bioresource Technology*, *103*(1), 249-258.

193. Patel, B., & Gami, B. (2012). Biomass characterization and its use as solid fuel for combustion. *Iranica Journal of Energy & Environment*, *3*(2), 123-128.

194. Designation, A. S. T. M. D. 3173-87 (1988). Standard Test Method for Moisture in the Analysis Sample of Coal and Coke. *Annual Book of ASTM Standards*, *5*, 295-296.

195. The Bioenergy System Planners Handbook, The ash composition. http://bisyplan.bioenarea.eu/ash_appendix.html

196. Sluiter, A., Hames, B., Ruiz, R., Scarlata, C., Sluiter, J., & Templeton, D. (2004). Determination of ash in biomass: LAP-005 NREL analytical procedure. *National Renewable Energy Laboratory, Golden*.

197. Quaak, P., Knoef, H., & Stassen, H. E. (1999). *Energy from biomass: a review of combustion and gasification technologies* (Vol. 23). World Bank Publications.

198. ASTM, D. 3175-07 (2007). Standard method for volatile matter in the analysis sample of coal and coke. *Annual Book of ASTM standards. American Society for Testing and Materials*.

199. Demirbaş, A. (1997). Calculation of higher heating values of biomass fuels. *Fuel*, *76*(5), 431-434.

200. Ledakowicz, S., & Stolarek, P. (2003). Kinetics of biomass thermal decomposition. *Chemical Papers-Slovak Academy of Sciences*, *56*(6), 378-381.

201. Saddawi, A., Jones, J. M., Williams, A., & Wojtowicz, M. A. (2009). Kinetics of the thermal decomposition of biomass. *Energy & Fuels*, *24*(2), 1274-1282.

202. Kim, T. H., Kim, J. S., Sunwoo, C., & Lee, Y. Y. (2003). Pretreatment of corn stover by aqueous ammonia. *Bioresource Technology*, *90*(1), 39-47.

203. Xu, N., Zhang, W., Ren, S., Liu, F., Zhao, C., Liao, H., ... & Yu, B. (2012). Hemicelluloses negatively affect lignocellulose crystallinity for high biomass digestibility under NaOH and H_2SO_4 pretreatments in Miscanthus. *Biotechnology for Biofuels*, *5*(1), 58.

204. Bansal, P., Hall, M., Realff, M. J., Lee, J. H., & Bommarius, A. S. (2010). Multivariate statistical analysis of X-ray data from cellulose: a new method to determine degree of crystallinity and predict hydrolysis rates. *Bioresource Technology*, *101*(12), 4461-4471.

205. de Moraes Rocha, G. J., Martin, C., Soares, I. B., Maior, A. M. S., Baudel, H. M., & De Abreu, C. A. M. (2011). Dilute mixed-acid pretreatment of sugarcane bagasse for ethanol production. *Biomass and Bioenergy*, *35*(1), 663-670.

206. Segal, L. G. J. M. A., Creely, J. J., Martin Jr, A. E., & Conrad, C. M. (1959). An empirical method for estimating the degree of crystallinity of native cellulose using the X-ray diffractometer. *Textile Research Journal*, *29*(10), 786-794.

207. Basu, P. (2013). *Biomass gasification, pyrolysis and torrefaction: practical design and theory*. Academic press.

208. Standard, A. S. T. M. E 711-87 (2004). Standard Test Method for Gross Calorific Value of Refuse-Derived Fuel by the Bomb Calorimeter. ASTM International, West Conshohocken, PA.

209. Prakash, N., & Karunanithi, T. (2008). Kinetic modeling in biomass pyrolysis–a review. *Journal of Applied Sciences Research*, *4*(12), 1627-1636.

210. Adapa, P. K., Schonenau, L. G., Canam, T., & Dumonceaux, T. (2011). Quantitative analysis of lignocellulosic components of non-treated and steam exploded barley, canola, oat and wheat straw using Fourier transform infrared spectroscopy. *Journal of Agricultural Science and Technology*, 177-188.

211. d'Almeida, A. L. F. S., Barreto, D. W., Calado, V., & d'Almeida, J. R. M. (2008). Thermal analysis of less common lignocellulose fibers. *Journal of Thermal Analysis and Calorimetry*, *91*(2), 405-408.

212. Kissinger, H. E. (1957). Reaction kinetics in differential thermal analysis. *Analytical chemistry*, *29*(11), 1702-1706.

213. Ozawa, T. (1970). Kinetic analysis of derivative curves in thermal analysis. *Journal of Thermal Analysis and Calorimetry*, *2*(3), 301-324.

214. Khuri, A. I., & Mukhopadhyay, S. (2010). Response surface methodology. *Wiley Interdisciplinary Reviews: Computational Statistics*, *2*(2), 128-149.

215. Noordin, M. Y., Venkatesh, V. C., Sharif, S., Elting, S., & Abdullah, A. (2004). Application of response surface methodology in describing the performance of coated carbide tools when turning AISI 1045 steel. *Journal of materials processing technology*, *145*(1), 46-58.

216. Montgomery, D. C. (2017). *Design and Analysis of Experiments*. John Wiley & Sons.

217. Baş, D., & Boyacı, İ. H. (2007). Modeling and optimization I: Usability of response surface methodology. *Journal of Food Engineering*, *78*(3), 836-845.

218. Arabi, S., & Sohrabi, M. R. (2014). Experimental design and response surface modelling for optimization of vat dye from water by nano zero valent iron (NZVI). *Acta Chimica Slovenica*, *60*(4), 853-860.

219. Adney, B., & Baker, J. (2008). *Measurement of cellulase activities: laboratory analytical procedure (LAP). National Renewable Energy Laboratory*. Technical Report.

220. Nelson, M. L., & O'Connor, R. T. (1964). Relation of certain infrared bands to cellulose crystallinity and crystal latticed type. Part I. Spectra of lattice types I, II, III and of amorphous cellulose. *Journal of Applied Polymer Science*, *8*(3), 1311-1324.

221. Bin, Y., & Hongzhang, C. (2010). Effect of the ash on enzymatic hydrolysis of steam-exploded rice straw. *Bioresource Technology*, *101*(23), 9114-9119.

222. Miao, Z., Shastri, Y., Grift, T. E., Hansen, A. C., & Ting, K. C. (2012). Lignocellulosic biomass feedstock transportation alternatives, logistics, equipment configurations, and modeling. *Biofuels, Bioproducts and Biorefining*, *6*(3), 351-362.

223. Pasangulapati, V., Ramachandriya, K. D., Kumar, A., Wilkins, M. R., Jones, C. L., & Huhnke, R. L. (2012). Effects of cellulose, hemicellulose and lignin on thermochemical conversion characteristics of the selected biomass. *Bioresource Technology*, *114*, 663-669.

224. Abdullah, S. S., Yusup, S., Ahmad, M. M., Ramli, A., & Ismail, L. (2010). Thermogravimetry study on pyrolysis of various lignocellulosic biomass for potential hydrogen production. *International Journal of Chemical and Biological Engineering*, *3*(3), 137-141.

225.Chen, W. H., Tu, Y. J., & Sheen, H. K. (2010). Impact of dilute acid pretreatment on the structure of bagasse for bioethanol production. *International Journal of Energy Research*, *34*(3), 265-274.

226.Mulinari, D. R., Voorwald, H. J., Cioffi, M. O. H., Da Silva, M. L. C., da Cruz, T. G., & Saron, C. (2009). Sugarcane bagasse cellulose/HDPE composites obtained by extrusion. *Composites Science and Technology*, *69*(2), 214-219.

227.Cheng, G., Varanasi, P., Li, C., Liu, H., Melnichenko, Y. B., Simmons, B. A., Kent, M.S., & Singh, S. (2011). Transition of cellulose crystalline structure and surface morphology of biomass as a function of ionic liquid pretreatment and its relation to enzymatic hydrolysis. *Biomacromolecules*, *12*(4), 933-941.

228.Popescu, C. M., Singurel, G., Popescu, M. C., Vasile, C., Argyropoulos, D. S., & Willför, S. (2009). Vibrational spectroscopy and X-ray diffraction methods to establish the differences between hardwood and softwood. *Carbohydrate Polymers*, *77*(4), 851-857.

229.Claramunt, J., Ardanuy, M., & García-Hortal, J. A. (2010). Effect of drying and rewetting cycles on the structure and physicochemical characteristics of softwood fibres for reinforcement of cementitious composites. *Carbohydrate Polymers*, *79*(1), 200-205.

230.Gandolfi, S., Ottolina, G., Riva, S., Fantoni, G. P., & Patel, I. (2013). Complete chemical analysis of carmagnola hemp hurds and structural features of its components. *Bioresources*, *8*(2), 2641-2656.

231.Eberhardt, T. L., Catallo, W. J., & Shupe, T. F. (2010). Hydrothermal transformation of Chinese privet seed biomass to gas-phase and semi-volatile products. *Bioresource Technology*, *101*(11), 4198-4204.

232.Min, F. F., Zhang, M. X., & Chen, Q. R. (2007). Non-isothermal kinetics of pyrolysis of three kinds of fresh biomass. *Journal of China University of Mining and Technology*, *17*(1), 105-111.

233.Lv, G. J., Wu, S. B., & Lou, R. (2010). Kinetic study for the thermal decomposition of hemicellulose isolated from corn stalk. *Bioresources*, *5*(2), 1281-1291.

234.Varhegyi, G., Antal, M. J., Jakab, E., & Szabó, P. (1997). Kinetic modeling of biomass pyrolysis. *Journal of Analytical and Applied Pyrolysis*, *42*(1), 73-87.

235.Zheng, G., & Koziński, J. A. (2000). Thermal events occurring during the combustion of biomass residue. *Fuel*, *79*(2), 181-192.

236. Brown Jr, R. D., & Jurasek, L. (Eds.). (1979). *Hydrolysis of cellulose: mechanisms of enzymatic and acid catalysis*. American Chemical Society.

237. Krishna, S. H., Prabhakar, Y., & Rao, R. J. (1997). Saccharification studies of lignocellulosic biomass from Antigonum leptopus Linn. *Indian Journal of Pharmaceutical Sciences*, *59*(1), 39.

238. Hsu, T. C., Guo, G. L., Chen, W. H., & Hwang, W. S. (2010). Effect of dilute acid pretreatment of rice straw on structural properties and enzymatic hydrolysis. *Bioresource Technology*, *101*(13), 4907-4913.

239. Fan, L. T., Lee, Y. H., & Beardmore, D. H. (1980). Mechanism of the enzymatic hydrolysis of cellulose: effects of major structural features of cellulose on enzymatic hydrolysis. *Biotechnology and Bioengineering*, *22*(1), 177-199.

240. Fan, L. T., Lee, Y. H., & Beardmore, D. R. (1981). The influence of major structural features of cellulose on rate of enzymatic hydrolysis. *Biotechnology and Bioengineering*, *23*(2), 419-424.

241. Puri, V. P. (1984). Effect of crystallinity and degree of polymerization of cellulose on enzymatic saccharification. *Biotechnology and Bioengineering*, *26*(10), 1219-1222.

242. Camesasca, L., Ramírez, M. B., Guigou, M., Ferrari, M. D., & Lareo, C. (2015). Evaluation of dilute acid and alkaline pretreatments, enzymatic hydrolysis and fermentation of napier grass for fuel ethanol production. *Biomass and Bioenergy*, *74*, 193-201.

243. Hallett, J. P., & Welton, T. (2011). Room-temperature ionic liquids: solvents for synthesis and catalysis. 2. *Chemical reviews*, *111*(5), 3508-3576.

244. Payal, R. S., Bejagam, K. K., Mondal, A., & Balasubramanian, S. (2015). Dissolution of cellulose in room temperature ionic liquids: Anion dependence. *The Journal of Physical Chemistry B*, *119*(4), 1654-1659.

245. Arora, R., Manisseri, C., Li, C., Ong, M. D., Scheller, H. V., Vogel, K., Simmons, B. A.; & Singh, S. (2010). Monitoring and analyzing process streams towards understanding ionic liquid pretreatment of switchgrass (Panicum virgatum L.). *BioEnergy Research*, *3*(2), 134-145.

246. Cruz, A. G., Scullin, C., Mu, C., Cheng, G., Stavila, V., Varanasi, P., Xu, D.; Mentel, J.; Chuang, Y- D.; Simmons, B. A.; & Singh, S. (2013). Impact of high biomass loading on ionic liquid pretreatment. *Biotechnology for Biofuels*, *6*(1), 52.

247. Wang, X., Li, H., Cao, Y., & Tang, Q. (2011). Cellulose extraction from wood chip in an ionic liquid 1-allyl-3-methylimidazolium chloride (AmimCl). *Bioresource Technology*, *102*(17), 7959-7965.

248. Kumar, S., Gupta, R., Lee, Y. Y., & Gupta, R. B. (2010). Cellulose pretreatment in subcritical water: effect of temperature on molecular structure and enzymatic reactivity. *Bioresource Technology*, *101*(4), 1337-1347.

249. Wang, K., Jiang, J. X., Xu, F., & Sun, R. C. (2009). Influence of steaming explosion time on the physic-chemical properties of cellulose from Lespedeza stalks (Lespedeza crytobotrya). *Bioresource Technology*, *100*(21), 5288-5294.

250. Ang, T. N., Ngoh, G. C., Chua, A. S. M., & Lee, M. G. (2012). Elucidation of the effect of ionic liquid pretreatment on rice husk via structural analyses. *Biotechnology for Biofuels*, *5*(1), 67.

251. Dong, S. J., Zhang, B. X., Gao, Y. F., & Hu, X. M. (2015). An efficient process for pretreatment of lignocelluloses in functional ionic liquids. *International Journal of Polymer Science*, *2015*.

252. Poletto, M., Ornaghi, H. L., & Zattera, A. J. (2014). Native cellulose: structure, characterization and thermal properties. *Materials*, *7*(9), 6105-6119.

253. Morais, A. R. C., Pinto, J. V., Nunes, D., Roseiro, L. B., Oliveira, M. C., Fortunato, E., & Bogel-Łukasik, R. (2016). Imidazole: prospect solvent for lignocellulosic biomass fractionation and delignification. *ACS Sustainable Chemistry & Engineering*, *4*(3), 1643-1652.

254. Auxenfans, T., Crônier, D., Chabbert, B., & Paës, G. (2017). Understanding the structural and chemical changes of plant biomass following steam explosion pretreatment. *Biotechnology for Biofuels*, *10*(1), 36.

RESEARCH OUTPUT

In Peer Reviewed Journals

- M. Dash, V.V. Dasu, K. Mohanty, Non-isothermal kinetic study of three lignocellulosic biomass using model-free methods, **Journal of Renewable and Sustainable Energy,** 5 (**2013**) 063101.
- M. Dash, V.V. Dasu, K. Mohanty, Physico-chemical characterization of Miscanthus, Castor, and Jatropha towards biofuel production**, Journal of Renewable and Sustainable Energy,** 7 (**2015**) 043124.
- M. Dash, K. Mohanty, Effect of different ionic liquids and anti-solvents on dissolution and regeneration of Miscanthus and glucose yield (Submitted).
- M. Dash, K. Mohanty, Optimization of dilute acid pre-treatment using RSM for up gradation and increased conversion of cellulose of Miscanthus towards efficient bio-ethanol production through SSF (Submitted).

Manuscripts under preparation

- M. Dash, K. Mohanty, Understanding the role of ionic liquid pretreatment parameters on physico-chemical property of regenerated lignocellulosic biomass and its relation to fermentable sugar yield through enzymatic hydrolysis.

International /National Conference Proceedings

- M. Dash, V.V. Dasu, K. Mohanty, "Kinetic study of lignocellulosic biomass using non-isothermal model-free methods towards biofuel production" International conference on Frontiers in Energy, Environment, Health and Materials research (**EEMR-2013**) , Bhubaneswar, (12-13th August **2013**).
- M. Dash, V.V. Dasu, K. Mohanty, "Physico-chemical characterization of Miscanthus towards renewable energy production"Workshop on Frontier Energy Research with Industry Academia Partnership (**FERIAP**), Centre For Energy, IIT Guwahati, (20-21st March **2015**).

- M. Dash, V.V. Dasu, K. Mohanty, "Conversion of Miscanthus into fermentable sugars through optimization of dilute acid pretreatment followed by enzymatic saccharification" Indian Chemical Engineering Congress, 68th Annual Session of Indian Institute of Chemical Engineers (**Chemcon 2015**), Department of Chemical Engineering, IIT Guwahati, (27-30 December 2015).
